AD-A089 168 NAVAL RESEARCH LAB WASHINGTON DC F/G 17/7
SUMMARY REPORT ON NRL PARTICIPATION IN THE MICROWAVE LANDING SY--ETC(U)
AUG 80 J P SHELTON, J K HSIAO DOT-FA75WAI-556
UNCLASSIFIED NRL-MR-4305 NL

1 OF 2
AD A089168

# Summary Report on NRL Participation in the Microwave Landing System Program

J. Paul Skillman and Harris Anderson

Target Characteristics Branch
Radar Division

August 19, 1980



Prepared under Interagency Agreement DOT-FA75WAI-596

NAVAL RESEARCH LABORATORY
Washington, D.C.

SECURITY CLASSIFICATION OF THIS PAGE (When Data Entered)

# REPORT DOCUMENTATION PAGE

READ INSTRUCTIONS BEFORE COMPLETING FORM

| | |
|---|---|
| 1. REPORT NUMBER: NRL Memorandum Report 4305 | 2. GOVT ACCESSION NO. |
| 3. RECIPIENT'S CATALOG NUMBER: NRL MR-4305 | |
| 4. TITLE (and Subtitle): SUMMARY REPORT ON NRL PARTICIPATION IN THE MICROWAVE LANDING SYSTEM PROGRAM | 5. TYPE OF REPORT & PERIOD COVERED: Interim report on a continuing NRL problem. |
| | 6. PERFORMING ORG. REPORT NUMBER: DOT-FA75WAI-556 |
| 7. AUTHOR(s): J. Paul Shelton and James K. Hsiao | 8. CONTRACT OR GRANT NUMBER(s) |
| 9. PERFORMING ORGANIZATION NAME AND ADDRESS: Naval Research Laboratory, Washington, D.C. 20375 | 10. PROGRAM ELEMENT, PROJECT, TASK AREA & WORK UNIT NUMBERS: 53-0649-0-0 |
| 11. CONTROLLING OFFICE NAME AND ADDRESS: Department of Transportation, Washington, D.C. 20591 | 12. REPORT DATE: 29 August 1980 |
| | 13. NUMBER OF PAGES: 106 |
| 14. MONITORING AGENCY NAME & ADDRESS (if different from Controlling Office) | 15. SECURITY CLASS. (of this report): UNCLASSIFIED |
| | 15a. DECLASSIFICATION/DOWNGRADING SCHEDULE |

16. DISTRIBUTION STATEMENT (of this Report)

Approved for public release; distribution unlimited.

17. DISTRIBUTION STATEMENT (of the abstract entered in Block 20, if different from Report)

18. SUPPLEMENTARY NOTES

19. KEY WORDS (Continue on reverse side if necessary and identify by block number)

Microwave Landing System
Scanning antennas
Microwave optics
Phased arrays

20. ABSTRACT (Continue on reverse side if necessary and identify by block number)

This report summarizes activity by the Radar Division of the Naval Research Laboratory in support of the Microwave Landing System program in the time period May 1975 through September 1979. This technical support was primarily associated with the ground scanning antennas. Initial emphasis was on microwave optical scanning techniques. This phase of the effort resulted in significant innovative contributions, but the more pressing objectives of the program shifted to the analysis of problems associated with phased array antennas. The Naval Research Laboratory contributed to the study of phased arrays in several ways. Computer simulations of internal monitoring systems, which can locate failed components, were carried out. A performance simulation of a general phased array using digital phase shifters was written. The performance characteristics of digital phase (Abstract continues)

DD FORM 1 JAN 73 1473 EDITION OF 1 NOV 65 IS OBSOLETE
S/N 0102-LF-014-6601

SECURITY CLASSIFICATION OF THIS PAGE (When Data Entered)

20. (Abstract continued)
shifters were measured and statistically analyzed. Several research contracts for promising phased array techniques were awarded to industrial contractors. In addition to research on the primary MLS functions, which involve scanning linear phased array antennas, NRL has studied the realization of a 360-degree scanning antenna utilizing a circular array. This report contains a nontechnical review of all activities, supported by technical appendices and a listing of reports and memoranda.

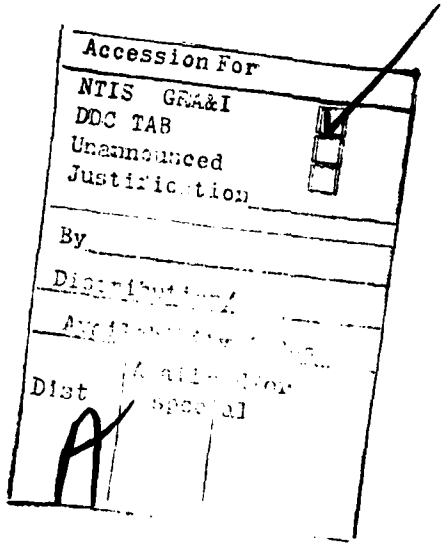

Table of Contents

# NRL PARTICIPATION IN THE MICROWAVE LANDING SYSTEM PROGRAM

## 1. INTRODUCTION

### 1.1 Purpose

This report summarizes work performed by the Radar Division, Naval Research Laboratory, under Interagency Agreement No. DOT-FA75WAI-556. This agreement was initiated in May 1975 between the Federal Aviation Administration (FAA) and the Naval Research Laboratory (NRL). This report covers activity during the period, May 1975 through September 1979.

This report is the final summary report (FY-79) called for in paragraph L, Article V, in Modification 10 to the Interagency Agreement. The Interagency Agreement has been further modified to extend the effort through FY-80. Therefore, this research program is continuing, and this report is not final in the strict sense. However, several phases of the program have been completed, and it is feasible to present a cohesive summary of activity and progress to date.

The general objective of this research program is to study scanning beam antenna designs and to make recommendations to the FAA as to the applicability of these designs to the Microwave Landing System (MLS). NRL is participating in this program because of its expertise in the technology being utilized in MLS antennas. During the period covered by this report, the MLS program devoted very little of its resources to military applications of MLS, and NRL has devoted only a very slight fraction of its effort to consideration of military application of MLS. Thus, this research program has been concerned with MLS as an advanced precision landing system for civil aviation. Appendix A contains the Statement of Work from the original Interagency Agreement and subsequent modifications thereto.

Although the MLS program is predominantly directed to civil aviation applications, DoD and the Navy clearly have strong interest both in the MLS program in particular and in advanced air traffic control technology in general. Thus, it is considered to be in the mutual interest of FAA and the Navy to have NRL participate in this program. From the standpoint of the Radar Division, where the NRL work on this program has been performed, the technology interchange relating to system concepts and detailed design techniques has been valuable.

**Manuscript submitted June 17, 1980**

For those readers who are not familiar with the Microwave Landing System, Appendix B is included as a brief introduction with both historical and technical information.

Unfortunately, there has been relatively little treatment of the MLS in the open literature. The background and general guidelines for the U.S. development effort are given in the final report of RTCA Special Committee 117 [1]. The FAA sponsored MLS symposia in 1972 and 1973, for which records are published [2,3]. Some general descriptions of landing systems can be found [4,5,6]. Workers from Bendix and Hazeltine have described the results of some of their efforts [7,8,9]. Articles in news-type publications such as Aviation Week and Electronic News, or even the general news media, emphasized the adversary aspects of the ICAO process. Other articles contained self-admitted bias [10] or were based on a general misunderstanding of the issues and processes involved [11]. The general subject of air traffic control is receiving increased popular coverage, and the MLS program was recently mentioned in National Geographic Magazine [12].

## 1.2 Outline of NRL Activity

Because of NRL's participation in the MLS program in the capacity of expert consultants, because of NRL's close proximity to FAA, and because of the wide range of activities being pursued by FAA during the time period covered by this report, a variety of tasks were undertaken by NRL in accomplishing the objectives of the statement of work. As has been previously stated, the initial research objective was to make recommendations to FAA as to the applicability of scanning antenna designs to the MLS program.

At the outset, NRL addressed microwave optical techniques for the reasons that (a) the Phase III programs being undertaken by Bendix and Texas Instruments (TI) were both using microwave optical designs and (b) the Australian INTERSCAN MLS, with which the U.S. had aligned itself at the conclusion of the selection process at the end of 1974, used microwave optical designs. Therefore, intensive interaction was required between NRL and Bendix, TI, and the Radio Physics Laboratory of the Commonwealth Scientific and Industrial Research Organization of Australia (CSIRO). Part of this interaction was achieved through the medium of the Design Review Board, to which NRL was a consultant, which reviewed the progress of Bendix and TI on the Phase III program during 1975-76.

A basic purpose for making antenna recommendations to FAA was to strengthen the U.S.'s submission to ICAO, which was initially made in December 1975. Further, the ICAO submission was defended and modified during the ICAO meetings of 1976-77.

NRL evaluated proprietary proposals from ITT Gilfillan and Hazeltine in 1975 and eventually awarded research contracts to those companies

for studies of novel phased array techniques. These studies were completed in 1976, and a second contract was awarded to Hazeltine for modification and additional testing of its technique. A study contract was awarded to Myer Associates in 1979 to assist with NRL's performance and monitoring simulations.

As a result of various cost and technical factors, emphasis shifted from microwave optical techniques to phased arrays in early 1976. Consequently, NRL also devoted increasing effort to phased array studies, initially considering the design and performance of thinned arrays, and later addressing the monitoring and performance simulation of all types of digitally scanned arrays.

### 1.3 Introduction to Report

This report is organized with the hope of providing the reader with a broad overview of NRL's participation in the MLS program during the 1975-77 time period. Although no attempt is made to completely satisfy all types of readers, it is hoped that the information contained herein will be useful to a wide variety of readers, ranging from engineers with specific design interests to those individuals with more general interest in the recent history and evolution of the MLS program.

Sections 3 and 4 are a glossary of terms and references, respectively. Sections 5 and 6 list documents generated by NRL and personnel participating in the program. Appendices A, B, and C include the work statement from the interagency agreement, a brief description of the Microwave Landing System, and a description of contract research supported by NRL.

Appendix D is a listing in chronological order of the significant events and milestones relating to NRL's activities in the MLS program. In many cases the milestones are also highly significant to the overall program, so that the chronology reasonably reflects the U.S. and ICAO MLS activity during the period.

Appendix E is a description of the performance simulation which has been developed by Dr. J. K. Hsiao, and Appendix F is an analysis of the digital filter used in that simulation.

Appendix G describes the optimum beam steering technique generated at NRL. Appendix H described the circular array design study carried out in 1978-79. Appendix I describes 3D bootlace lenses which were developed on another NRL task but which have direct application to the original microwave optical scanning studies and the circular array study. Appendix J describes how to feed a linear array with a 3D lens.

## 2. DISCUSSION OF ACTIVITIES

### 2.1 Microwave Optical Research

The original statement of work, agreed upon between NRL and FAA and reproduced in Appendix A, listed the following seven subjects for consideration.

1. Microwave optics.
2. Feed commutation.
3. Monitoring and redundancy.
4. Beam shaping.
5. Phased-array/microwave optics trade-off studies.
6. Alternate proposal for ICAO.
7. Design review activities.

The emphasis was very strongly on scanning antennas utilizing microwave optics. The Phase III contracts were just underway in mid-1975, and both TI and Bendix were using microwave optical designs for the Basic Narrow (narrow referring to the aperture size) configuration, in which the azimuth antenna beamwidth is about two degrees and the elevation antenna beamwidth is about 1.5 degrees. Bendix used Gent bootlace lenses (also known as Rotman) for their Phase III equipment, and TI used a bifocal folded pillbox for the elevation unit and a parabolic torus for the azimuth unit.

Although these microwave optical designs were felt to be cost effective in the Basic Narrow configuration, they were not considered practical for the Basic Wide configuration, which requires 3.66m (12-foot) apertures to produce one-degree beamwidths. Thus, two objectives of the microwave optical studies were (a) to review all possible microwave optical techniques to determine what would be the preferred design approach, and (b) to ascertain whether there was a practical microwave optical design for use in the Basic Wide configuration.

In addition to the microwave optical design activity underway at Bendix and TI in 1975, the Australian INTERSCAN MLS program was committed to microwave optical scanning antennas. The principal MLS research activity in Australia has taken place at the Radio Physics Laboratory of CSIRO in Sydney, under the leadership of Dr. J. P. Wild and, later, H. Minnett. The principal MLS design and fabrication contractor has been Australasian Wireless Amalgamated.

Immediately upon execution of the interagency agreement, it was deemed desirable to coordinate the research programs at NRL and CSIRO. To this end, meetings were held during a two-week period in June 1975 in Paris and Sydney. The American representatives in these discussions were J. P. Shelton of NRL and S. R. Jones of MITRE.* Initial and final discussions were held with J. P. Wild in Paris, and detailed technical discussions were held with H. Minnett, associate director of the Radio Physics Laboratory, and other workers. The outcome of these meetings was an agreement to pursue an intensive cooperative antenna study program during the period July-September 1975, with another meeting at the

*MITRE Corporation was an overall technical consultant to FAA on the MLS program, and S. R. Jones was the MITRE project leader until 1977.

end of the study to decide upon an appropriate hardware development program. The Australians described two antenna concepts which they regarded as proprietary: One was the use of curved waveguide slot array radiators in circular azimuth arrays, which eliminates beamwidth broadening at high elevation angles. The other was a cylindrical geodesic dielectric-loaded lens, which appeared equivalent to the Myers geodesic. The agreed-upon study program included the following objectives:

1. Antennas with one-degree beamwidth, obtained with an effective aperture of $75\lambda$. In the case of circular configurations, the feed radius will be no greater than $40\lambda$.

2. CSIRO would pursue (a) complex modulation analysis and simulation, (b) experimental improvement of torus antenna to demonstrate one-degree beamwidth, (c) design of column waveguide arrays and shaped reflectors, and (d) study of new disk and cylinder lenses.

3. NRL would pursue (a) general lens studies, (b) feed network concepts, and would provide any possible information on lens references and slot array design.

4. Both groups agreed to study monitoring, redundancy, cost, and error budget.

It was estimated that the next meeting would be about mid-September. The subsequent meeting actually occurred on 1 December 1975, at CSIRO in Sydney. The American group consisted of J. P. Shelton, NRL, S. R. Jones, MITRE, and G. Jensen and R. Normoyle of FAA. This two-week meeting produced significant results, although they were not predicted by the objectives listed above. The cooperative antenna study program was remarkable in producing innovative concepts; it is doubtful that these innovations would have been generated without the impetus of the cooperative program.

The following developments were presented by CSIRO:

1. J. P. Wild described his "Opera House" lens, so named because of its resemblance to the Sydney opera house. This bootlace lens configuration utilizes a spherical geodesic surface rather than the conventional planar internal propagation region. It has been shown that Wild's lens is the optimum trifocal bootlace configuration.

2. Torus efforts included experimental development of an eight-phase complex modulator, plus theoretical design of a compact torus with $R = 77.5\lambda$ (the objective was $75\lambda$).

3. Parallel-plate lens designs for feeding circular arrays included flat disk lenses and spherical geodesic configurations with linear angle transformations.

The following developments were presented by NRL:

1. Redundant switching and modulation networks had been developed in mid-October for inclusion in the ICAO submission. Both types of network rely on PIN diode control devices configured so that the network can sustain the failure of one diode without hindering operation. The switches use hybrid matrix networks with typically 4, 8, or 16 ports on each side. Available switch configurations for these matrices are SP3T, SP7T, and SP15T with nonisolated outputs or SP2T, SP4T, and SP8T with all ports isolated and matched.* The redundant modulator technique uses diode phase shifters with a Fourier transforming Butler matrix or equivalent lens to transform from phase scan to lateral feed motion.

2. A simplified analysis of Gent-Rotman lenses was carried out to establish the performance limitations of the lens. It was concluded that the Gent-Rotman lens can be used to generate one-degree beams with $\pm 40$ degrees coverage with the required precision. It was also concluded that the optimum lens design has front-back symmetry.

3. A modular Rotman lens configuration was described, which uses small lenses to build larger lenses analogous to the building-block assembly of Butler matrices.

4. Parallel-plate lenses with circular symmetry were described. Technical memoranda on (a) a family of folded disk lenses, (b) a geodesic Luneburg design, and (c) a bootlace-corrected trifocal Schmidt system were presented. To aid in the realization of parallel-plate lens structures, a parallel-plate directional coupler was proposed.

At the conclusion of the December 1975 meeting at CSIRO, plans were made to progress from Stage I of the cooperative antenna program into Stage II, which would involve experimental testing of some of the proposed novel techniques.

Although work on microwave optical techniques continued at CSIRO, effort at NRL was diverted from microwave optics into phased-array technology early in 1976. Subsequent efforts are described in the following sections.

## 2.2 Phased-Array Studies

### 2.2.1 Background for Phased-Array Effort

The cooperative NRL-CSIRO microwave optical study effort produced notable results. However, in terms of the broader requirements

*It was subsequently learned that this switch configuration was not original. The basic matrix switching configuration was proposed by H. Schrank in the 60's (Schrank, Hooper, and David, "A Study of Array Beam Switching Techniques," RADC-TR-65-546, Feb. 65) and C. Lee more recently reinvented the SP3T version (U.S. Pat. 3,996,533, 7 Dec 76).

of the U.S. MLS program and the presssures of the ICAO selection process, it was decided in early 1976 to adopt phased arrays as the preferred design approach for the U.S. TRSB MLS. The following factors contributed to this decision:

1. Although techniques for achieving redundancy in the switching and modulation portions of the microwave optical antenna systems were proposed, it became clear that experimental validation and field testing of these techniques could not be accomplished soon enough to make an impact on the ICAO process.

2. The cost of phase shifters was dropping dramatically, with the result that the cost advantage of microwave optical systems was becoming much less significant.

3. Although microwave optical antennas could be designed to meet the MLS requirements for one-degree beamwidths, the lens structures were always larger than the aperture length. For the one-degree beamwidth, this leads to integral planar structures with dimensions of about 3.66m (12 feet), which is excessively bulky for equipment which must be transportable on a world-wide basis.

NRL's involvement in these phased-array studies can be divided roughly into three stages. The first stage consisted of a theoretical investigation of thinned arrays. This work coincided with experimental field tests of the Bendix azimuth phased array at NAFEC, modified to a thinned configuration. The second stage of the NRL phased-array effort consisted of a study of integral RF monitoring techniques for fault detection and isolation, carried out through computer simulation. The third stage involved the development of a performance simulation applicable to all of the phased array configurations under consideration. In addition, NRL has established a procedure for testing phase shifters that are intended for use in MLS phased arrays.

### 2.2.2 Thinned Arrays

It was decided early in 1976 to prepare a case for the use of thinned phased arrays at airports where multipath is not a serious problem. The thinned array is realized by quasi-random removal of elements from a filled array. The resultant system can be made to exhibit essentially unchanged pattern shape near the main beam at the cost of much higher far-out sidelobes, together with the lower gain associated with a smaller number of radiators.

The questions to be answered during the thinned array study related to the effects of thinning on accuracy, reliability, multipath vulnerability, monitorability, and cost. These topics were treated in a report titled "Preferred Time Reference Scanning Beam Phased Array Implementation for MLS," by S.R. Jones, MITRE, J.P. Shelton, NRL, and R.E. Willey,

Bendix. The report was entered as a Background Information Paper to the Washington meeting of Working Group A of AWOP, held in May 1976. NRL contributed about two-thirds of this report with the following sections:

2.0 Design Concepts

2.1 Aperture Features and Beam Scanning Effects

2.1.1 Sidelobe Performance of Thinned Arrays

2.1.2 Beam Scanning Effects in Phased Arrays

2.1.2.1 Effect of Phase Shifter Bit Reduction on Sidelobe Level

2.1.2.2 The Beam-Pointing Accuracy of a Phased Array

2.2 Failure Characteristics of Phased Arrays

3.0 Hardware Considerations

3.2 Advanced Techniques

3.2.1 Integrated Diode-Controlled Phased Array Technique

3.2.2 Network Techniques for Limited Scan Arrays (COMPACT)

Appendix A: A Review of Thinning Techniques for Linear Arrays (by J. K. Hsiao)

Meanwhile, preparations were underway at Bendix to perform accuracy measurements of a thinned azimuth array at NAFEC. The array was the one developed by Bendix during Phase II in the 1973/74 time period. Thinning was accomplished by removing phase shifters from the filled array. The performance of the thinned array had been predicted by simulations carried out at Bendix. The measured performance, obtained in a series of tests carried out in June 1976, was in good agreement with the simulation results. Furthermore, phase shifter failures were measured and simulated, and the graceful degradation of the phased array, even in the thinned condition, was amply demonstrated. These test results were submitted to the AWOP WGA meeting held at The Hague in July 1976.

2.2.3 Phased Array Monitoring Studies

After the July WGA meeting at The Hague, the U.S. TRSB proposal was modified to include both thinned and filled phased arrays, and emphasis was placed on analysis of a fault-locating monitoring system for phased arrays.

A monitoring simulation program was begun at NRL in August 1976. The objective was to complete the simulation so that the results could be

used at the London WGA meeting scheduled for November 1976. The simulation was sufficiently complete so that the fault isolation capability of the proposed U.S. monitoring system could be confirmed. The outcome of the London meeting was the desired one: that monitoring was not a discriminant between DMLS and TRSB MLS.

2.2.4 Phased Array Performance Simulation

After the AWOP meeting at Montreal in May 1977 and the vote by AWOP in favor of the U.S. system, a decision was made by the MLS office to develop an "in-house" performance simulation to provide the capability for comparing the various phased array configurations and beam-scanning algorithms being proposed by industry. It was decided that NRL would develop this simulation, and effort was begun in April 1977. Appendix E describes the present status of this simulation.

2.2.5 Phase Shifter Measurements

In the fall of 1977 FAA became interested in the performance that could be expected from phase shifters that might be used in MLS antennas and the effect of component tolerances on system performance. In 1975 Bendix had purchased 180 phase shifters from EMS for possible use in the Phase III equipment development program. Although these units were not used in Phase III equipment, it was decided that they would be used in the Basic Wide system.

Therefore, NRL was tasked to measure a small number of phase shifters, about 10, at the outset, then a group of about 30, and finally the entire available inventory of 180.

Although these units were purchased under a set of specifications, it was necessary to evaluate their actual performance so that the measured performance of the system could be related to the actual phase shifter characteristics.

Initially, a group of about seven Bendix/EMS ferrite latching four-bit units and two TI diode four-bit units were tested using an automatic network analyzer available at NRL. A computer program was written for compiling statistical data on the measurements, which reads out insertion phase characteristics and standard deviation of the variation of phase shift from the desired values, together with mean and standard deviation of insertion loss and VSWR. Subsequently, NRL was tasked with testing 180 Bendix/EMS units. At this point it was realized that the manual transfer of data, by means of punched cards, from the printed output of the network analyzer to the computer was laborious, time-consuming, and error-prone. Therefore, a somewhat circuitous but fully mechanized procedure was devised, whereby the test data was recorded on magnetic tape, then transcribed to a disk and input to the computer.

Testing and analysis of the 180 units was performed in FY-79. It was planned that a subset of this group would be retained at NRL for temperature testing. Unfortunately, Bendix called for return of these remaining units before the testing could be completed.

2.2.6 Optimum Beam Steering Technique

In the course of the research effort on phased arrays, it was noted that all contractors had proprietary beam steering algorithms. Subsequently, J. P. Shelton of NRL proposed an optimum beam steering technique which uniquely determines the sequence in which phase shifters will be stepped. This technique is described in Appendix G.

## 2.3 Investigation of 360-degree Ground Scanning Azimuth Antenna

Following the selection by ICAO in April 1978 of the TRSB/MLS and a decision at that meeting that the design of a 360-degree ground scanning azimuth antenna should be developed, a portion of NRL's effort has been devoted to this problem.

In May 1978 J. P. Shelton of NRL proposed a three-dimensional bootlace lens configuration which is applicable to the generation of multiple beams from linear arrays. This development has impact on two problem areas in the MLS. It had already been found that some of the feed systems which would be used for the 360-degree system require lenses with dimensions larger than those of the circular array. The 3D lens will have dimensions much smaller than those of the corresponding 2D lens. Thus, it is possible to use a 3D lens in the 360-degree antenna system which is smaller than the circular array.

Furthermore, the 3D lens solves the original problem which NRL was tasked with in 1975. It is now possible to feed the one-degree-beamwidth azimuth array with a lens structure which is small relative to the size of the array.

Appendix H is a discussion of the circular array design study. Appendix I describes two 3D lens configurations which have been derived. Appendix J gives the procedure for applying the 3D lens to a linear array.

## 2.4 Design Review Board and Contractor Interaction

In order to monitor the progress of the Phase III development contracts at Bendix and TI, the MLS office organized a Design Review Board (DRB) which was active during the critical phases of the contracts--from the summer of 1975 through the spring of 1976. Meetings were held at the contractors' various facilities at roughly monthly intervals. NRL participated in the DRB process as an expert consultant and provided an attendee to most of the DRB meetings.

In addition, NRL acted as a source of consulting expertise to the contractors. Indeed, the interaction between NRL and the contractors was of great benefit to all parties. The degree of interaction was more or less, depending on such factors as location or the disposition of the contractor to discuss his activities. (Some contractors show a marked disinclination to discuss technical matters except when a contract is in the offing.) The results of these factors were as follows for the various contractors:

Bendix - Strong because of both location and disposition and also heavy and continuing MLS activity.

TI - Weak primarily because of location.

ITT Gilfillan - Weak because of remote location and brief period of activity.

Hazeltine - Negligible because of disposition.

## 2.5 ICAO Participation

It has already been pointed out that NRL submitted material for inclusion in the U.S. MLS ICAO proposal, which was submitted in December 1975. To some extent, all MLS activity by FAA has been directed to the ICAO process because of the absolute necessity of winning that contest. Subsequent to the submission of proposals to ICAO by Australia, UK, FRG, and US, there were four AWOP WGA meetings in 1976 followed by an AWOP meeting in March 1977.

NRL participated in the preparation of the thinned phased array proposals that were entered into the ICAO process at the Washington meeting in May 1976 and at The Hague meeting in July 1976.

J. P. Shelton of NRL attended the London WGA meeting in November 1976 and the Montreal AWOP meeting in March 1977.

Russian delegations visited Washington in November 1975 and November 1977, the Russians supported TRSB MLS. NRL participated in the discussions with the Russian delegations.

## 2.6 Contracts with ITT Gilfillan and Hazeltine

In mid-1975 when NRL entered the MLS program, the Phase III contracts with TI and Bendix were also underway. Thus, all of the developmental effort being funded by FAA at that time was directed toward microwave optical scanning antennas, and there was no effort being directed to phased arrays.

At roughly the same time, ITT Gilfillan and Hazeltine came forward with unsolicited proprietary proposals for novel phased-array

techniques. It was decided that it would be advantageous to the MLS program to investigate these techniques. NRL was deemed the logical organization to issue and monitor the necessary contracts.

One technique, proposed by ITT Gilfillan, employs a "vari-phase coupler" to integrate the power distribution to the array elements with a diode phase-shift procedure. The technique offers the advantages of a compact physical package, low losses, and low cost with the possible disadvantages of three-bit phase control and amplitude variation with phase state. This integrated phased array technique is described in Appendix C.

ITT Gilfillan fabricated a 44-element horizontal array with three-degree beamwidth under their contract. The array is fed at the center.

The other technique, under development at Hazeltine and acronymed COMPACT, employs a network between the array and the phase shifters to form near-optimum sector element patterns so that a minimum number of phase shifters can be used in limited scan applications, such as the MLS elevation antennas. The network requires that the number of phase shifters be one-half the number of inputs to the array, and the technique is limited to coverage of about 40 to 50 degrees. The limited-scan network technique is also described in Appendix C.

Hazeltine fabricated, under their research contract, a 96-element vertical array with one-degree beamwidth which can be scanned by 24 phase shifters. The 96 elements consist of 48 element pairs, which are fed by the COMPACT network.

NRL issued and monitored contracts for both of these techniques, and both contractors completed their contracts in mid-1976. Final reports were submitted, and the experimental measurements showed excellent agreement with the performance predicted for the techniques. In addition, NRL awarded a second contract to Hazeltine in April 1977 for additional testing of the COMPACT antenna.

In July 1979 NRL issued a contract to Meyer Associates for a simulation and monitoring study. This study encompassed the following tasks:

1. Review the NRL MLS performance simulation program and develop procedures for validating it.
2. Study the performance of the field monitor under conditions of component failures and develop a suitable simulation procedure and validation process.
3. Review present and future requirements for maintenance monitoring in the MLS ground scanning antennas.
4. Design an experimental maintenance monitor for evaluating phase shifter performance.

## 3. GLOSSARY OF TERMS

| | |
|---|---|
| ALPA | Airline Pilots' Association |
| ATA | Air Transport Association |
| AWA | Australiasian Wireless Amalgamated |
| AWOP | All-weather Operations Panel |
| COMPACT | Cost Minimized Phased Array Circuit Technique (proprietary to Hazeltine) |
| CSIRO | Commonwealth Scientific and Industrial Research Organization (Australia) |
| DLS | DME-based Landing System (West Germany) |
| DMLS | Doppler Microwave Landing System (U.K.) |
| DRB | Design Review Board |
| FAA | Federal Aviation Administration |
| FRSB | Frequency Reference Scanning Beam |
| IATA | International Air Transport Association |
| ICAO | International Civil Aviation Organization |
| IFALPA | International Federation of Airline Pilots' Associations |
| ILS | Instrument Landing System |
| INTERSCAN | Australian TRSB MLS |
| MLS | Microwave Landing System |
| NAFEC | National Airport Facilities Evaluation Center, Atlantic City, N.J. |
| NRL | Naval Research Laboratory |
| TDM | Time Division Multiplex |
| TI | Texas Instruments |
| TRSB | Time Reference Scanning Beam |
| WGA | Working Group A |

## 4. REFERENCES


1. "A New Guidance System for Approach and Landing," RTCA SC-117, Doc. No. 148, Dec 18, 1970.
2. Systems Research and Development Service, United States Microwave Landing System (MLS) Development Program Symposium, Symposium Record, FAA-RD-73-95, FAA Report, Jun 1973.
3. Systems Research and Development Service, International Microwave Landing System (MLS) Symposium, Symposium Record, FAA-RD-74-56, RAA Report, Apr 1974.

4. L. L. Sanders and V. J. Fritch, Jr., "Instrument Landing Systems," IEEE Trans. COM, Vol COM-21, No. 5, pp 435-453, May 1973.
5. Frank B. Brady, "Landing Guidance Systems," AGARD Monograph on Air Traffic Control, Feb 1975.
6. R. A. Moore, H. W. Cooper, and R. S. Littlepage, "Trends in Aircraft Landing Systems," presented at EASCON '76, Sep 1976.
7. R. M. Cox and J. R. Sebring, "MLS-A Practical Application of Microwave Technology," IEEE Trans MTT, Vol. MTT-24, No. 12, pp 964-971, Dec 1976.
8. A. R. Lopez, "Scanning-Beam Microwave Landing System - Multipath Errors and Antenna Design Philosophy," IEEE Trans AP, Vol. AP-25, No. 3, pp 290-296, May 1977.
9. R. J. Kelly, "Guidance Accuracy Considerations for the Microwave Landing System," presented at NAECON '76, May 1976.
10. R. S. Barratt, "The UK Approach to MLS," Microwave Journal, Vol. 19, No. 10, pp 19-22, Oct 1976.
11. C. E. White, "MLS - A Decision Required," (editorial), Microwave Journal, Vol. 19, No. 9, p 24, Sep 1976.
12. Michael E. Long, "The Air-Safety Challenge," National Geographic, Vol. 152, No. 2, pp 209-234, Aug 1977.

## 5. DOCUMENTS GENERATED BY NRL

The following reports, documents, papers, and publications have been generated during the performance of the tasks in this program.

Reports, papers, and publications:

J. K. Hsiao, "A Review of Thinning Techniques for Linear Arrays," NRL Memo Report 3495, May 1977.
J. P. Shelton, "Focusing Characteristics of Symmetrically Configured Bootlace Lenses," NRL Memo Report 3483, Apr 1977.
J. K. Hsiao and J. P. Shelton, "A Phased Array Maintenance Monitoring System: Part I," NRL Memo Report 3613, Sep 1977.
J. K. Hsiao and J. P. Shelton, "A Phased Array Maintenance Monitoring System: Part II," NRL Memo Report 3737, Mar 1978.
J. P. Shelton, "Focusing Characteristics of Symmetrically Configured Bootlace Lenses," IEEE Transactions on Antennas and Propagation, Vol. AP-26, No. 4, Jul 1978, pp 513-518. This paper received "Best Paper of 1978" award from AP-S Transactions.
J. K. Hsiao and J. P. Shelton, "A Phased Array Maintenance Monitoring System," IEE International Radar-77 Conference, Oct 1977, London, England. Conference Publication No. 155, p 447.
J. K. Hsiao and J. P. Shelton, "Maintenance Monitoring System for Microwave Landing System Array Antennas," 1978 IEEE/AP-S International Symposium Digest, May 1978.

J. K. Hsiao and J. P. Shelton, "Phased-Array Maintenance Monitoring System," U.S. Patent No. 4,176,354, Nov 27, 1979.
J. P. Shelton, "Three Dimensional Bootlace Lenses," 1980 IEEE/AP-S International Symposium, Jun 1980.

Memoranda:

W. F. Gabriel, "Cylindrical Array/Geodesic Luneberg MLS Antenna," Sep 1975.
R. M. Brown, "Schmidt Antennas for MLS," Nov 1975.
R. M. Brown, "Off-Axis Corrected Bootlace Schmidt Lenses," Nov 1975.
J. P. Shelton, "A Modular Lens Antennas System for the MLS Antenna Program," Aug 1975.
J. P. Shelton, "A Family of Concentric Lenses," Nov 1975.
Material for ICAO Submission, Oct 1975
Sections on: Modular Gent Lens Antenna System
Redundancy in Microwave Optics Scanning with Fail-Safe Switches and Modulators
Sector Element Patterns for Phased Arrays
Five Circular Array Microwave Optical Designs
J. P. Shelton and J. K. Hsiao, contributions to "Preferred Time Reference Scanning Beam Phased Array Implementation for MLS, May 1976 (AKA "The Yellow Book")
Sections on: Sidelobe Performance of Thinned Arrays
Effect of Phase Shifter Bit Reduction on Sidelobe Level
The Beam-Pointing Accuracy of a Phased Array
Failure Characteristics of Phased Arrays
J. P. Shelton, "Hadamard Transform Algorithm for Phased Array Monitoring," 24 Jun 1977.
J. P. Shelton, "Optimum Beam-Steering Technique for a Scanned Phased Array Antenna," Invention Disclosure, Jul 1978.
Code 5340, NRL, "Report on Network Analysis," 11 Apr 1979.
J. P. Shelton, "Design of a 360-Degree Azimuth Antenna for the Microwave Landing System," May 1979.

## 6. PERSONNEL PARTICIPATING IN PROGRAM

The following personnel have contributed to the tasks described in this report and are listed roughly in descending order of amount of participation:

J. P. Shelton, Principal investigator; Head, Target Characteristics Branch, Code 5340
J. K. Hsiao, Associate investigator, Consultant
V. C. Cavaleri, Electronics technician
P. A. Minthorn, Engineering aide
W. F. Gabriel, Electronics engineer; Head, Antenna systems group
R. M. Brown, Electronics engineer
B. Wright, Electronics technician

## APPENDIX A

### Interagency Agreement Work Statement and Modifications Thereto

The original work statement contained in the Interagency Agreement of May 1975 is as follows:

III. STATEMENT OF WORK

NRL shall provide all the required personnel, facilities equipment, materials and services necessary to perform the effort herewith set forth:

A. This development effort shall include assessments of antenna designs and performance, consideration of alternative design techniques, and trade-off analyses.

1. Microwave Optics. Focusing systems for microwave optical scanners shall be investigated. Both wide- and narrow-angle scan sectors shall be considered, as well as linear and circular apertures. An extensive investigation shall be made of scanning microwave optical systems, and their applicability to the MLS shall be assessed. Where necessary, as in the case of the torus, for example, a ray tracking computer program shall be generated to assess pattern performance. An attempt shall be made to establish the general limitations of circularly symmetric collimators, with a view toward relating the number of degrees of freedom available in the structure to the wavefront tolerance, and thereby the limiting aperture size.

2. Feed Commutation. The Technology of beam scan by commutating a feed array shall be reviewed. Relationships among beam shape continuity and linearity of scan, feed radiator density, feed array length and mutual coupling effects shall be examined. The possibility of aberration correction by commutation power division shall be investigated. Methods of minimizing insertion losses shall be sought.

3. Monitoring and Redundancy. Internal monitoring systems shall be studied for all scanning techniques of interest. Monitoring systems shall be assessed in terms of accuracy, complexity, and reliability. The details of location of monitoring components shall be worked out for the different types of antenna configurations. Redundancy shall be studied from the standpoints of failure modes of commutated feed systems

and required parallel stand-by components. The effect of redundant design on cost and performance shall be analyzed.

4. Beam Shaping. The effect of the requirement for elevation beam shaping on the design of the azimuth antenna shall be analyzed. A ray-tracing computer program shall be used to compute patterns for circular arrays of column radiators, for a linear aperture feeding a cylindrical shaped-beam reflector, and for a toroidal aperture (see III.A.1.).

5. Phased-Array/Microwave Optics Trade-off Studies. This trade-off analysis shall evaluate a number of commutating techniques and phased-array designs according to several criteria, such as size, initial cost, operating cost, logistics, reliability, monitorability, and maintainability.

6. Alternate Antenna Proposal for ICAO. NRL shall prepare an alternate antenna proposal to be included in the U.S. MLS submission to ICAO. This proposal shall specify prime alternate antenna designs appropriate for TRSB MLS; a preferred alternate design approach shall be identified taking into account the results of other antenna design activity in the MLS Program. This choice shall be well supported by available analyses, simulations, bench tests and in-depth considerations of monitoring, redundancy requirements, cost factors and possible failure modes. In sum, this effort shall yield a well thought out proposal to ICAO of desirable alternate TRSB antenna designs.

7. Design Review Activities. NRL shall participate in Design Review activities as appropriate. These reviews will be held with the two prime industrial teams at 3-6 week intervals throughout the MLS phase III. The FAA anticipates NRL attendance at those Design Reviews where antenna configurations are a primary topic. This activity shall include comment and critique of these configurations.

In September 1975 the following paragraph was added to the Work Statement by means of Modification No. 1:

8. Analysis of New Antenna Concepts. NRL shall evaluate new antenna designs showing promise for cost savings in phased arrays.

The purpose of this modification was to provide for NRL's activity in phased array studies and in supporting outside contracts for promising phased array techniques.

In February 1977 with Modification No. 5, the Work Statement was further modified as follows:

1. Paragraph A.2., after the last sentence add the following:

"Study beam steering algorithms and required logic hardware for phased arrays including fully filled, limited scan, such as the Cost Minimized Phased Array Circuit Technique (COMPACT), and thinned configurations."

2. Paragraph A.3., after the last sentence add the following:

"Conduct studies of rf monitoring techniques for phased arrays. Address system requirements, analyze and simulate proposed techniques, and fabricate breadboard systems as required. Establish appropriate rf component tolerances to match the operation of the monitor to the required operating performance of the Time Reference Scanning Beam (TRSB) antenna."

3. Paragraph A.8., as contained in Modification 1, after the last sentence add the following:

"Antennas acquired shall be tested to compare the performance with the low cost design goals. Review the current state-of-the-art in phase shifter technology."

In October 1977 with Modification No. 7 the Work Statement was further modified as follows:

1. Paragraph A2 as amended by Modification No. 5, after the last sentence add the following:

"Digital simulation of phased array antenna configurations will be utilized to investigate current MLS designs. NRL will provide comment and critique to FAA with respect to system design considerations."

2. Add the following Paragraph A9.

"NRL shall test components such as slotted wave guide radiators, phase shifters, and shall perform microwave network analysis. Data shall be taken for inclusion in a report."

In March 1979 with Modification No. 10 the Work Statement was further modified as follows:

Article IV. Deliverable Items, add the following paragraphs

K. Draft Summary Report - (FY-79)

Submit three copies of the draft report documenting the results of the work accomplished during the period October 1, 1978 through September 30, 1979, on Items III A 3 and 3. Prepare in NRL format.

L. Final Summary Report - (FY-79)

Submit one reproducible copy of the report generated under the Task in Item III A 2 and 3.

Article V. Completion of Work & Delivery, Paragraph I, Draft of Network Analysis Report, as amended in Modification No. 7

"Delete July 31, 1978, and in lieu therefor insert March 31, 1979"

Paragraph J. Network Analysis Report, as amended in Modification No. 7

"Delete September 30, 1978 and in lieu thereof insert May 31, 1979."

Add the following paragraphs:

"K. Draft Summary Report (FY-79)

Submit not later than October 30, 1979. The FAA will require thirty (30) days to review, approve, disapprove, or request changes to this report."

"L. Final Summary Report (FY-79)

Submit not later than December 31, 1979."

## APPENDIX B

### A Brief Description of the Microwave Landing System

History - The first commercial ILS was demonstrated in 1939. The use of ILS expanded rapidly, and it was adopted by ICAO as the international standard in 1949. Efforts to develop a second-generation landing guidance system were initiated in the late 1950's. As a result of a request by ATA to the FAA in 1967, special committee 117 (SC-117) of the Radio Technical Commission for Aeronautics was formed in December 1967 to develop a precision guidance system concept for approach and landing. The U.S. Government formed an interagency planning group to establish a coordinated national plan for the development of the Microwave Landing System. The resulting plan provided for FAA leadership in developing an MLS suitable for submission to ICAO as an international standard.

In 1973 FAA funded the development of doppler and scanning beam systems. In December 1974 Time Reference Scanning Beam was selected as the United States candidate MLS. TRSB MLS was submitted to ICAO by the FAA in December 1975. The All Weather Operations Panel (AWOP) of ICAO voted in favor of TRSB MLS in March 1977, and ICAO ratified the AWOP decision at its world wide meeting in April 1978.

Thus, NRL has been participating in the MLS program under this Interagency Agreement since shortly after the TRSB selection was made. Some further details of MLS programs both in the U.S. and elsewhere during the time period from about 1973 to the present are germane to this discussion.

The FAA funding of the development of both doppler and scanning beam systems was referred to as Phase II of the MLS program. The doppler systems were designed by ITT Gilfillan and Hazeltine. The scanning beam systems were designed by Texas Instruments and Bendix. The scanning beam systems utilized frequency reference (FRSB), and TI used mechanically scanning antennas, while Bendix used electronically scanned phased arrays. These systems were installed and tested at NAFEC and Wallops Island.

Meanwhile, MLS development was being actively pursued by other governments. Australia was developing an electronic scan TRSB system referred to as INTERSCAN. The U.K. has pioneered doppler MLS (DMLS) and was developing that system. France, West Germany, and Russia were

developing systems, but with somewhat less intensity. West Germany evenutally proposed their DMR-based landing system (DLS) to ICAO.

This then was the situation in the fall of 1974 when the FAA entered its selection process, which included representatives from other agencies of the Government, such as NASA and DoD, from other governments such as Australia, U.K., France, and West Germany, and from other organizations such as ATA and ALPA.

It was realized during the selection process that TRSB is superior to FRSB from the standpoint of spectrum occupancy, although TRSB precludes the use of mechanically scanned antennas. The option of mechanical scan was dropped, and FRSB was replaced by TRSB as the scanning beam candidate. Finally, TRSB was selected over doppler.

Subsequent to the selection process the FAA contracted with Bendix and TI in 1975 for Phase III systems, which involved electronically scanned microwave optical antennas and which were derived from the Australian INTERSCAN system.

Finally, as the cost of microwave electronic phase shifters designed specifically for the MLS application fell dramatically, the FAA placed increasing emphasis on phased arrays, especially for the most capable systems, beginning in 1976.

The selection of TRSB by the U.S. was viewed with alarm and consternation by the U.K. There had apparently been a basic misunderstanding relative to the FAA selection process: The U.S. assumed that the U.K. would align its position to the candidate selected by the FAA, and the U.K. assumed that the U.S. would select the doppler system. Neither the U.S. nor the U.K. apparently considered the alternative outcomes, and the result of this shortsightedness was a bitterly fought contest for adoption by ICAO, which was waged through the four Working Group A meetings of 1976, through the AWOP meeting of March 1977 (at which the vote was in favor of TRSB), and continued unabated into the world wide ICAO meeting which was held in April 1978. At that meeting the U.S./Australian TRSB/MLS was the winner.

Technical - A technical description of MLS is best introduced by stating the general requirements of the system. The highest category of service to be provided by MLS is IIIC, as defined by ICAO. This will provide guidance information to the aircraft of sufficient precision to allow automatic landing. MLS provides azimuth angle information over a region $\pm$60 deg. relative to runway center line with vertical coverage to +20 deg. Elevation angle information is provided from 0 to 20 deg. Back azimuth or missed approach information is provided over a region $\pm$40 deg. relative to runway center line. Flare elevation information is provided from -2 to +8 deg. Data is also provided to identify function, airport, runway, nominal glide slope, minimum glide slope, and the like.

The U.S. and the Australian TRSB and the U.K. DMLS are closely related in several respects. The operating frequency is C-band, 5030 to 5090 MHz. Transmitters are on the ground, and receivers are in the aircraft; angle information is derived in the airborne receiver and displayed to the pilot.

The basic difference between the doppler and TRSB systems is that the doppler MLS codes the antenna in time and codes the coverage region in frequency, while TRSB codes the antenna in frequency and codes the coverage region in time. One is essentially the Fourier transform of the other, or in other words one is the dual of the other in terms of time and frequency. DMLS measures frequency in its airborne receiver, and TRSB measures time. For the same antenna apertures, both systems will have basically the same capability.

Therefore, the differences between the doppler and scanning beam techniques are found in the second-order design characteristics, such as the requirement for doppler to use two transmitters, one as a reference, or differences in data rates and signal formats.

To elaborate slightly on the operation of the scanning beam system, the most capable version will use four scanning antennas, each of which generates a fan beam. The azimuth and back azimuth antennas will produce vertical fans which scan to and fro in azimuth to provide azimuth information to an airborne receiver. The elevation and flare antennas will have horizontal fan beams which scan to and fro in elevation to provide elevation information to an airborne receiver. Suggested beamwidths for the fan beams are one degree for azimuth and elevation, three degrees for back azimuth, and one-half degree for flare. The resultant aperture sizes are roughly 3.6 m (12 feet), 1.2 m (4 feet), and 7.3 m (24 feet), respectively. The azimuth antenna is located on center line at the far end of the runway, and the back azimuth is located at the side of the runway opposite the desired touchdown region. The flare antenna is located at the side of the runway some distance beyond the touchdown region.

Angle information is time division multiplexed (TDM), and the transmitted rf signal is switched sequentially among the various antennas. For each scanning antenna, the beam is scanned in one direction and then the other. The time difference between the arrivals of the beam maxima of the to and fro scans is measured in the airborne receiver and is directly related to the angular position of the aircraft. Each scanning beam transmission is identified by a preceding data transmission.

Low cost has been one of the primary objectives of MLS antennas, because the system will be in widespread commercial use and it is planned that one version will be applicable to small community airports.

High precision is of course a dominant requirement. Scanning antenna accuracy of the order of 1/50 beamwidth is required to provide the specified overall system precision.

Because the system is involved with the most critical portion of the approach and landing procedure, it must not introduce any hazard. Thus, reliability, monitorability, maintainability, redundancy, and failure tolerance are all subjects of crucial importance to the program.

Finally, the concept of maintainability is important in two respects. First, the system must be easily and quickly maintainable so that it has a minimum of down time. Second, it must be easily maintainable by relatively unskilled personnel because it will be deployed world wide, and there must be no possibility of system malfunction because of improper maintenance.

## APPENDIX C

## Contractor Research Supported by NRL

This appendix contains qualitative descriptions of the concepts proposed by ITT Gilfillan and Hazeltine and supported by NRL contracts. Both of the techniques are novel, and the emphasis in this appendix is on a clear presentation of the basic concept.

### 1. E-PLANE VARIPHASE EXCITER

A diagram of an E-plane variphase exciter is shown in Figure C-1. The device employs deep slots in the narrow wall of a waveguide that intercept the longitudinal currents in the main series guide. When the diode pair in a slot is symmetrically biased in the forward or reverse state, the net coupling to the radiating element is zero. This is so because a slot intercepts equal and opposite rf currents on the top and bottom walls of the main guide, which results in a net coupling of zero to the $TE_{10}$ mode of the output guide. If now one diode of the pair is reverse biased, and the other diode is forward biased, a net imbalance in the currents results that will couple to the output guide with a reference phase of zero degrees. If now the diode biases are reversed, an imbalance of the currents in the opposite direction will result in the same magnitude of coupled signal but with the opposite polarity. The plus or minus quadrature signal can be excited as above with a second slot spaced one-quarter guide wavelength from the first slot, as illustrated.

Figure C-2 illustrates the eight possible quantized states for the variphase exciter. Four phase states are realized by $\pm I$ and $\pm Q$. An additional four phase states are realized with the combined states of the device. A total of eight phase states are therefore achievable with only four diodes. However, the coupling in the diagonal states is nominally 3 dB stronger than in the cardinal state.

The absolute value of coupling to the output element is controlled by the slot depth. Therefore, only one design of switching network comprising the printed-circuit exciter is required for a wide range of antenna designs.

Table C-I is a summary of the projected performance of a linear array utilizing the variphase exciter. The array has 110 elements and a nominal beamwidth of one degree. The phase-randomization function is quadratic with an edge phase value of 360 degrees, or one wavelength of curvature. The overall beam position accuracy and sidelobe performance are similar to a conventional array with three-bit phase shifters.

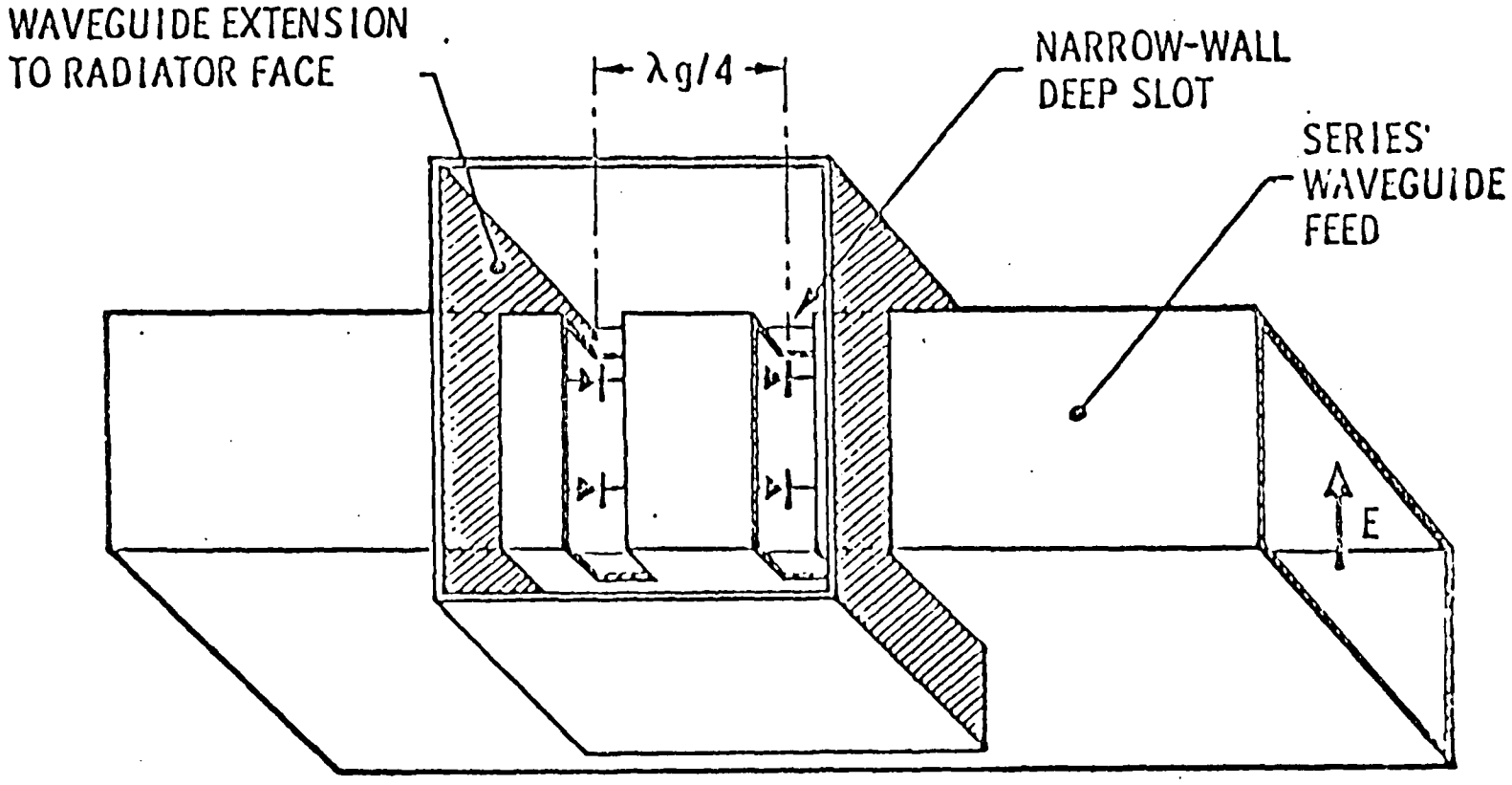


Fig. C-1 — Variphase exciter (narrow wall edge slots).

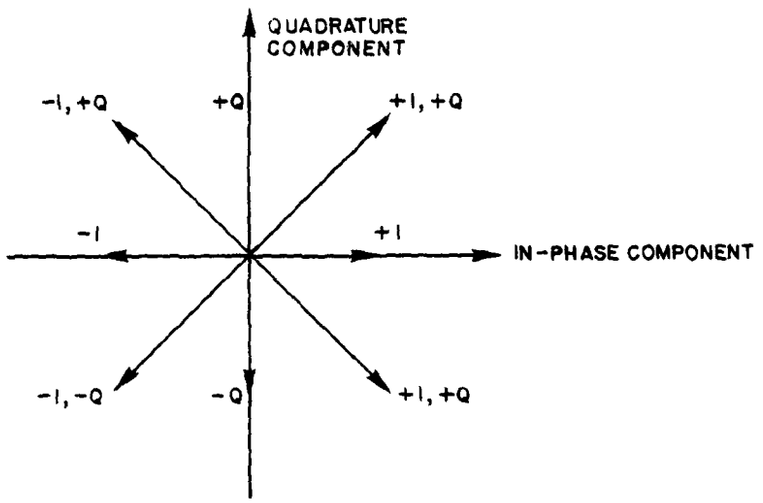


Fig. C-2 — Quantized states of variphase exciter.

Table C-I

Projected performance of a 110-element linear array

| Nominal Scan Angle (Degrees) | Beam Position Error (Degrees) | Peak Sidelobe Level (dB) | RMS Sidelobe Level (dB) |
|---|---|---|---|
| 0 | 0.00 | -23 | -31 |
| 1 | .01 | -22 | -31 |
| 2 | .00 | -23 | -31 |
| 3 | -.01 | -22 | -31 |
| 4 | .-1 | -24 | -31 |
| 5 | -.01 | -21 | -30 |
| 6 | .00 | -22 | -31 |
| 7 | .00 | -24 | -31 |
| 8 | -.01 | -21 | -31 |
| 9 | -.01 | -23 | -32 |
| 10 | -.01 | -23 | -31 |
| 15 | .01 | -24 | -31 |
| 20 | .00 | -24 | -31 |
| 25 | .00 | -22 | -31 |
| 30 | -.02 | -21 | -30 |
| 35 | .01 | -22 | -30 |
| 40 | .03 | -22 | -30 |
| 45 | -.01 | -21 | -30 |

## 2. THE COMPACT ANTENNA

Figure C-3 shows that the ideal COMPACT element pattern is obtained by an element that produces an aperture excitation that is in the form of sin x/x. The width of the "main-lobe" of the distribution in wavelengths and the sharpness of the pattern cut-off is proportional to the antenna aperture size, typically on the order of a few degrees wide.

Figure C-4 shows a block diagram of a typical COMPACT antenna. It consists of a power divider network, one phase shifter per effective element, a coupling network and individual radiators. The power divider network is used to excite the element terminals with a tapered distribution that yields an acceptable sidelobe level for the scanning beam pattern. The phase shifters shown at the element terminals are exercised to scan the narrow beam. Inserted between the element terminals and the radiators in the aperture is a coupling network. This network is a key component whose function is to provide the sin x/x element terminals. The network must provide translational symmetry; that is, each element terminal excites the same sin x/x distribution in the aperture only translated in the aperture by the separation of the element terminals.

Before describing the actual COMPACT coupling network, the basic method of generating sin x/x with translational symmetry is shown in Figure C-5. The network synthesis starts with a horizontal coupling line and vertical element lines connected to it by identical directional couplers. A portion of a signal input at one of the element lines is directly transmitted to the output of that element line and the remaining portion then excites all element lines to the right of the input by means of the directional couplers. This repeated coupling process results in an amplitude distribution which monotonically decreases to the right of the element terminal input. The phasing along the coupling line between directional couplers is $\pi$ radians (180° of phase shift). This value of phase is chosen to produce the correct in-phase polarity of the output distribution mainlobe and the alternating-phase polarity of the sidelobes, as in the sin x/x function. As shown in the figure, the inherent property of a directional coupler is that the coupled output is in quadrature (j) (90° of phase shift) with the directly transmitted output. By tracking the signal input through this basic network, it can be seen that the proper polarities are achieved. This network, however, generates only one half of the desired aperture excitation, and the sampling points of sin x/x are rather widely spaced. To generate the complete sin x/x function and with more sample points, two identical coupling lines are interleaved and combined at the bottom of the network to form the element terminal. The directional couplers in the top coupling line excite one side of the aperture. The directional couplers in the bottom coupling line excite the opposite side of the aperture. The couplers are identical in both coupling lines only oriented in opposite directions. By tracking signals through this network, it can be seen that an element terminal excites a sin x/x type distribution in

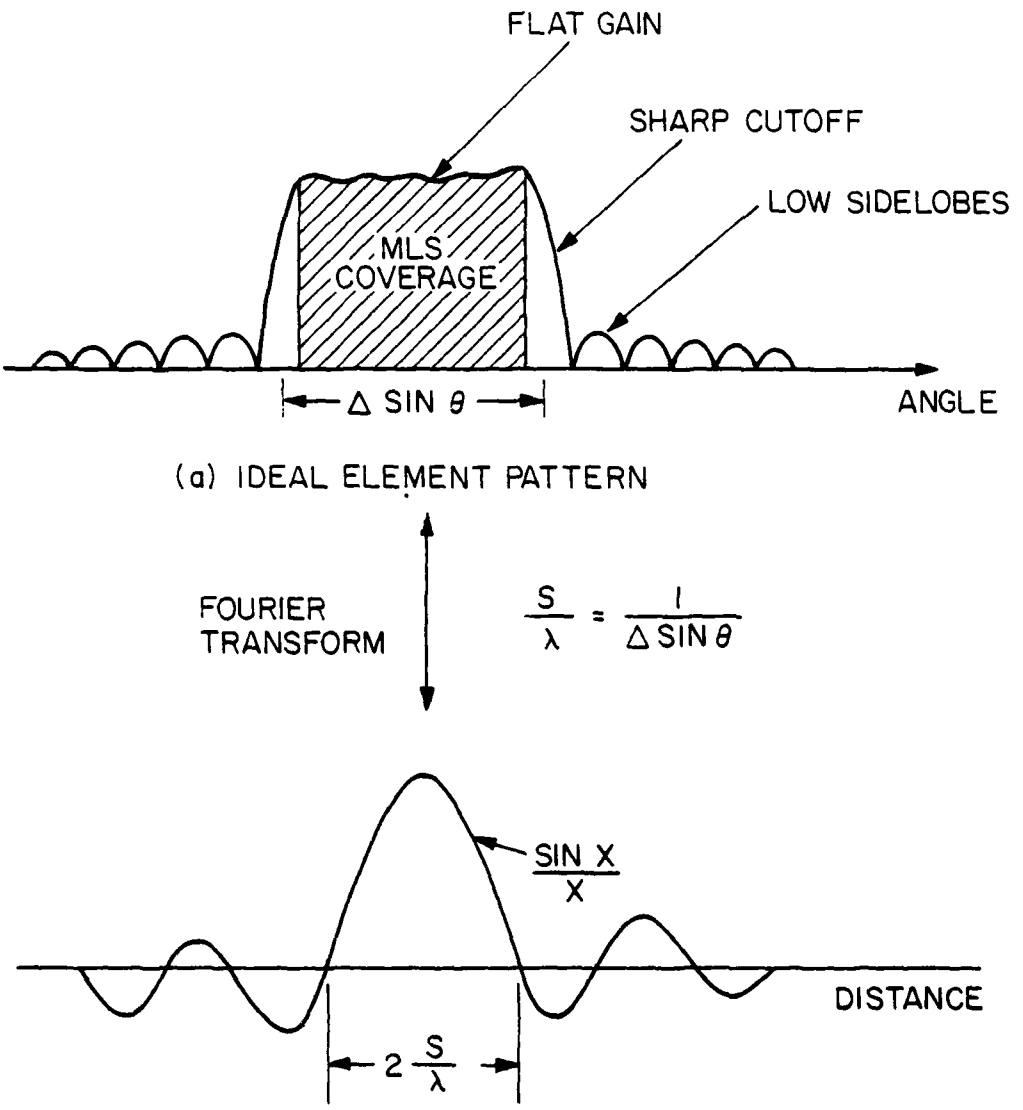


Fig. C-3 — Ideal COMPACT element pattern and aperture excitation.

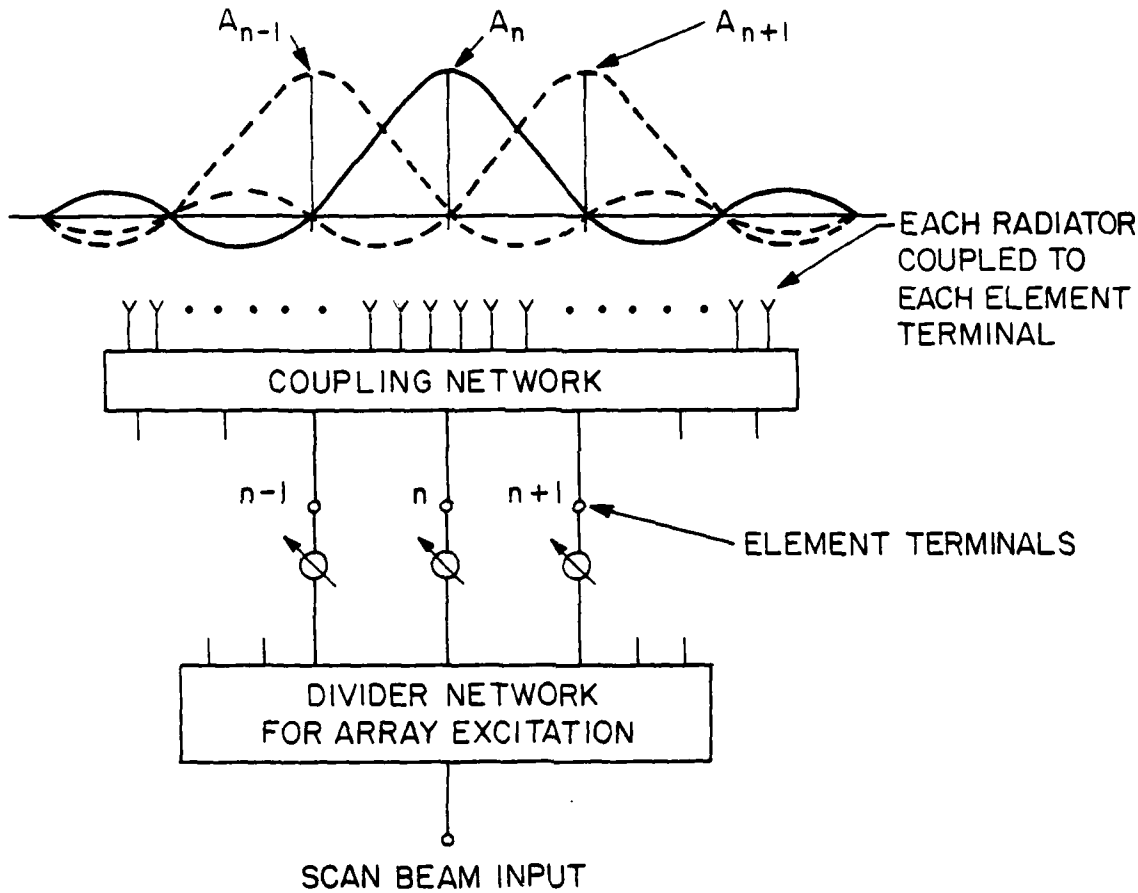


Fig. C-4 — Block diagram of a COMPACT antenna.

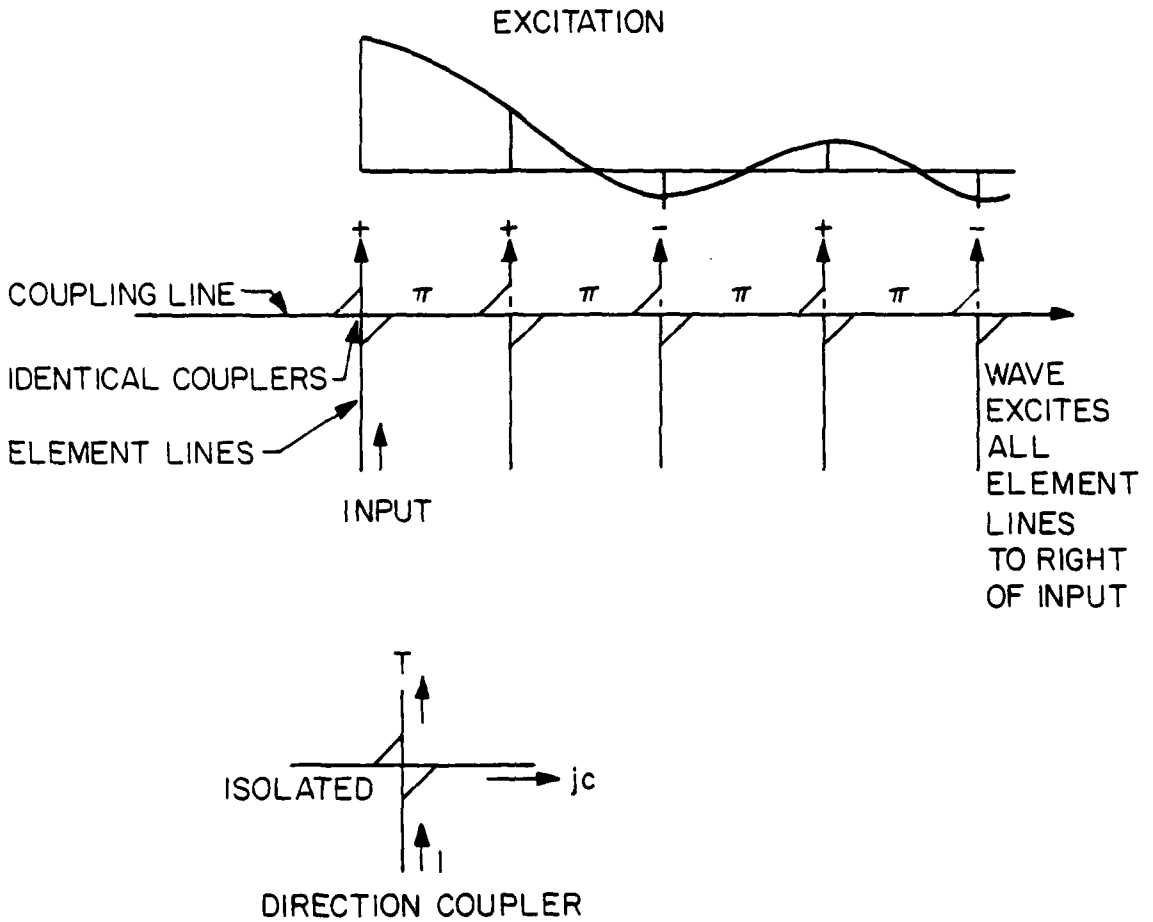





Fig. C-5 — Principle of COMPACT coupling network.

the aperture with four samples within the main lobe, one sample at each of the zeros, and one sample at the peak of each sidelobe. This network is representative of the coupling network required in COMPACT.

The network of Figure C-6 has the required translational symmetry to form an array antenna. Each element terminal excites the same aperture distribution only displaced by the element spacing because the network is identical as seen from each element terminal.

The implementation for coupling networks is shown in Figure C-7. The network previously described is used with a slight modification. This modification is the location of resistive components between each directional coupler along the coupling lines. Each attenuator is identical, as are the couplers, and its main purpose is to provide one additional degree of control of the element aperture excitation. This results in a closer approximation to the desired sin x/x and closer realization of the ideal element radiation pattern. The value of coupling and resistive components are both approximately -3 dB with a network loss of about -2 dB.

- INTERLEAVE TWO OPPOSITE COUPLING LINES
- COMBINE ELEMENT LINES IN PAIRS TO FORM TERMINAL

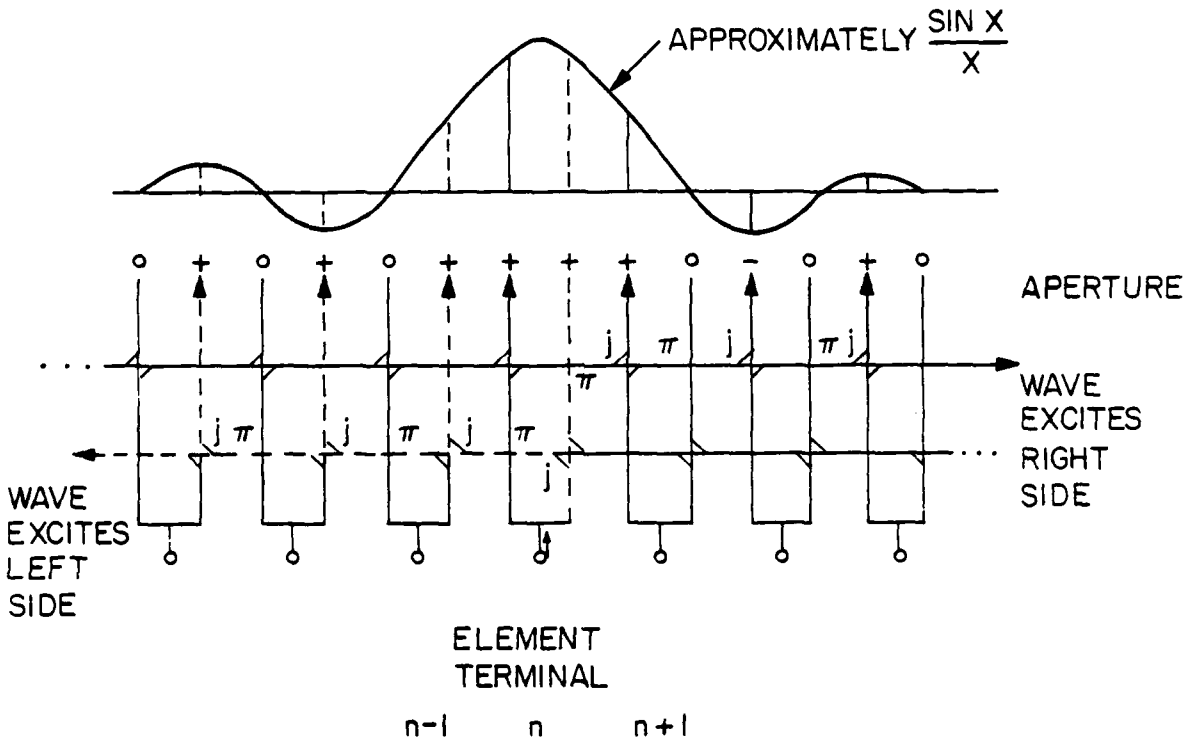


Fig. C-6 — Typical COMPACT coupling network.

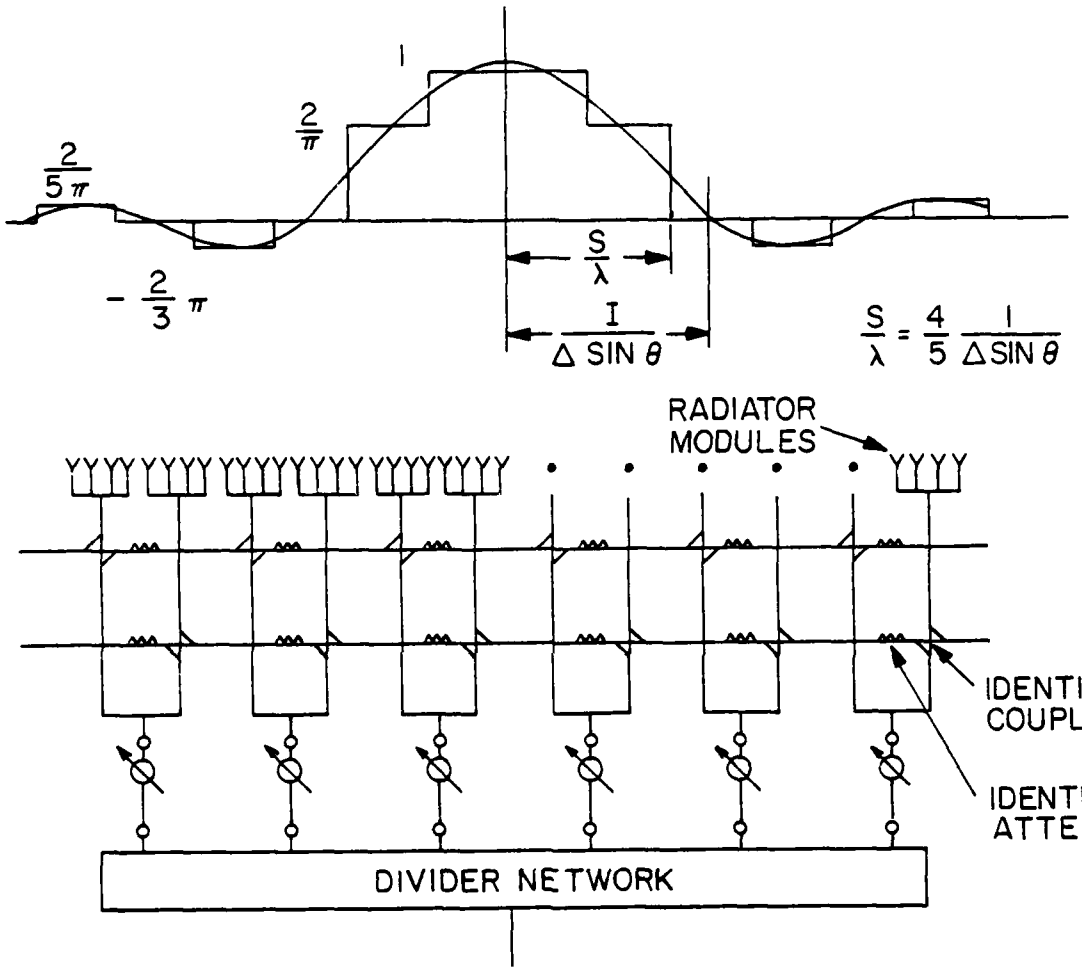


$$\Delta \text{SIN}\,\theta = \text{SIN}\,\theta_{max} - \text{SIN}\,\theta_{min} + \left(\frac{2\lambda}{D}\right)^{*}$$

* MARGIN FOR FINITE ANTENNA BEAMWIDTH AND ELEMENT PATTERN CUTOFF WHEN BEAM SCANNED TO $\theta_{max}$ AND $\theta_{min}$

Fig. C-7 — Implementation of the COMPACT coupling network.

## APPENDIX D

### Chronology of Events and Milestones of NRL Participation in MLS under Interagency Agreement

| Date | Description |
|---|---|
| **1975** | |
| May | Initiation of interagency agreement. |
| June | COMPACT proprietary proposal by Hazeltine. |
| | Meetings with Australians and French in Paris and Sydney. |
| July | Proprietary proposal by ITT Gilfillan. |
| August | DRB meeting at Bendix, Towson, MD. |
| September | DRB meetings at TI, Dallas and Bendix, Ft. Lauderdale. |
| October | Preparation of contributions to U.S. ICAO submission. |
| November | Visit by Russian delegation to U.S. |
| | DRB meeting at Bendix, Towson, MD. |
| December | Meeting with Australians in Sydney. |
| | Contract award to ITT Gilfillan. |
| **1976** | |
| February | Contract award to Hazeltine. |
| | (WGA meeting in Germany - no NRL participation.) |
| March | DRB meeting at Bendix, Towson, MD. |
| April | Completion of thinned array analysis. |
| May | Phased array background paper completed. |
| | ITT Gilfillan contract complete. |
| | WGA meeting in Washington. |
| June | Thinned-array test program at NAFEC. |
| July | (WGA meeting at The Hague - no NRL participation.) |
| | Hazeltine contract complete. |
| August | Phased array monitoring simulation begun. |
| September | Dispute over delivery of Hazeltine COMPACT antenna. |
| November | WGA meeting in London. |
| **1977** | |
| January | Review of NASA Basic Wide proposals. |
| March | AWOP meeting in Montreal. |
| April | Contract award to Hazeltine for testing of COMPACT antenna at NAFEC. |
| | Performance simulation begun. |
| June | Proposal of Hadamard monitoring algorithm. |

1977

| | |
|---|---|
| June | Completion of phased array monitoring report. |
| October | Phase shifter measurements begun. |

1978

| | |
|---|---|
| May | Proposal of 3D bootlace lens techniques. |
| July | Proposal of optimum beam steering technique. |
| September | Visit to DOT and CSIRO in Australia. |
| November | Presentation of 360-deg antenna design study to visiting Russian delegation. |

1979

| | |
|---|---|
| May | Visit to Russia. |
| July | Contract award to Myers Associates. |

# APPENDIX E
# PERFORMANCE SIMULATION OF MLS PHASED ARRAYS

## 1. INTRODUCTION

The Federal Aviation Administration's (FAA) Microwave Landing System (MLS) uses a Time Reference Scanning Beam (TRSB) system. This TRSB system is an air-derived data system which operates at C-band (5030-5090 MHz) to provide precision landing guidance information on an aircraft's azimuth and elevation positions. The angular position of the aircraft is determined by receiving separate azimuth and elevation fan beams generated from two linear phased arrays (in the cases treated here) which scan "TO" and "FRO" across the coverage sector in both azimuth and elevation directions. The airborne subsystem measures the elapsed time between a given "TO" and "FRO" scan. This time difference is directly proportional to the aircraft's angular position (see Fig. E-1). In order to determine the aircraft's precise angular location, it is of utmost importance to measure accurately the time the main beam passes the aircraft. The stringent MLS operational requirements set this position measurement at an accuracy of $\pm$.02 degree with a one degree beamwidth [1]. The accuracy of this measurement depends on both the antenna beam shape and the method used to detect the peak of the beam [2]. The dynamic antenna pattern is affected by both the multipath reflections and the array radiation pattern. The multipath effect in turn depends on the environment of the antenna site, the array design and the beam peak detection algorithm.

A computer simulation has been developed which represents the performance of the various phased array antenna systems which are being considered for use in the Microwave Landing System. The purpose of this simulation is to assess the angular accuracy of MLS in terms of its design parameters, tolerance effects, component and subsystem failures, multipath, and angle detection algorithm.

In this way it is hoped that a basis can be established for specifying parameter values and tolerances for the ground scanning antennas and for determining its failure modes and vulnerability. Important applications of this process are the phase and amplitude tolerances on the antenna array, which are in turn related to the specifications on the phase shifters and distribution networks.

Once the design parameters and tolerances and the failure modes are specified, another simulation which involves the fault location monitoring system can be used to determine whether an out-of-limits accuracy condition can be detected in a timely fashion.

In the following sections of this appendix, the simulation of the antenna array and its feed system is discussed. Then the computation of the radiation patterns is described. The measurement of angle by the airborne receiver is analyzed. The effects of receiver location and multipath are treated. Finally, the various simulation output formats are presented, and a flow diagram for the entire simulation is given with instructions for using it.

## 2. SIMULATIONS OF ARRAYS

This program simulates the performance of linear phased arrays used in the TRSB system. Two types of arrays are simulated. The first type is a conventional phased array in which each radiating element is equipped with a beam steering phase shifter. The second type is a COMPACT array. Several antenna radiating elements in this array may share a common phase shifter. The operational principles of this array are included in Appendix C. Array data such as element spacing, number of phase shifters, number of radiating elements per phase shifter and the phase shifter's number of bits are all variable inputs to the simulation program. The maximum number of radiating elements in this simulation program is limited to 120 while the number of phase shifter bits must be no more than 6.

It is assumed that both errors and failures exist in the array. In the following, simulations of errors and failures are described.

(a) Errors:

All components in the array, which includes the feed network, rf power source and phase shifters, contribute both amplitude and phase errors. In the simulation program, errors from all sources are lumped together and assigned to each phase shifter. The distribution of these errors is assumed to be Gaussian in view of the fact that they are contributed from many independent sources.

Amplitude and phase errors are assumed. Amplitude of radiating power from each phase shifter is assumed normally to be unity. Due to feed network variation and phase shifter attenuation, amplitude of rf power varies from element to element. This variation is assumed to be Gaussian centered at unity. The standard deviation, in percent, of this variation must be specified. As for phase error, two types are assumed. The first one is an insertion phase error which is assumed to be associated with each phase shifter, and the second one is a phase shifter error which is associated with each phase state of each phase shifter. The former varies from element to element while the latter varies from phase state to phase state of each phase shifter. Both of these errors are assumed to be Gaussian centered at a normal value. Standard deviations of these errors are inputs to the program. Besides these, a constant insertion phase can be added to each phase shifter across the array.

For a COMPACT array, additional phase and amplitude errors are assigned to the coupling network. Again these errors are assumed to be Gaussian centered at the normal value with a prescribed standard deviation. For amplitude error, its standard deviation is in percent while phase errors are stated in degrees. These standard deviations are input to the simulation program. A subprogram which generates Gaussian random numbers with zero mean and unit standard deviation is included in the simulation program. Outputs from this subprogram, multiplied by the appropriate standard deviation value are used as the simulated errors. At the beginning of each sample of simulation, the amplitude error and the insertion phase error associated with each phase shifter and the phase error of each phase state are generated and are stored in accordance with the location and phase state of each phase shifter. For a COMPACT array, errors of amplitude and phase in the coupling network are stored in accordance with the output port of the network. These recorded values are used for computation of the radiating energy level received by the MLS receiver.

(b) Failures:

The number of failures is an input parameter to the simulation program. These failures can occur on any phase shifter element and at any bit of that phase shifter element. Three modes of failures are assumed. The first one is an open circuit failure. This may be taken into account for any point along the feed network from rf source to the radiating element. A prescribed probability, an input to the simulation program, is assigned to this open-circuit failure. The second and third types of failures are failures of the phase shifter element itself.

The second type is a failure such that a phase shifter may stick to a certain phase state and fail to respond to the beam steering command. Probability of occurrence of this type of failure is assumed to be known. The third type is a failure of one of the phase shifter bits. This may be a stuck-to-zero or a stuck-to-one failure. The probability of any phase state in each phase shifter to develop an error of the second type is assumed to be equal. Similarly, all bits in a phase shifter have equal probability to develop either a stuck-to-zero or a stuck-to-one failure.

A subprogram which generates uniformly distributed random numbers is included in the simulation program. By use of the random numbers generated from this subprogram, locations and types of failures are determined. The procedure for performing such a task in the simulation program is as follows.

For each failure specified, a random number is drawn first. Since this random number has a uniform distribution from 0 to 1, multiplying this random number by the number of array elements and truncating the fraction portion can determine the location of a randomly failed element. By the same token, a second random number can be used to determine

the type of failure. The random number which has a range from 0 to 1 is divided into three regions. Each region represents a type of failure. For example, if we specify .1 for open circuit failure and .2 for stuck-phase-state failure, then random numbers lying between zero and .1 represents open circuit failure, .1 to .2 represents stuck-phase-state failure, and greater than .2 represents the case of bit failure. A third random number is then used to determine which bit or which phase state is failing.

Additional failures may occur in the coupling network of a COMPACT array. These failures are assumed to be open circuit. They may occur at any input port, output port or coupling line with equal probability. Locations of these failures can be determined by the uniform random number generator. The number of failures in the COMPACT array must also be specified.

Distributions of these errors and failures are generated at the beginning of each simulation sample. In order to achieve some statistical distribution of the effects of these errors and failures on the performances of the array, a number of simulation samples usually are performed. However, among all these samples, the number of failures, the probability of certain types of failures and the standard deviations of errors are maintained at a constant value. The number of simulation samples is an input variable, and is specified at the beginning of the program.

## 3. ARRAY PATTERN COMPUTATION

For each simulation sample, a number of receiver locations are allowed. At each receiver location, the direct phase path and the reflection phase path (if multipath is assumed) from each radiating element to the receiver are computed and stored. For most cases, except for the monitor output, the receiver is assumed to be located in the far zone region. Hence, the phase path is a function only of the receiver's location angle. This phase can be represented as

$$P(\theta,n) = \exp [j2\pi nd/\lambda \sin \theta],$$

where $\theta$ is the receiver position angle with respect to the normal to the plane of the array, n is the index of the array element and d is the element spacing. The reflection phase path depends on the nature of the reflection surface. This will be discussed in a later section. For the case of the monitor output, the monitor range is small, and its phase path is calculated based on the actual distance from monitor receiver to the array, which can be represented as

$$D_n^2 = (H_2 - H_1 + nd)^2 + R^2$$

$$P(\theta,n) = \exp [j2\pi D_n/\lambda],$$

where $H_2$ and R are the receiver height and range, respectively, and $H_1$ is the antenna height at the center of the array.

The array beam scans from one side of the receiver to the other. This constitutes a "TO" scan, and reversed scan constitutes a "FRO" scan. The scan algorithm or beam steering algorithm is predetermined and is generated in a subprogram that will be described in a later section. In order to reduce simulation computation, received signals are computed only in a small sector which is approximately equal to one beamwidth centered at the receiver's angle position. At each beam steering step, the required phase settings are first computed in accordance with the beam steering algorithm. The previously stored phase state settings, which include both amplitude and phase errors and failures, are then called and used to compute the field radiating from each element in the direction of the receiver. This radiating field is then translated through both the direct path and the reflection phase path from the element to the receiver. The total field reaching the receiver at this beam position is the sum of the field components from the radiating elements. This total radiated field at each beam steering step in both "TO" and "FRO" directions is stored for angle processing by the receiver.

A Taylor weighted illumination subprogram is included in the simulation program. One may specify the desired sidelobe level and the design parameter $\bar{n}$. The subprogram generates the required array illumination function.

For a COMPACT array, besides tapered illumination, the program also provides variations of the coupling coefficient and attenuation in the "COMPACT" coupling network, tilting of the element pattern to a desired angle and the effect of changing the operating frequency. Dummy elements can be added at each end of the array.

## 4. ANGLE RESOLUTION

The stored dynamic pattern data is first smoothed by a two-pole digital Butterworth filter. Details of the filter design are given in Appendix F. These smoothed data are then used for angle resolution.

There are several methods to determine the receiver location angle. The one used in this simulation program is that proposed by Bendix in which the two half power points of the scanning dynamic pattern are first located [3]. The center of the beam is taken as the average of these two points. In the actual system, the array beam scans continuously in the coverage sector from $-\theta_1$ to $+\theta_1$ (see Fig. E-1). The airborne receiver senses the radiated energy, smooths it, determines the 3-dB points and records the time of the middle point, as it passes the aircraft. The time difference between a "TO" and "FRO" scan is used to determine the aircraft's angle location. However, in a simulation, the amount of computation required to scan over the entire coverage

sector is excessive. Therefore, in the simulation program the dynamic pattern is simulated only in the main beam region. Since the beam scans in discrete steps, each beam position in the coverage section is indexed in the simulation program in accordance with the beam steering algorithm. It is further assumed that for both the "TO" and "FRO" scans, the beam starts precisely at the same beam positions. In the simulation program, all angle positions are referenced to the beam indices in order to achieve better accuracy and avoid computer truncation error. Two problems have to be addressed. The first is that due to multipath effects, the beam shape may be deformed and the main beam may be widened. Starting the beam at the half-beamwidth point of an ideal pattern may not include the actual 3-dB points. To overcome this difficulty, an adaptive algorithm is built into the simulation program. The dynamic pattern is first computed taking into account the effect of multipath, errors and failures. The 3-dB points are then searched. If no 3-dB point can be found at one side of the dynamic pattern, that side of the pattern is extended and recomputed. This extension will continue until either a 3-dB point is reached or the pattern level is not reducing any more. Another problem is the transient response of the digital filter. To avoid this problem the computed dynamic pattern must have enough lead time to avoid the transient region. This difficulty is avoided by first examining the delay of the impulse response of the digital filter. In the subsequent pattern computation, the range of the pattern is extended to cover this transient delay region. By use of both the "TO" and "FRO" patterns the effect of delay due to filtering is removed.

## 5. RECEIVER LOCATION

For each simulation sample, a number of different receiver locations may be simulated. However, in all these simulations, the phase shifter and feed network errors and the failures remain the same. The number of different receiver locations to be simulated is an input parameter. There are five ways to specify these receiver locations.

a. The receiver's locations are specified in height and range. These heights and ranges are read-in to the program. The antenna height at array center must also be specified. The location of the monitor receiver can be entered in this way.

b. Both receiver height and range are generated randomly with a uniform probability within a given range. Antenna height must be specified.

c. In most cases, the receiver is in the far field of the antenna, and only the angle position of the receiver is of interest. In these cases the receiver angle locations may be read in.

d. Given the angle ranges, the receiver angle locations may be generated in random with uniform probability within a specified angle range.

e. For pole tests, the receiver is located at a fixed range and the height of the receiver is increased by a fixed amount until a certain height is reached or a given number of pole test positions are evaluated. For this case, the antenna height must also be specified.

6. MULTIPATH EFFECT

The multipath effect is calculated for the elevation antenna on the assumption that the ground is flat. The ground reflection angle (see Fig. E-2a) is then

$$\psi = - \tan^{-1} \left( \frac{H_2 + H_1}{R} \right)$$

where $H_1$ and $H_2$ are the antenna height and receiver height, respectively, and R is the range. The phase of the reflected energy is

$$\theta_p = 4\pi H_1 H_2 / R\lambda + \phi$$

Where $\lambda$ is the wavelength and $\phi$ is the ground reflection phase which along with the ground reflection coefficient must be specified. For the case when receiver location is specified only by elevation angle, the ground reflection angle $\psi = -\theta$, where $\theta$ is elevation angle. The ground reflection phase is then chosen randomly in the range from 0 to $2\pi$.

7. BEAM STEERING ALGORITHM

Four beam steering algorithms are incorporated into the simulation program. However, any other steering algorithm can be adopted easily by changing a subprogram which is used to generate these steering algorithms. The four beam steering algorithms are described in the following:

a. Bendix algorithm - The algorithm was developed by Bendix for a conventional array. In this algorithm, the array phase settings are computed at larger coarse steps. However, from one coarse step to the next coarse step, the phase shifters are switched one pair at a time. Thus there are N/2 fine steps between each coarse step, where N is the total number of phase shifters (even) in the array. To assure uniform scan from one coarse step to the next, Bendix has developed a special sequence to achieve this goal. That sequence is used in this simulation program.

b. Random sequence - This is similar to that of the Bendix algorithm. However, the switching sequence between coarse steps is random and is generated in accordance with a random number sequence.

c. Hazeltine sequence - This sequence was developed by Hazeltine for use in their COMPACT array. In this sequence a single phase shifter at

a time is switched. The interval of switching time is 2/7 μsec. For an array scan rate of 20,000 degrees per second, this gives a scan step of approximately .0057 degree. The Hazeltine sequence steers the beam from -1° to 10 degrees.

d. Conventional step - In this straightforward procedure, for the required steering angle at any step, the necessary phase settings at that step are computed and switched accordingly.

8. SIMULATION OUTPUT

Several different kinds of simulations can be implemented with this program. These simulations and their outputs are described in the following paragraphs and an example of each is presented.

a. Angle error statistic - The main purpose of this implementation is to establish a statistical correlation between angle error and component tolerance (array errors) and the number of failures in the array. The output of this simulation is a plot of the cumulative probability of angle error, given the number of failures and the standard deviations of amplitude and phase errors. In the example of Fig. E-3, the probability distributions of angle errors for a conventional 96-element array are presented. The array elements are subject to a Gaussian amplitude and phase error with standard deviations of .05 for amplitude and 5 degrees for phase. Three curves are presented, one for zero failure, one for 6 failures and the third for a 12 failure case. For example, when the array has no failure, the probability that the angle error is less than .02 degrees is 95%, while for a 6 failure case, this becomes 91% and for 12 failures it drops to about 80%.

This statistic is generated by performing a number of simulation samples. For each sample, a number of receiver locations are chosen. In this case, these receiver locations are chosen at random with a coverage section of -60° to +60°. In this particular type of simulation the number of error/failure distributions is 30 while the number of receiver locations is 40. This gives a statistical sample of 1200. The curves of Fig. E-3 are generated by these samples.

b. Pole test - the pole test is used in the field to measure the system performance. In this test, a receiver is located at a given distance from the array antenna, and a series of measurements is made at given increments of height. The output of these simulations is shown in Fig. E-4a. This plot is for the case of a COMPACT array with 24 phase shifters. No failure is assigned to the array. Five percent and five degree standard deviations are assigned respectively to the amplitude and phase distributions of the array errors. The receiver is at a range of 280.4 meters (920 ft), starting at an initial height of .61 meter (2 ft) and increasing in .61 meter (2 ft) steps until it reaches 20.7 meters (68 ft). At each step 16 simulations are performed. For each simulation, the array failures and errors remain the same; however, each phase shifter is incremented by one phase state. This process

is known as phase cycling. Angle errors for each simulation at each receiver height are then computed. The mean, standard deviation, minimum and maximum of this angle error are then plotted for each receiver height. It can be seen that due to the multipath effect, angle errors are very large at lower receiver heights. Furthermore, because the element pattern of this array is tilted 12 degrees upwards, a bias angle error exists. In this example, the increment of the phase shifter is set at one bit (360/16 degrees for a 4 bit phase shifter). However, the program has provision to accommodate any odd increment of insertion phase.

Hazeltine developed a beam steering algorithm which can effectively compensate this bias error. One of the examples is shown in Fig. E-4b. In this figure, the pole test was performed in the elevation range from 2.25 to 3.75 degrees with 11 angle positions evenly distributed within this range. At each angle position, 10 samples are computed. Each sample has phase cycling similar to the case discussed above. Two sets of data are presented side by side at each angle position. The circles are the mean value of the 16 phase cycling results. At each angle position, there are 10 such samples. To the right of these samples are the mean, standard deviation, minimum, and maximum of these samples. The global mean is the average value of all the mean values at each angle position, while standard deviation is the mean value at each angle position deviated from this global mean. The bias angle errors are seen to be removed for this example.

c. Dynamic pattern - In order to examine closely the effects of multipath, beam steering algorithms and the digital filter, the scanning dynamic pattern is plotted. This pattern is the radiated energy received by the receiver at a fixed position. One of the examples is shown in Fig. E-5. This is a dynamic pattern of a receiver at the horizon for a conventional array. There are four curves on this plot. Two of the curves which are almost coincident are the dynamic pattern for both "TO" and "FRO" cases before filtering. The two curves with cross marks are the patterns after filtering. Delays due to filtering for "TO" and "FRO" cases are in opposite directions. One may see that at angles which are below the horizon (below receiver's height), the pattern shapes are strongly modified by the ground reflections. Furthermore, no 3-dB point exists at the lower angle side, even with the pattern extended further as shown in this figure.

d. Monitor output - The monitor output is a plot of the dynamic pattern for a monitor receiver situated at close range. Because the receiver is located at a closer range, the pattern is not computed on the assumption that the receiver is at infinity. Instead, the actual distance from each element to the receiver is computed and the actual phases of both the direct radiation and the reflection from the ground surface are used to compute the dynamic pattern. An example for a COMPACT array is shown in Fig. E-6. In this plot the mulipath effect is ignored.

e. Array or element pattern - Sometimes it is desirable to be able to examine the array pattern or the element pattern (for COMPACT array). This pattern may be used to examine the effects of failures and errors in the array. It also can be used to examine the effect of element pattern tilt, frequency shifting and other effects on the element pattern of a COMPACT array. For a COMPACT array one must specify the particular element in the array to be plotted and also the pattern tilt angle, frequency shifts, etc. One example is shown in Fig. E-7. This is a plot of the element pattern of a COMPACT array. The element is at the center of the array of 116 radiating elements and 24 phase shifters with 8 dummy radiating elements located at each end of the array. The element is tilted at a 12° angle. The operating frequency is at the center band.

f. Phase shifter switching histogram - For a given steering algorithm it is of interest to examine the number of phase shifters switched at each coarse step. This statistic may be useful in designing steering algorithms. The beam steering algorithm in this example is that proposed by Bendix. The coarse step is .2 degree. Fig. E-8 shows the number of phase shifters switched at each coarse step. It is interesting to note that about one third of the phase shifters are not switched during any given coarse step.

g. Digital filter response - A digital filter is used to smooth the dynamic pattern data before they are used for angle resolution. The response of this filter can be plotted as shown in Fig. E-9. Both frequency and impulse responses are shown in this figure.

## 9. FLOW DIAGRAM

A flow diagram of this simulation program is shown in Fig. E-10. The simulation program starts with a read-in of all pertinent simulation data. A list of such data is shown in Table E-1. If the simulation is to plot the smoothing filter response, it will jump to the subroutine for generating such filter, plot its responses and terminate the program. Otherwise, the program will first initiate the random number generator. Before computing the radiating scan pattern, the program generates the beam steering algorithm, sets up the receiver's angle positions, computes the phase and amplitude of the multiple path reflection wave, generates smoothing digital filter and computes the phase paths of array elements to each receiver position. The program has three layers of do-loops. The outer loop is the sample loop in which the failure modes and locations and the array errors are determined for each simulation sample. The second loop is the phase cycling loop in which a constant phase is added to each array element for phase cycling purposes. The third loop performs the computation of the dynamic array pattern at each receiver position. After that, the angle position will be determined and compared with the actual angle position. Results are then plotted. A pre-scan at each receiver angle position is performed to make sure that the computed dynamic pattern includes the 3-dB points and avoids the transient effect of the smoothing filter.

Table E-1 — Data Read-in Procedure for Simulation

```
C
C************FIRST DATA CARD, USE I5 FORMAT*******************************
C      NL, NUMBER OF PHASE SHIFTERS
C      NM, NUMBER OF RADIATING ELEMENTS PER PHASE SHIFTER
C      NM=1,    CONVENTIONAL ARRAY
C      NBIT, NUMBER OF PHASE SHIFTER BITS
C      NSAMP, NO. OF SIMULATION SAMPLES
C      NSAG, NUMBER OF DIFFERENT RECEIVER ANGLE POSITIONS
C      NF, NUMBER OF PLOTS OF   DIFFERENT NUMBER OF FAILURES,OR DIFFERENT
C         ELEMENT ERRORS
C      NF POSITIVE FOR DIFFERENT ELEMENT ERRORS
C      NF NEGATIVE FOR DIFFERENT NUMBER OF FAILURES
C      LTALR EQUAL 1 USE TAYLOR WEIGHT
C      LPKI, INITIAL PHASE STATE FOR POLE TEST
C         IF LPKI .GT. 2**NBIT, PLOT OUT EACH INSERTION PHASE STATE
C      JPRT PRINT ALL DATA AT JTH ANGLE POSTION AT THE FIRST SAMPLE FOR
C         DIAGNOSIS PURPOSE
C      LLCT=0,  NO LABEL
C      LREF=0      NO REFLECTION IS CONSIDERED
C      LPOLE=0 ,  NO POLE TEST
C      LPOLE GT 0,   PERFORM POLE TEST,NUMBER OF RUN IN EACH TEST EQUALS
C         TO LPOLE, SAME PHASE ADDED TO AND FRO SCAN
C      LPOLE LT 0,           DIFFERENT PHASE IS ADDED AT TO AND FRO SCAN
C      LPLT=0 SUPRRESS ALL PLOTS
C      LPLT=1,   PLOT ANGLE ERROR STATISTIC OR POLE TEST
C      LPLT=11,PLOT ANGLE ERROR STATISTIC WITH PHASE CYCLING,
C         NO. OF OF CYCLINGS EQUAL TO LEAP
C         LPLT=21, PLOT ONLY MEAN VALUE OF THE PHASE CYCLING
C      LPLT=31, DO POLE TEST FOR MANY SAMPLES AND PLT ONLY THE MEAN OF
C         PHASE CYCLING
C         LPLT=41, DO POLE TEST AT ONE SAMPLE AND PLOT PHASE CYCLING
C             RESULTS
C         LPLT=51, PLOT INDIVIDUAL SAMPLE FOR SPACIAL VARIATIONS
C         LPLT=61, DO BOTH LPLT=51, AND 41
C      LPLT=2,   PLOT DYNAMIC PATTERN
C      LPLT=3,   PLOT ARRAY PATTERN OR ELEMENT PATTERN
C      LPLT=4, PLOT PHASE SHIFTER SWITCHING HISTOGRAM
C      LPLT=5, PLOT OUTPUT OF MONITOR
C      LPLT=6, PLOT FILTER FREQUENCY AND IMPULSE RESPONSES
C      INIT, RANDOM NUMBER INITIALIZATION SEED
C         FIRST DIGIT OF INIT IS USED TO SET INITIAL RANDOM SEQUENCE
C         2ND DIGIT MULTIPLIED BY SAMPLE INDEX SETS THE SAMPLE SEQUENCE
C      LEAP=0,NO PATTERN PLOT,LEAP=1, PLOT ELEMENT PATTERN, LEAP=2, PLOT
C         THE FULL ARRAY PATTERN
C         WHEN LPLT=21,31,41,51,61, LEAP IS USED AS TH INDEX OF THE
C              REFERENCE TO COMPUTE RMS DEVIATION
C      LSEQ, BEAM STEERING SEQUENCE CONTROL
C         LSEQ=0, NO SEQUENCE
C         LSEQ=1, USE NAFEC SEQUENCE
C         LSEQ=2, USE RANDOM SEQUENCE
C         LSEQ=3, USE HAZETINE'S SEQUENCE
C
C************SECOND DATA CARD USE F10.6 FORMAT*****************************
C      FAC, COURSE INCREMENT (IN DEGREES)
C      CPA ARRAY TILTING ANGLE
C      REF REFLECTION COFFICIENT
C      DX,  RADIATING ELEMENT SPACING
C      RATIO SCAN PATTERN SEARCH CUT-OFF POINT,PER CENT OF MAX. POWER
C      OMEGA, FILTER CUT-OFF FREQUENCY
C      PTSR, PLOT SCALE RANGE
C      TAGLLT SCAN ANGLE LIMITATION BELOW HORIZON
```

Table E-1 — (continued)

```
C************THIRD DATA CARD USE F10.6 FORMAT, SKIP IT IF NOT COMPACT ARRAY
C      TLAG, COMPACT ARRAY ELEMENT PATTERN TILTING ANGLE
C      FRAT, PER CENT OF FREQUENCY DEVIATION FROM CENTER FREQUENCY
C      FA,  THE FACTOR THAT THREE DB COUPLER DEVIATES FROM UNIT WHEN
C         FREQUENCY IS CHANGED
C      ENL, THE ELEMENT THAT THE ELEMENT PATTERN TO BE PLOTTED
C      XR, YR COMPENSATION COEFF. FOR COMPACT ARRAY
C      ELVOD, NUMBER OF DUMMY ELEMENTS IN A COMPACT ARRAY
C
C************FOURTH DATA CARD USE F10.6 FORMAT**************************
C      H1, ANTENNA HEIGHT
C      H2 TARGET HEIGHT OR RANGE OF TARGET HEIGHTS
C      H3, FOR POLE TEST INCREMENT OF RECEIVER HEIGHT
C         FOR MONITOR , LIMIT OF LOWER ANGLE
C      OR RANGE OF TARGET DISTANCE
C      SCANR, BEAM SCAN RANGE(INCLUDING POSITIVE AND NEGATIVE ANGLES)
C         FOR MONITOR RECEIVER UPPER ANGLE LIMIT
C      HT, ARRAY TO STORE TARGET HEIGHTS
C      ORT, ARRAY TO STORE TARGET RANGE
C      FMC, OPERATING FREQUENCY IN MHZ
C      RLL=1, READ IN HEIGHT AND DISTANCE
C      RLL=2, RANDOM HEIGHT AND DISTANCE
C      RLL=3, READ-IN ANGLES
C         IF THE FIRST ANGLE READING IS GREAT THAN 1000, READS INCREMENT
C         OF ANGLES. THE SECOND NUMBER IS THE INITIAL ANGLE AND THE THIRD
C         NUMBER IS THE INCREMENT OF ANGLES IN DEGREES
C      RLL=4, RANDOM ANGLES
C      PTMPPS, POLE TEST MULTIPLE PATH PHASE
C
C************IF READ ANGLE OR HEIGHT AND RANGE, ENTER DATA CARDT HERE
C               USE F10.6 FORMAT
C
C      FOR CONVENTIONAL ARRAYS,IF ARRAY PATTERN IS PLOTTED, ENTER DATA FOR
C         FINE STEPS BEYOND THE POSITION ANGLE JUST READ IN, USE I5 FORMAT
C
C
C************FIFTH DATA CARD, USE I5 FORMAT*****************************
C      NFAL, NO. OF FAILURES IN THE ARRAY
C      NCFL, NO. OF FAILURES IN COMPACT NETWORK
C
C************SIXTH DATA CARD USE F10.6 FORMAT***************************
C      AER, ST. DEVIATION OF AMPLITUDE ERROR IN PER CENT,PHASE SHIFTER
C      PER, ST.DEVIATION OF ANGLE ERROR IN DEGREES, PHASE SHIFTER
C      PMEAN, ST. DEV. OF MEAN INSERTION PHASE
C      POPEN, PROBABILITY PF OPEN CIRCUIT ON PHASE SHIFTERS
C      PPSSTE, PROB OF A PHASE SHIFTER STUCK TO A CERTAIN PHASE STATE
C         THE PROB. OF EACH PHASE STATE IS UNIFORM
C      PINST FIXED INSERTION PHASE FOR PHASE CYCLING
C      PEBIT, ST.DEVIATION OF PHASE ERROR IN EACH PHASE SHIFTER BIT
C         IF PEBIT LT 1., THIS ERROR IS IN PER CENT OF THE PHASE SHIFTER
C           BIT
C         IF PEBIT GE TO 1. THIS ERROR IS IN DEGREES
C
C************SEVENTH DATA CARD USE F10.6 FORMAT**************************
C      NEEDED ONLY FOR COMPACT ARRAYS
C      CAER, ST. DEVIATION OF AMPLITUDE IN PER CENT, COUPLE NETWORK
C      CPER, ST. DEVIATION OF ANGLE ERROR IN DEGREES, COUPLE NETWORK
C
C************************************************************************
C      IF HAZETINE'S STERRING ALGORITHM IS USED ENTER THE SEQUENCE HERE
C         USE I2 FORMAT
C
```

If the program is required to compute the static array pattern or to plot the dynamic pattern or to generate the phase shifter switching histogram, the program will be terminated after the respective task is completed.

## 10. SUMMARY

In summary, this simulation program has the following outputs.

a. Statistical distribution of angle errors for target at random positions.

b. Statistical distribution of angle errors for fixed elevation and range or at a fixed azimuth angle (pole test).

c. Dynamic scan pattern at a fixed angle. Before and after filtering for both "TO" and "FRO" cases.

d. Output of a monitor which is located at a close-in range (phase errors are corrected).

e. Array element pattern and array pattern for both conventional arrays and COMPACT arrays.

The condition in which this simulation is performed is summarized as follows:

a. Type of array (conventional or COMPACT).

b. Number of elements.

c. Phase and amplitude error is assumed to have a normal distribution (input st. deviation).

d. Phase shifter truncation (input no. of phase shifter bits).

e. Multiple-path effect (input reflection coefficient and phase).

f. Band-pass filter to smooth data (input cut-off frequency of the filter).

g. Failures in phase shifter and in COMPACT network (input number of failures and type of failures).

h. Variation of beam scan algorithms. (Four algorithms are included: Bendix, Hazeltine No. 1, Hazeltine No. 2, Random.)

i. For pole test the angle error is averaged over a number of runs, each with a different constant insertion phase. (Input No. of runs and insertion phase.)

j. Compensation of bias error of COMPACT array due to tilting of element pattern.

k. Each plot is labeled with all the simulation conditions.

l. Scan limit.

11. REFERENCES:


1. "Guidance Accuracy Considerations for the Microwave Landing System," Robert J. Kelly, NAECON 76, Dayton, Ohio. 18 May 1976.

2. "Comparison Study of MLS Airborne Signal Processing Techniques," R. J. Kelly and E. F. C. Laberge, NAECON 78, Dayton, Ohio, 16-18 May 1978.

3. "MLS Basic Wide Configuration" Bendix Communication Division, Proposal No. 1601, Jan 4, 1977.

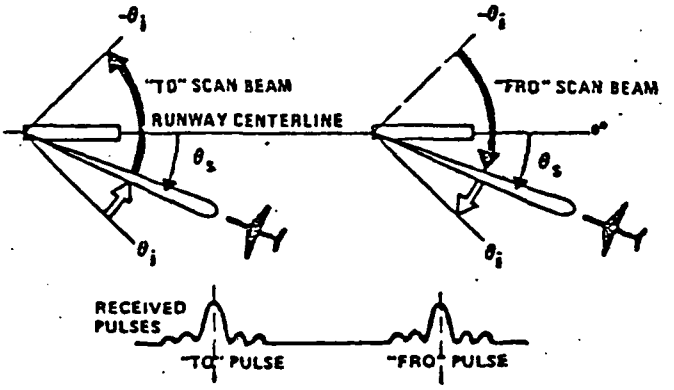


Fig. E-1 — Principle of TRSB angle measurement.

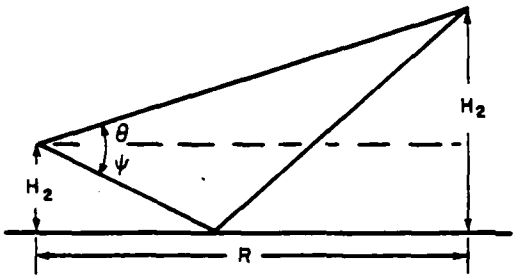


Fig. E-2(a) — Multipath reflection for close receiver.

Fig. E-2(b) — Multipath reflection for receiver at far zone field.

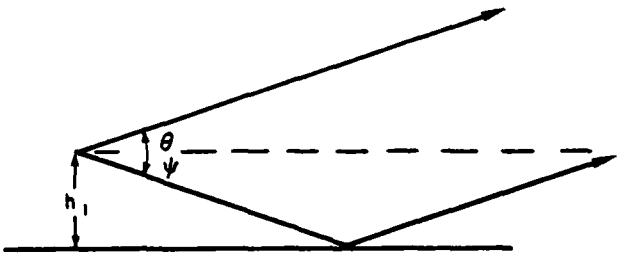

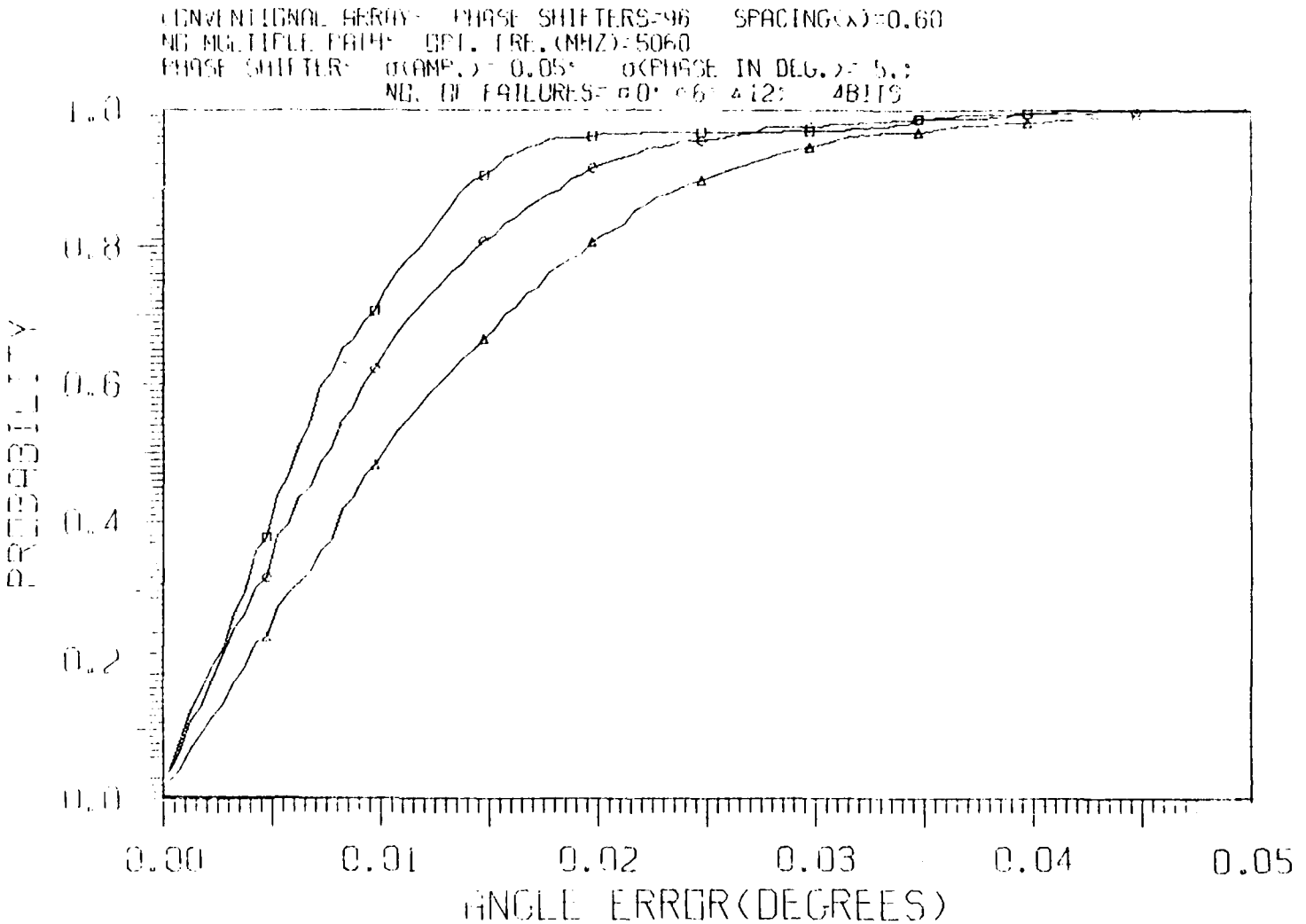


Fig. E-3 — Statistical distribution of angle errors.

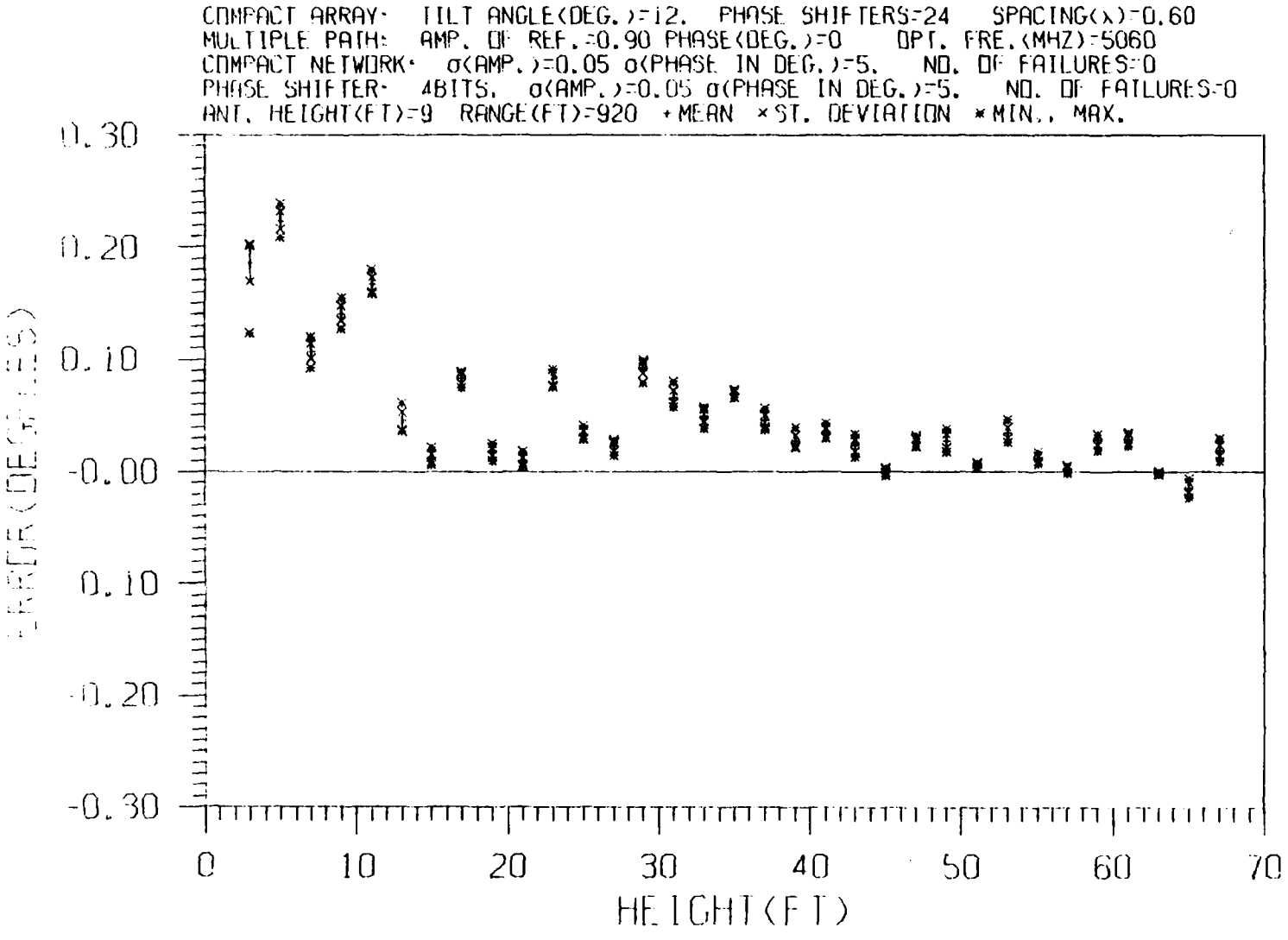


Fig. E-4(a) — Pole test results.

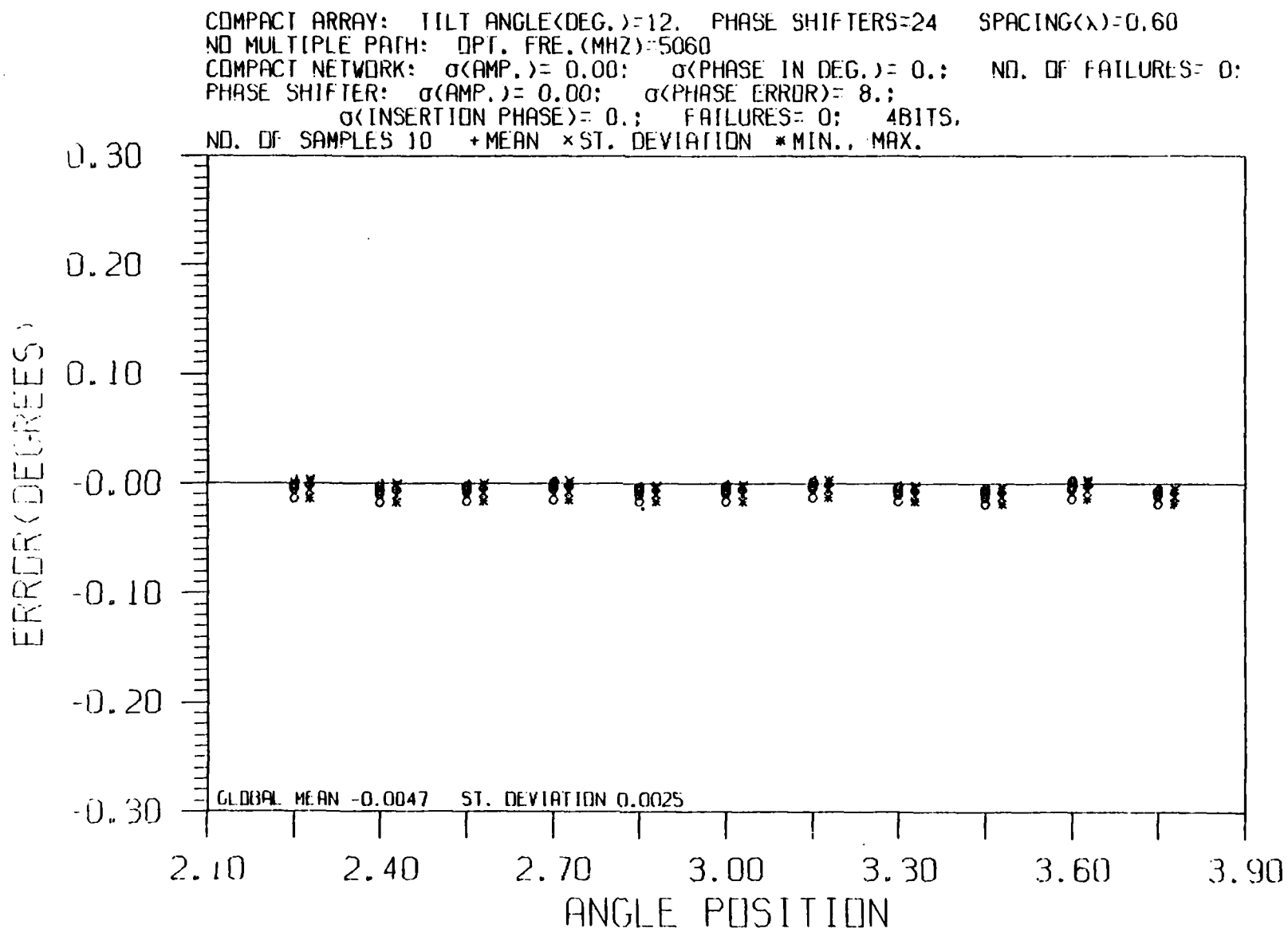


**Fig. E-4(b) — Pole test results — bias error compensated.**

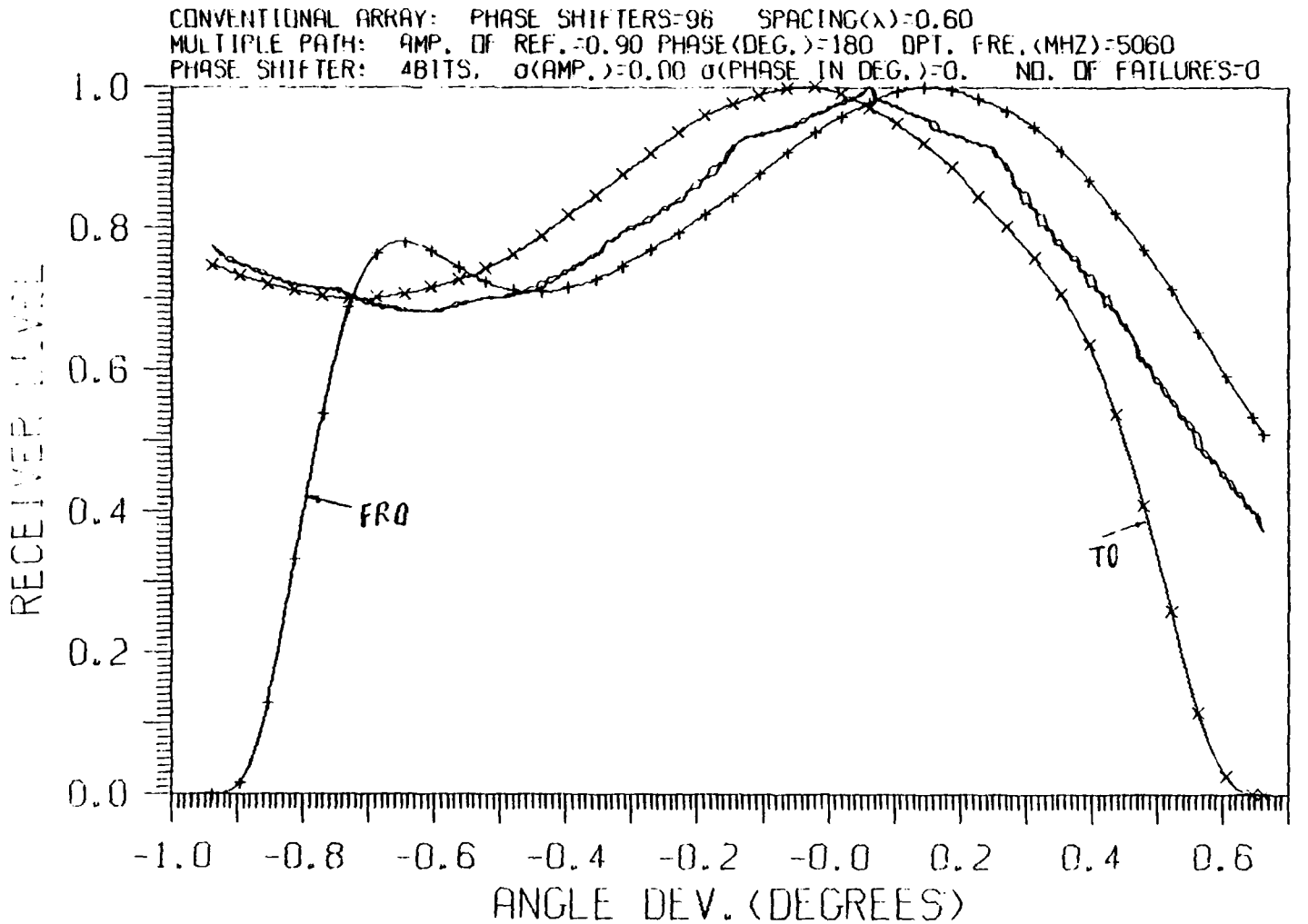


Fig. E-5 — Dynamic pattern of a scanning array.

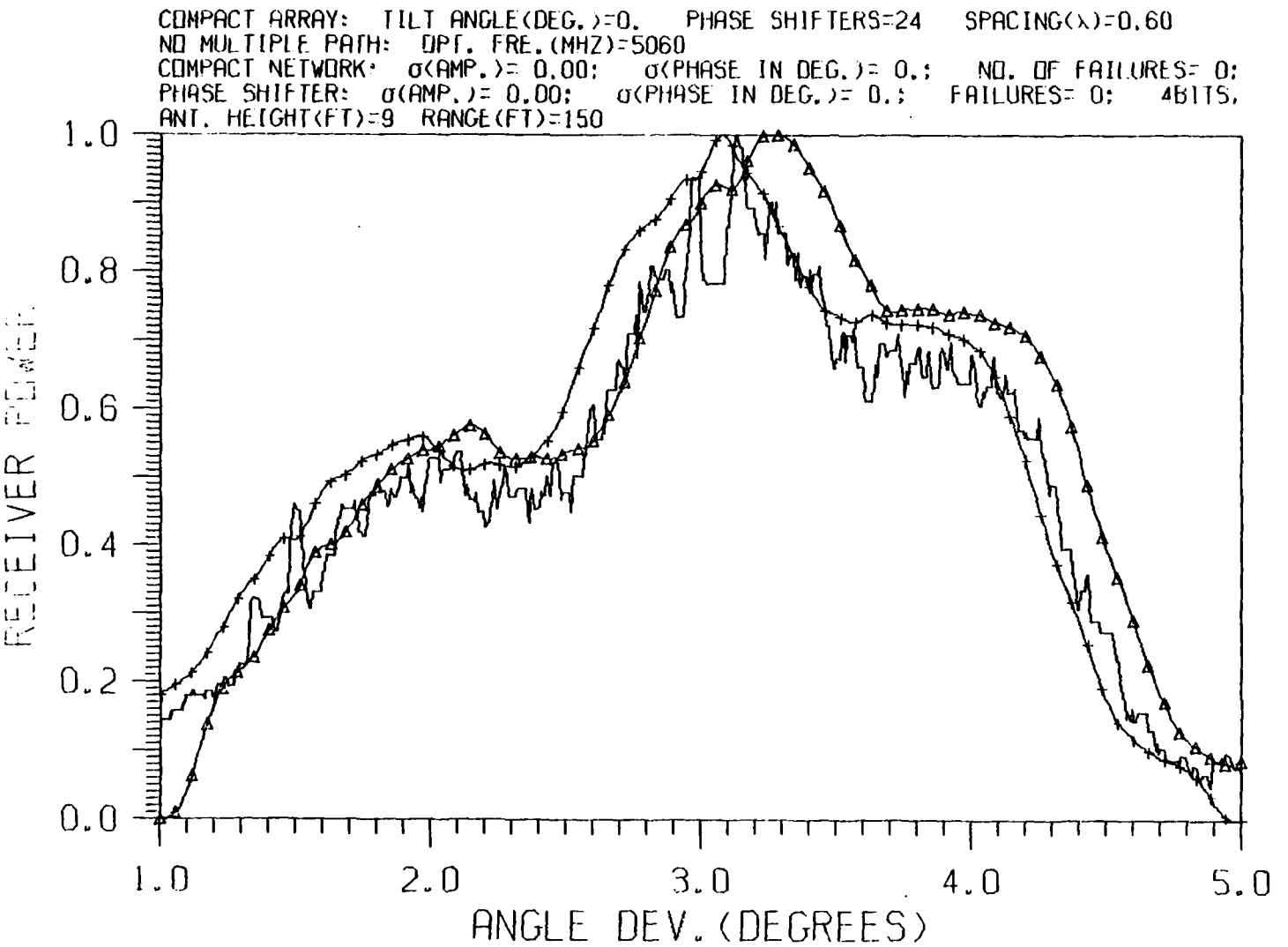


**Fig. E-6 — Monitor output.**

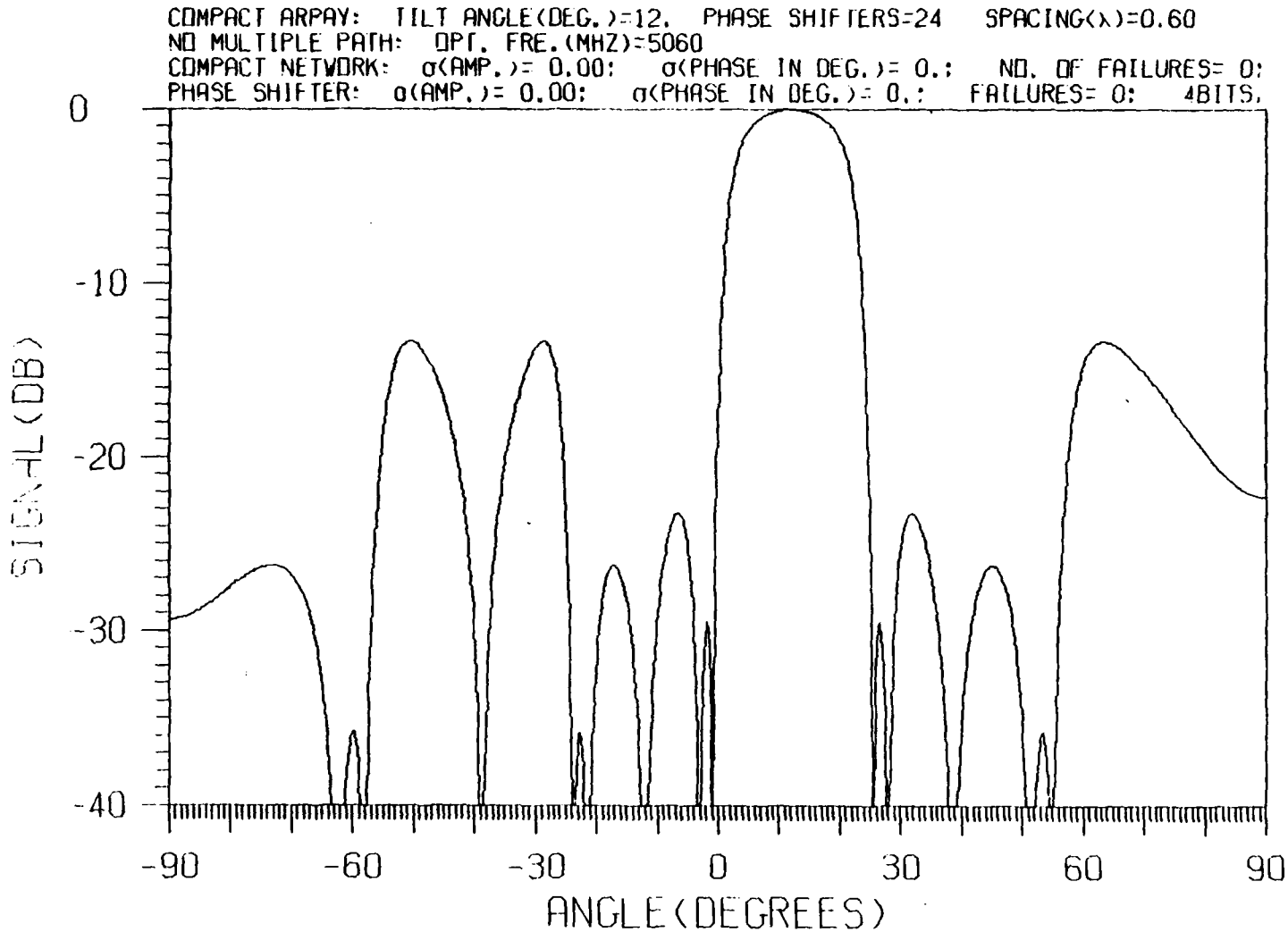


**Fig. E-7 — Element pattern of a COMPACT array.**

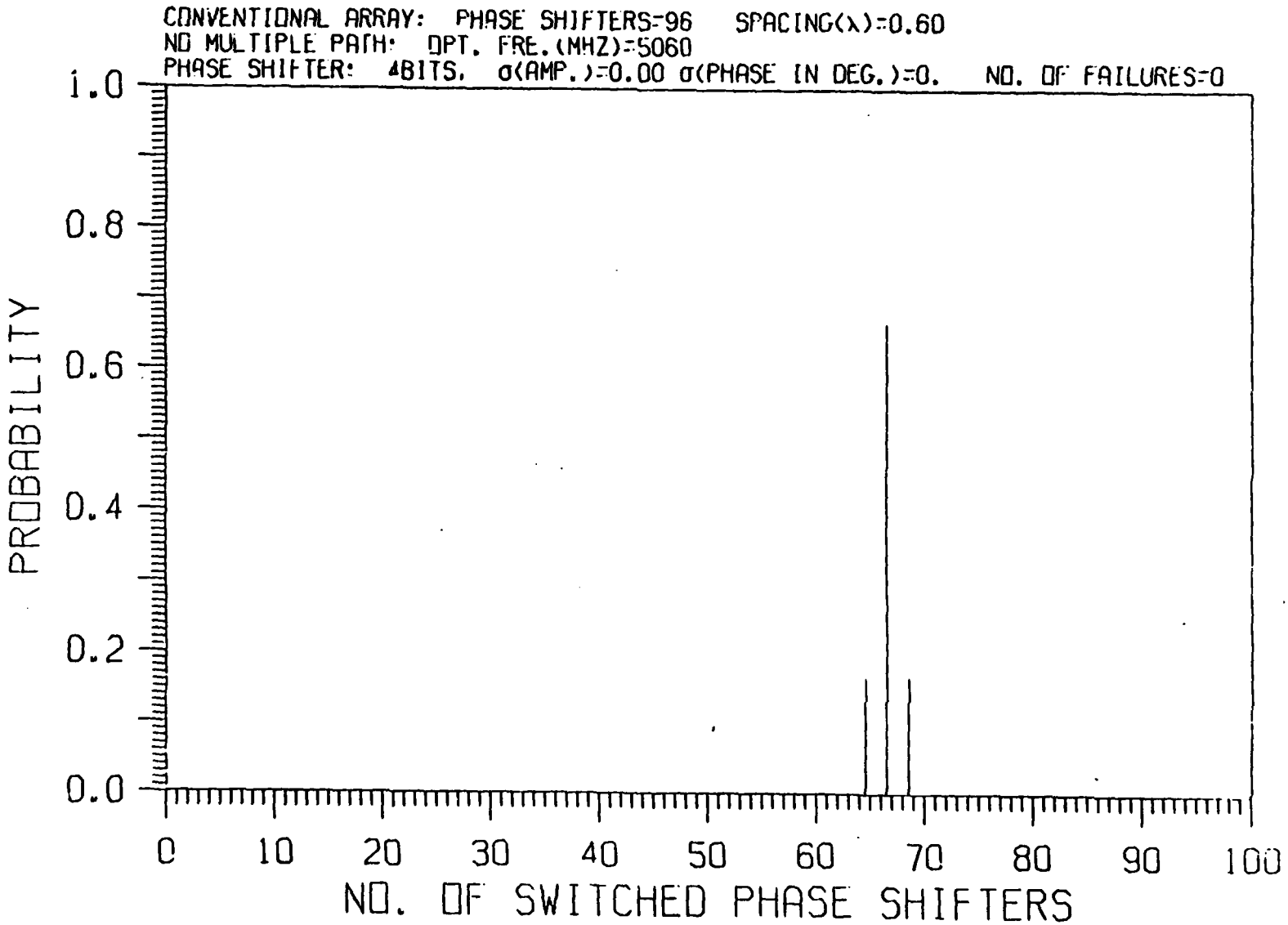


Fig. E-8 — Histogram of phase shifter switching.

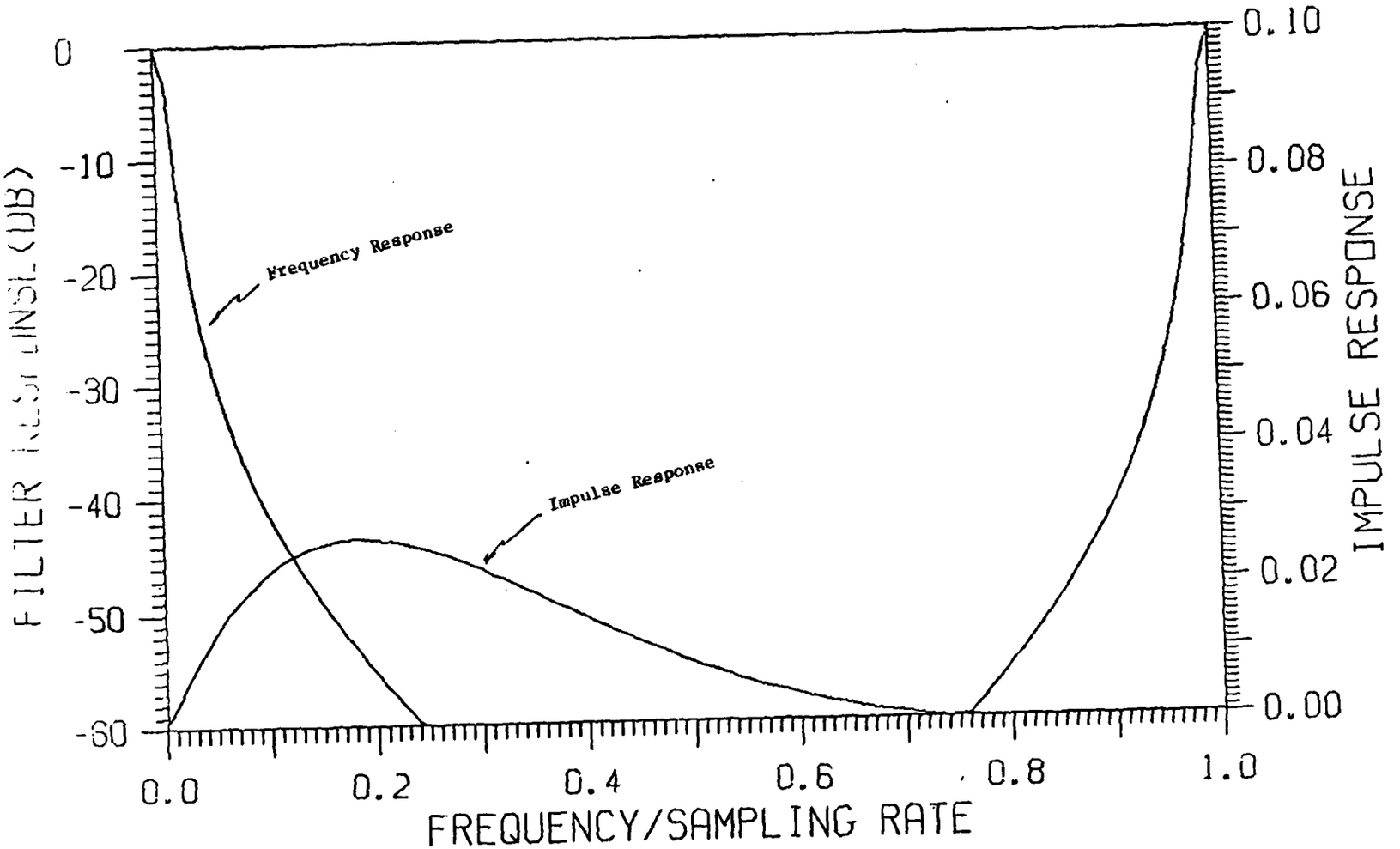


Fig. E-9 — Digital filter responses.

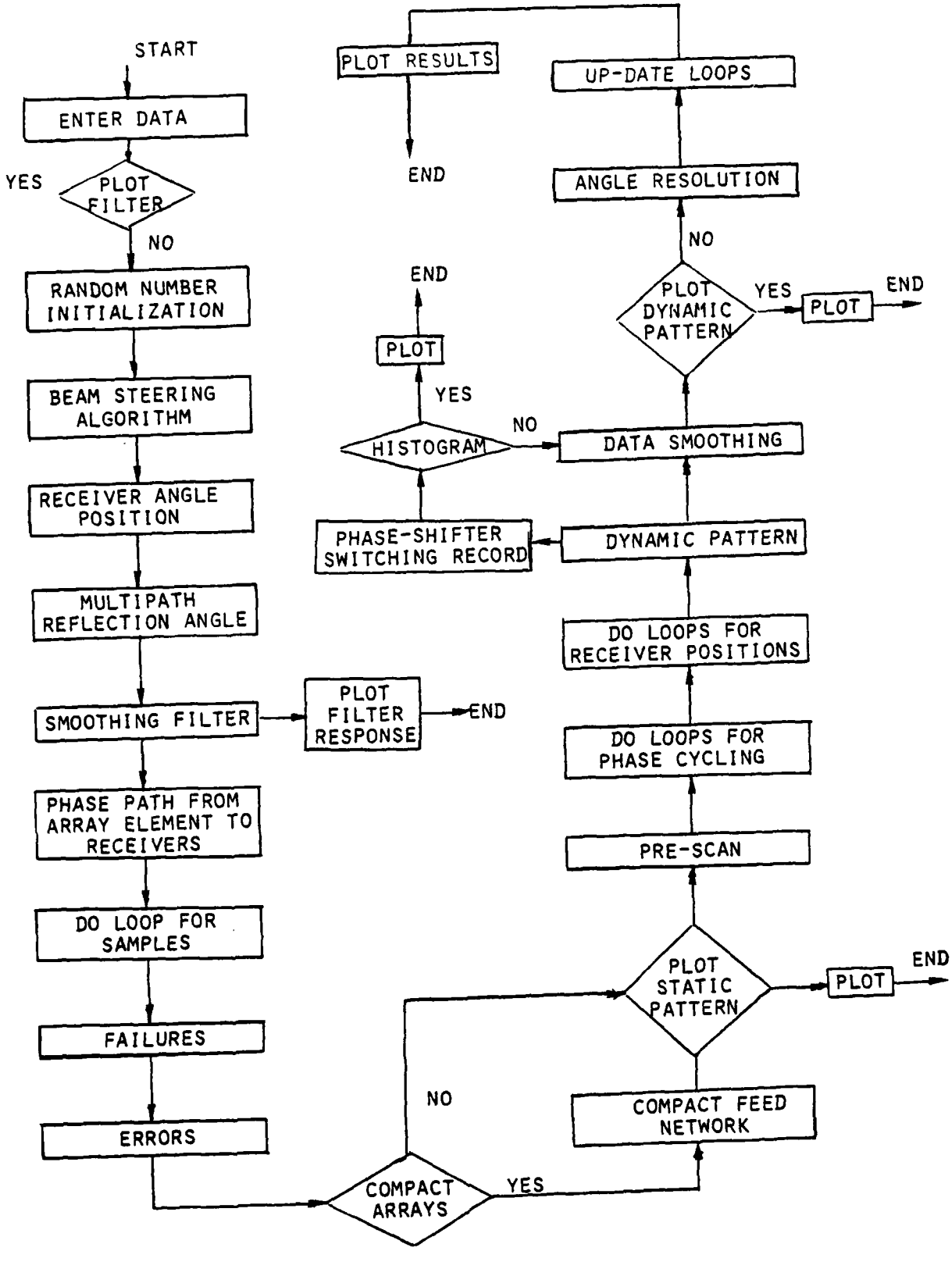


Fig. E-10 — Flow diagram.

## APPENDIX F
## DIGITAL FILTER DESIGN

A typical digital filter is shown in Fig. F-1, where $\tau$ represents the delay time in seconds. This filter can be realized either by delay lines or by digital units, provided the input signal is sampled at a rate satisfying the Nyquist criterion. The impulse response of such a filter is

$$h(t) = \sum_{n=o}^{N} a_n \, \delta(t-n\tau) \qquad \text{(F1)}$$

where $\delta(t)$ is an impulse function.

The transfer function in the frequency domain of such a filter is but the Fourier transform of the impulse response; hence,

$$H(f) = \sum_{n=o}^{N} a_n \exp\left(-j2\pi n \frac{f}{f_r}\right) \qquad \text{(F2)}$$

where $f_r = 1/\tau$ represents the sampling rate.

If a *z-transform*, such that

$$z = \exp\left(j2\pi \frac{f}{f_r}\right) \qquad \text{(F3)}$$

is performed on the filter impulse response, one finds

$$H(z) = \sum_{n=o}^{N} a_n \, z^{-n} \qquad \text{(F4)}$$

If feedback is provided as shown in Fig. F-2, the transfer function in the z plane becomes

$$H(z) = P(z)/Q(z) \qquad \text{(F5)}$$

where

$$P(z) = \sum_{n=o}^{N} a_n \, z^{-n} \qquad \text{(F5a)}$$

$$Q(z) = \sum_{n=0}^{N} b_n \, z^{-n} \qquad \text{(F5b)}$$

Thus a digital filter can be represented by a rational function in the z-domain. The design goal is to find such a rational function which has a prescribed amplitude behavior as a function of the frequency $f/f_r$. The transformation of equation (F3) establishes the relation between the frequency $f/f_r$ and the variable z.

The transformation specified by equation (F3) essentially maps the entire frequency axis (f) into a unit circle in the z plane. Furthermore, the magnitude of the transfer function shown in equation (F5) has a periodicity of $f_r$. Thus the absolute value of equation (F5) has an identical value at f and at $f + nf_r$ where n is an integer. Due to this periodicity, the frequency response can be viewed as limited to the range,

$$0 \leq f/f_r \leq 1$$

A digital filter in most applications is required to realize the properties of a conventional bandpass filter. An approach to design such a digital filter is hence to transform a known bandpass filter to a digital filter. Most conventional bandpass filter characteristics are specified as a function of the imaginary axis ($\omega$ axis) in the S plane, which extend from $-\infty$ to $+\infty$ .

Therefore, it is evident that in order to design a digital filter having a similar property, one is required to find a suitable transformation which will map the entire axis ($\omega$ axis) in the S plane into a unit circle in the z plane. Then, by use of this transformation, the properties of a bandpass filter which is synthesized in the S domain can be transferred into the z domain. Two pairs of such transformations which can achieve such a purpose are listed in the following:

$$\text{(a)} \quad z = \frac{\Omega + S}{\Omega - S} \tag{F6a}$$

$$S = \Omega \frac{z - 1}{z + 1} \tag{F6b}$$

$$\text{(b)} \quad z = \frac{S + \Omega}{S - \Omega} \tag{F7a}$$

$$S = \Omega \frac{z + 1}{z - 1} \tag{F7b}$$

Where $\Omega$ is an arbitrary constant.

We shall now discuss the significance of these transformations. From equation (F6a), if

$$z = \exp(j\phi)$$

then

$$S = j\,\Omega \tan \frac{\phi}{2}$$

Thus the entire imaginary axis in the S plane is mapped onto a unit circle in the z plane. Since $\Omega$ is an arbitrary constant, one may assume that

$$\Omega = \cot \frac{\phi_c}{2}$$

Under this condition, an arc between $\pm \phi_c$ on the unit circle in the z plane is mapped into a region, $S = \pm j$ in the S plane (see Fig. F-3).

According to equation (F3), frequencies such as $\phi_c \geq \frac{2\pi f}{f_r}$ correspond to the region in which $|\omega| \leq 1$. Thus a low-pass filter designed in the S domain having a cutoff frequency of unity can be transformed into the z domain where it will also be a low-pass filter having a corresponding cutoff frequency at

$$\frac{2\pi f_c}{f_r} = \phi_c$$

Similarly, a high-pass filter designed in the S domain can be transformed into the z domain to be a corresponding high-pass filter.

By similar reasoning, one finds that according to equation (F7a)

$$S = -j\,\Omega \cot \frac{\phi}{2}$$

If one sets

$$\Omega = \tan \frac{\phi_c}{2},$$

one finds that an arc between $\pm \phi_c$ such that $|\phi| \geq \phi_c$ will be mapped into a region $S = \pm j$ as shown in Fig. F-4. Hence, in this case, a low-pass filter having a cut-off frequency at unity in the S domain will become a high-pass filter in the z domain with a cut-off frequency

$$\frac{2\pi f_c}{f_r} = \phi_c$$

On the other hand a high-pass filter designed in the S domain will be transformed into a low-pass filter in the z domain.

The above transformations furnish a convenient way to transer any type of bandpass filter, either high-pass or low-pass.

The Butterworth low pass filter has a transfer function

$$T(j\omega)^2 = \frac{1}{1 + \varepsilon^2(\omega/\omega_c)^{2N}}$$

where N is the order of the rational function. The pole locations in the S plane are

$$\overline{S}_k = \frac{\omega_c}{\varepsilon^{1/N}} e^{j\left(\frac{\pi}{2} + \frac{2k-1}{2}\pi\right)}$$

where

$$k = 1,2,\ldots,N$$

and zeros at infinity.

One may transfer these poles and zeros in the S plane into the z plane by use of equation (F6a). From these poles and zeros in the z plane, a corresponding transfer function can be formed.

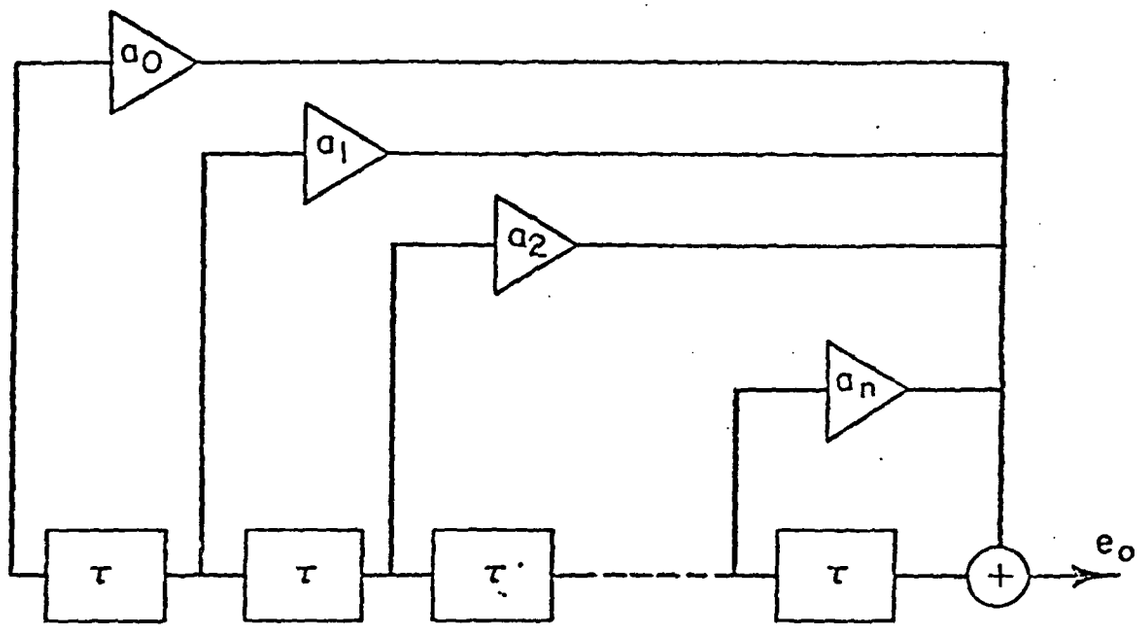


Fig. F-1 — A feed forward comb filter.

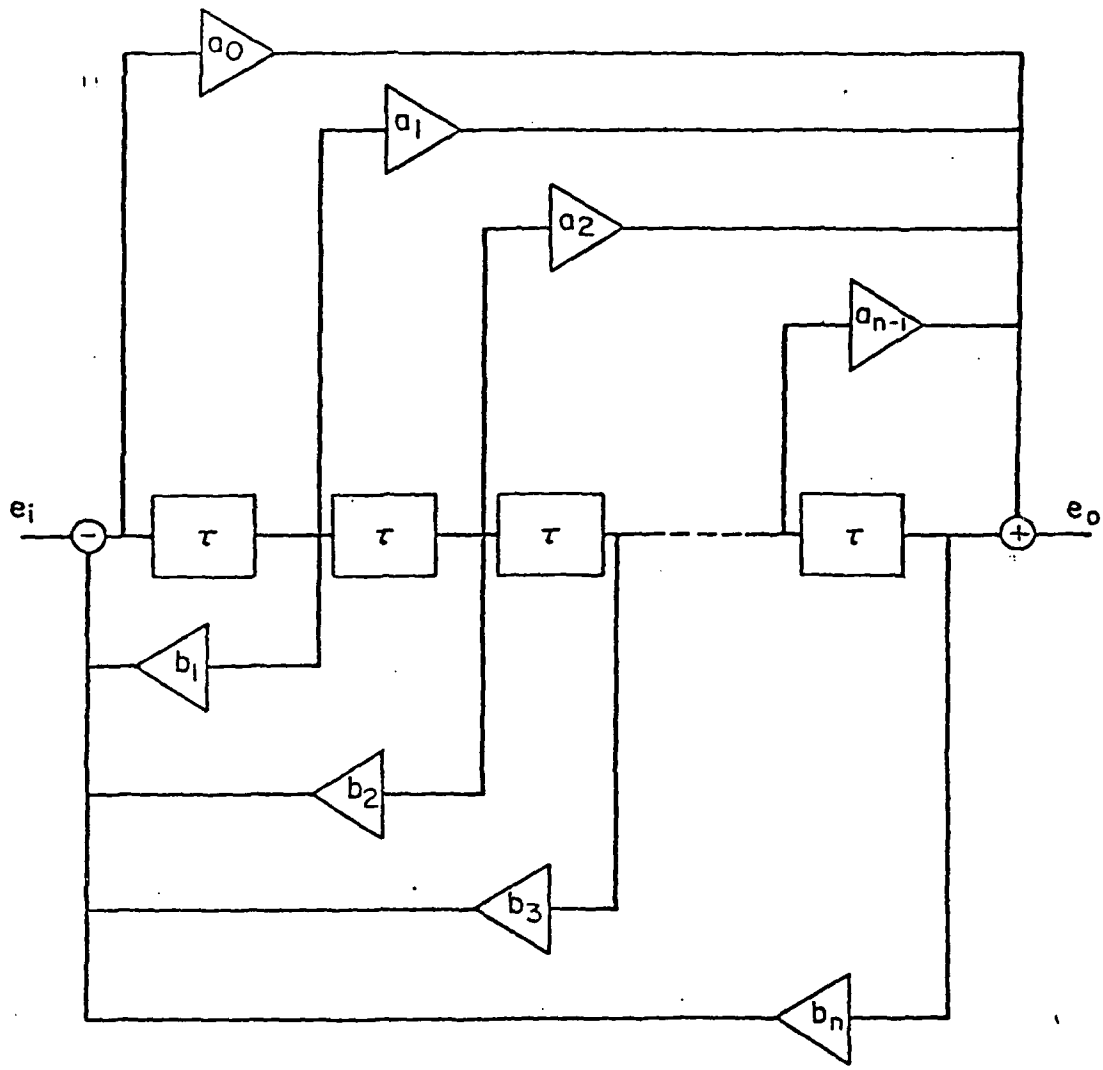


Fig. F-2 — A recursive type comb filter.

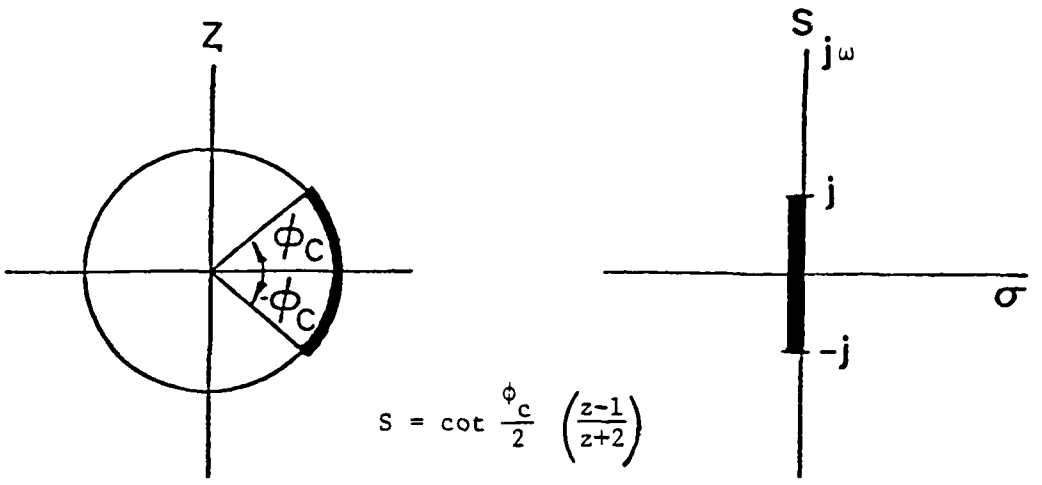


Fig. F-3 — Bilinear transformation map of a unit circle in the Z plane onto the imaginary axis in the S plane.

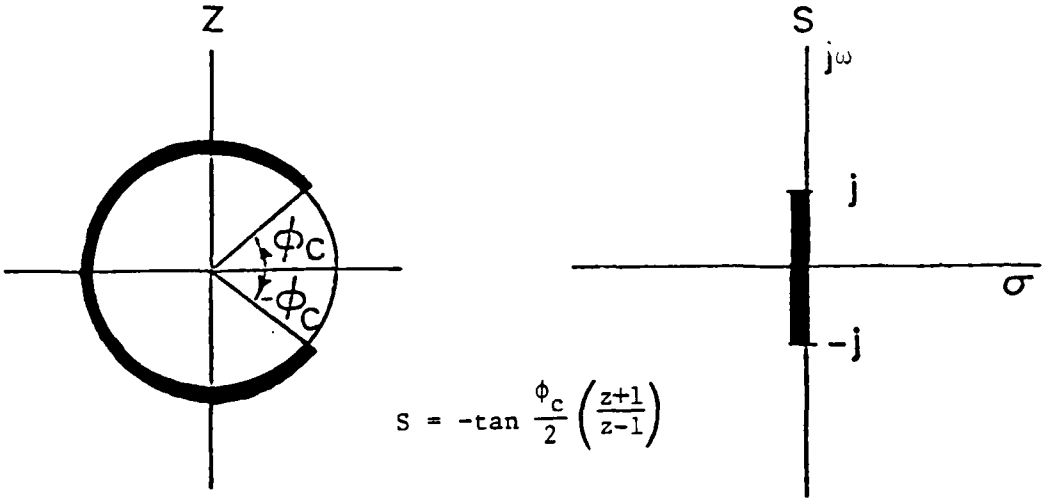


Fig. F-4 — Bilinear transformation map of a unit circle in the Z plane onto the imaginary axis in the S plane.

## APPENDIX G

## Optimum Beam Steering Technique

### 1. Introduction

This appendix describes a beam steering technique for a linear phased array antenna in which the phases of the individual phase shifters are determined by digital phase shifters with discrete settings. The objective of the beam steering technique is to provide maximum precision in beam pointing and minimum degradation in beam shape. The beam steering technique described in this appendix is felt to be optimum in the sense that it minimizes the energy lost from the designed aperture distribution. The technique uses a "recipe" consisting of a sequence of element numbers and phase settings for smooth sequential angular scan of the array, but the technique is not limited to a quasi-continuous scanning application.

### 2. Theory of Operation

The antenna system under consideration is shown in Fig. G-1. It consists of an array of N elements, where N can be even or odd. Each element is fed from the RF distribution network through a digitally controlled phase shifter. Associated with each element is a quiescent excitation, obtained when its phase shifter is set at zero. The amplitude is determined by the aperture distribution associated with the required pattern characteristics. The quiescent phase may be intentionally nonzero in the event that "stairstep" phase distributions are to be avoided. No random errors are assumed in the analysis. It is assumed that all settings of all phase shifters are exact, and that the overall condition of the array is always exactly calculable.

A digital phase shifter is defined as one which has $2^J$ phase states with a transmission phase difference between adjacent phase states of $2\pi/2^J$ rad. Thus, the transmission phase of a four-bit phase shifter can be set to any one of 16 values, ranging from 0 to $15\pi/8$ rad in $\pi/8$ rad steps.

The array can be stepped through the phase states shown in Fig. G-2 and put into a condition which is equivalent to the quiescent condition. Phase shifters to the right of array center are stepped positively in phase, and phase shifters to the left are stepped negatively in phase. The condition for which adjacent elements differ in phase by one phase

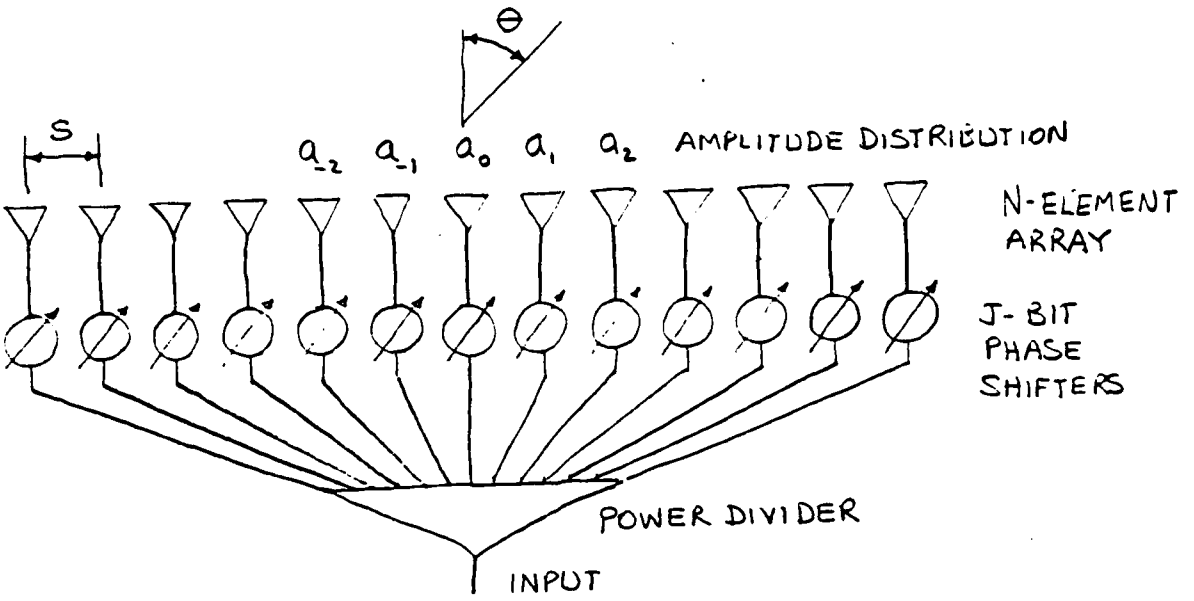


Fig. G-1 — N-element phased array with J-bit phase shifters.

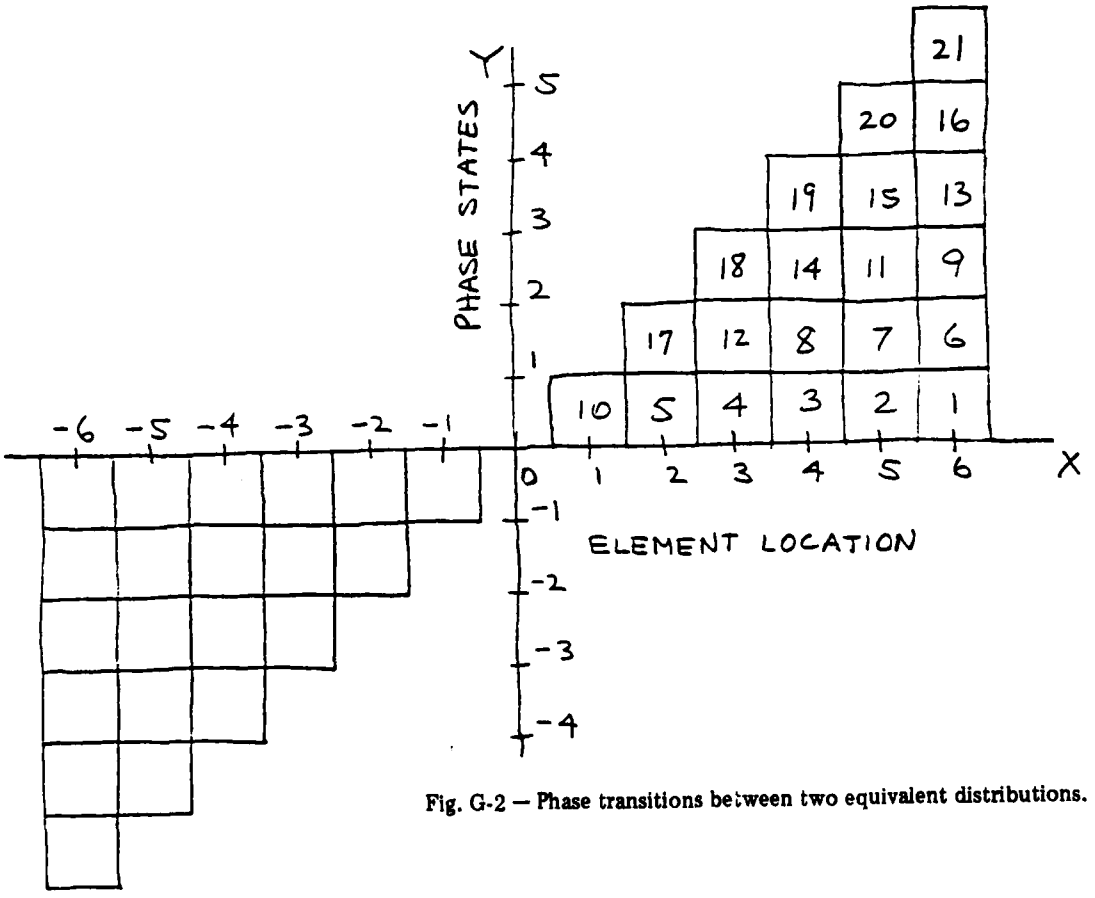


Fig. G-2 — Phase transitions between two equivalent distributions.

step is electrically equivalent to the original quiescent condition. Thus, it is only necessary to develop a beam steering technique for the beam motion implied by the phase states of Fig. G-2. The numbers in the boxes represent the sequence in which the phase shifters are stepped. Symmetrically opposed phase states are stepped alternately.

If the number of bits in the phase shifter is J, and the element spacing is s, the beam motion shown in Fig. G-2 after 21 phase steps is

$$\Delta(\sin\theta) = \frac{2\pi}{2^J} \cdot \frac{\lambda}{2\pi s} = \frac{\lambda}{s2^J} \qquad \text{(G-1)}$$

where $\theta$ is beam angle from Fig. G-1. Equation (G-1) is based on the relationship for the beam pointing direction of an array with linear phase progression of $\phi$ rad between adjacent elements, which is

$$\frac{2\pi s}{\lambda} \sin\theta = \phi.$$

Therefore, the change in $\sin\theta$ for a given change in $\phi$ is given by

$$\Delta(\sin\theta) = \frac{\lambda\Delta\phi}{2\pi s} .$$

For the example of Fig. G-2, $\Delta\phi = 2\pi/2^J$. The maximum number of steps that can be used to scan the beam through $\Delta(\sin\theta)$ is

$$M = \left(\frac{N-1}{2}\right)\left(\frac{N+1}{2}\right) = \frac{N^2-1}{4} \qquad \text{(N odd)}$$

Thus, the average step size is

$$\Delta_s(\sin\theta) = \frac{\Delta(\sin\theta)}{M} = \frac{\lambda}{s2^J} \cdot \frac{4}{(N^2-1)}$$

$$\approx \frac{4\lambda}{s2^J N^2} \qquad \text{(N large)} \qquad \text{(G-2)}$$

It is seen from Fig. G-2 that the available number of steps is cut in half by operating the phase shifters in pairs. It is seen from Equation (G-2) that the step size is doubled by removing one bit from the phase shifter.

The design problem addressed in this appendix is the choice of an optimum technique for stepping the phase shifters. This technique is based on a single criterion: the total error energy will always be minimized. Error energy is defined as the sum of the squares of the components obtained by taking the difference between actual element excitation and a weighted LMS fitted linear phase function. In addition, the beam direction is defined by the linear phase function.

To derive the steering technique, we use y as the phase coordinate and x as the element location coordinate. The location of the ith element and its associated phase are $x_i$ and $y_i$, respectively. The amplitude excitation is $a_i$, and the power excitation is $w_i = a_i^2$.

Although we allow for independent control of all phase shifters, we claim that the preferred phase distribution is always symmetric, and we calculate only symmetric distributions. Symmetric pairs can still be shifted in sequence.

We first derive a linear phase function, $y = bx$, such that the weighted sum of the squared error components is minimum.

The phase error for the ith component is

$$\Delta y_i = y_i - bx_i$$

The energy in the error component of the ith element is

$$\begin{aligned} E_i &= (a_i \Delta y_i)^2 \\ &= w_i (\Delta y_i)^2 \\ &= w_i (y_k^2 - 2bx_i y_i + b^2 x_i^2) \end{aligned}$$

The total energy is to be minimized with respect to b:

$$E = \Sigma w_i (y_i^2 - 2bx_i y_i + b^2 x_i^2) \qquad \text{(G-3)}$$

$$\frac{\delta E}{\delta b} = \Sigma w_i (-2x_i y_i + 2bx_i^2) \overset{\text{set}}{=} 0$$

$$b \Sigma w_i x_i^2 = \Sigma w_i x_i y_i$$

$$b = \frac{\Sigma w_i x_i y_i}{\Sigma w_i x_i^2} \qquad \text{(G-4)}$$

Substitution of Equation (G-4) into Equation (G-3) yields

$$E = \Sigma w_i y_i^2 - \frac{(\Sigma w_i x_i y_i)^2}{\Sigma w_i x_i^2}$$

If we now change the phase of the jth element by $\delta y_j$, the change in E is $\delta E_j$, and is given by

$$\delta E_j = w_j \delta y_j \left[ 2 \left\{ y_j - x_j \frac{\Sigma w_i x_i y_i}{\Sigma w_k x_i^2} \right\} + \delta y_j \left\{ 1 - \frac{w_j x_j^2}{\Sigma w_i x_i^2} \right\} \right] \quad \text{(G-5)}$$

Equation (G-5) allows us to apply the minimum energy criterion by always selecting that j which gives the minimum value of $\delta E_j$. In addition, it is found that beam motion is given by

$$\delta b_j = \frac{\delta y_j w_j x_j}{\Sigma w_i x_i^2} \quad \text{(G-6)}$$

Note that this beam steering technique is deterministic. There is always a preferred phase shifter to step (sometimes more than one with the same minimum $\delta E_j$). Thus, once an initial set of $y_i$ and an aperture distribution $w_i$ are specified, the beam stepping sequence is determined.

Table G-I gives samples of beam stepping sequences for three cases for a 13-element array. For the first case, the amplitude distribution is uniform ($w_i = 1$) and the initial phases are zero ($y_i = 0$). For the second case the amplitude distribution has been tapered to a cosine-squared on a pedestal in power. The values of $w_i$ are determined by $w_i = .3 + .7 \cos^2 (\frac{180i}{13})$. For the third case, the taper is retained, and a quasi-random set of initial phases has been introduced. The values of $y_i$ for i = 1 through 6 are .42, - .25, .08, .25, - .42, and - .08. The value of $\delta y_i$ is taken to be unity, so that one complete scan cycle is contained between b = 0 and b = 1. The beam stepping sequence is thereby normalized with respect to the number of bits in the phase shifters. That is, the same sequence is used regardless of the number of bits. The beam simply doesn't move as far if there are more bits.

Note that, for a given aperture distribution, the size of the beam step is determined by the element that is shifted as predicted by Equation (G-6). Note also that, for the cases for which all $y_i$ are initially zero, the stepping sequence is essentially symmetrical about the 11th step. On the 10th, 11th, and 12th steps, elements 1, 3, and 5 must be shifted, and no symmetry is possible for that portion of the sequence.

It is readily seen that the stepping sequence is strongly dependent on the initial values of $y_i$ and less strongly dependent on the aperture distribution. It is also pointed out that, whereas the ratio of maximum to minimum beam step sizes is (N-1)/2 (for N odd) or N-1 (for N even), for a uniform aperture distribution, it is always less for a tapered aperture distribution.

Table G-I. Examples of Beam Steering Technique Applied to a 13-Element Array

| Step No. | Uniform Amplitude $y_i = 0$ | | | Taper $y_i = 0$ | | | Taper $y_i \neq 0$; $b_o = -.0073$ | | |
|---|---|---|---|---|---|---|---|---|---|
| | j | b | ΔE | j | b | ΔE | j | b | ΔE |
| 1 | 6 | .0659 | .6044 | 6 | .0467 | .2232 | 5 | .0413 | -.0038 |
| 2 | 5 | .1209 | .0659 | 5 | .0953 | .1125 | 6 | .0880 | .0199 |
| 3 | 4 | .1648 | -.1429 | 4 | .1481 | .0138 | 2 | .1306 | .0534 |
| 4 | 3 | .1978 | -.0879 | 3 | .2002 | -.0311 | 4 | .1834 | .1284 |
| 5 | 2 | .2198 | .1648 | 2 | .2428 | .0968 | 3 | .2355 | -.0668 |
| 6 | 6 | .2857 | -.0330 | 6 | .2895 | -.0600 | 5 | .2841 | -.1699 |
| 7 | 5 | .3407 | -.1319 | 5 | .3381 | -.0535 | 6 | .3308 | -.2633 |
| 8 | 4 | .3846 | .0989 | 4 | .3909 | .0441 | 6 | .3775 | .1831 |
| 9 | 6 | .4505 | -.0110 | 6 | .4376 | .0090 | 5 | .4261 | .0552 |
| 10 | 1 | .4615 | .0879 | 1 | .4617 | .0967 | 4 | .4789 | -.0632 |
| 11 | 5 | .5165 | .1099 | 3 | .5137 | .0510 | 3 | .5310 | .0902 |
| 12 | 3 | .5495 | -.1978 | 5 | .5624 | -.1478 | 6 | .5777 | .0583 |
| 13 | 6 | .6154 | .0110 | 6 | .6091 | -.0090 | 5 | .6263 | .0544 |
| 14 | 4 | .6593 | -.0989 | 4 | .6619 | -.0441 | 2 | .6689 | -.0768 |
| 15 | 5 | .7143 | .1319 | 5 | .7105 | .0535 | 4 | .7217 | -.0329 |
| 16 | 6 | .7802 | .0330 | 6 | .7572 | .0600 | 6 | .7684 | -.0311 |
| 17 | 2 | .8022 | -.1648 | 2 | .7998 | -.0968 | 5 | .8170 | .0904 |
| 18 | 3 | .8352 | .0879 | 3 | .8519 | .0311 | 3 | .8691 | .0703 |
| 19 | 4 | .8791 | .1429 | 4 | .9047 | -.0138 | 6 | .9158 | .0405 |
| 20 | 5 | .9341 | -.0659 | 5 | .9533 | -.1125 | 4 | .9686 | -.0197 |
| 21 | 6 | 1.0000 | -.6044 | 6 | 1.000 | -.2232 | 1 | .9927 | -.1164 |

## 3. Hardware Application

In order to establish a quasi-continuous scanning pattern, a functional relationship must be defined between b and time, and the appropriate phase shifters will be shifted at the resulting times. In this arrangement both time and element values must be stored in the beam steering prescription. In practice it might be preferable to execute phase shifts at uniform time intervals, corresponding to a clock rate. For example, the 13-element array depicted in Table G-I actually takes 42 steps to scan from b = 0 to b = 1, counting both positive and negative element positions. If we specify that we want some number of evenly spaced steps, it is possible to combine groups of phase shifts in order to closely approximate the desired beam motion. There are a number of procedures by which steps could be combined, but the most straightforward appears to be to take the tabulated steps in order and group them so that the actual beam position during a particular dwell period is as close to the desired position as possible. For example, if we want ten beam positions between b = 0 and b = 1 uniformly spaced in time, Figure G-3 shows that the desired setting values of b should be .05, .15, .25,... .95. For the uniform amplitude and taper with $y_i \neq 0$ cases of Table G-I, the resulting process is shown in Table G-II. The error in b is shown for each beam position, and the RMS error in b is .0172 for the uniform case and .0162 for the tapered case. Based on 21 total available steps, which will give a maximum deviation from any desired setting of about 1/42 = .0238, and assuming a uniform distribution over $\pm$ .0238, we would expect an RMS error of $.0238/\sqrt{3}$ = .0137, which is in reasonable agreement with the results obtained.

So long as the number of steps used is less than the total number available, we would expect the RMS error to be independent of the number used. That is, the RMS error in $\sin\theta$ is approximately

$$\sigma = \lambda/(s2^{J+1}M\sqrt{3}) \approx \lambda/(s2^{J-1}N^2\sqrt{3})$$

where we have inserted the step size from Equations (G-1) and (G-2). Since the beamwidth B in $\sin\theta$ is approximately $\lambda/Ns$, the precision of beam steering relative to a beamwidth is

$$\sigma/B = 1/2^{J-1}N\sqrt{3}.$$

Two likely hardware realizations of these techniques both require the memorization of the stepping sequence in some form--it is not reasonable to expect to compute the sequences during the scan. One procedure, which is more applicable to a small number of phase shifters and/or a limited angular scan, is to commit the entire scanning sequence to memory and use it as a recipe from a ROM. Another procedure is to commit a single portion of the repeating sequence to memory and to calculate successive values of b, using the memorized sequence to determine the phase shifter steps for each clock interval. A third possibility is becoming

more feasible as the cost of semiconductor memory continues to decline. The entire stepping sequence for given phase shifter can be located at the phase shifter so that the central beam steering unit would consist of little more than an initializer and a clock.

Table G-II. Scanning Sequences for Uniform Step Size

| Uniform Amplitude | | | | Taper, $b_o$ = - 0.0073 | | | |
|---|---|---|---|---|---|---|---|
| Desired b | Realized b | Units Shifted | Error | Desired b | Realized b | Units Shifted | Error |
| .05 | .0659 | 6,6 | +.0159 | .043 | .0413 | 1,5 | -.0017 |
| .15 | .1648 | 4,5 | +.0148 | .143 | .1306 | 2,6 | -.0124 |
| .25 | .2198 | 2,3 | -.0302 | .243 | .2355 | 3,4 | -.0075 |
| .35 | .3407 | 5,6 | -.0093 | .343 | .3308 | 5,6 | -.0122 |
| .45 | .4505 | 4,6 | +.0005 | .443 | .4261 | 5,6 | -.0169 |
| .55 | .5495 | 1,3,5 | -.0005 | .543 | .5310 | 3,4 | -.0120 |
| .65 | .6593 | 4,6 | +.0093 | .643 | .6263 | 5,6 | -.0167 |
| .75 | .7802 | 5,6 | +.0302 | .743 | .7217 | 2,4 | -.0213 |
| .85 | .8352 | 2,3 | -.0148 | .843 | .8691 | 3,5,6 | +.0261 |
| .95 | .9341 | 4,5 | -.0159 | .943 | .9686 | 4,6 | +.0256 |

For the recipe approach, three examples are given, ranging from limited coverage and small number of phase shifters to full coverage and large array. Table G-III lists the parameters and the resulting required memory capacity.

Table G-III. Memory Required for Recipe Method of Beam Steering Control; 4-bit Phase Shifters

| No. Phase Shifters | Angle Coverage (deg) | Memory Size (k bits) |
|---|---|---|
| 30 | 0 - 15 | 2.7 |
| 100 | 0 - 15 | 35 |
| 100 | -40 - +40 | 180 |

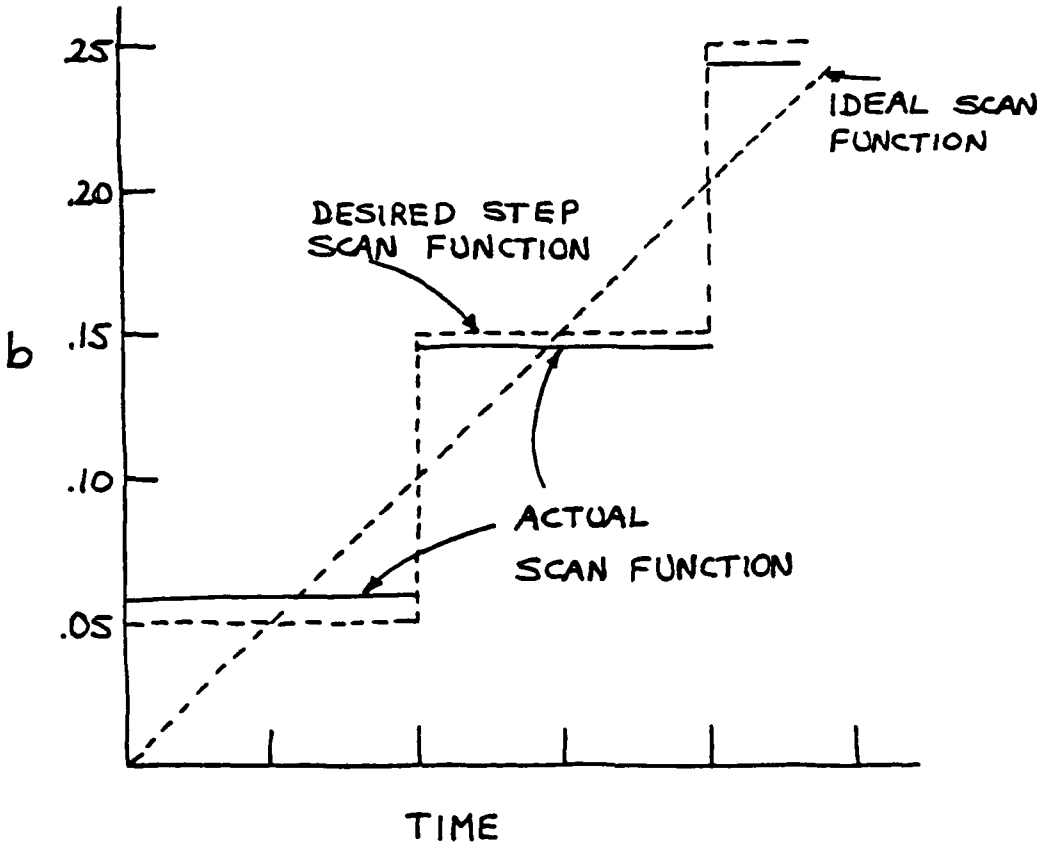


Fig. G-3 — Scan function for b vs time.

For the second technique, which is part ROM, part processing, the memory requirement for the ROM is about 8 k bits for the 100-element array of 4-bit phase shifters covering $\pm$ 40 degrees.

For the case in which all memory is located at the phase shifters, the memory requirement at each phase shifter would be about 3 k bits for the 100 element array of 4-bit phase shifters covering $\pm$ 40 degrees.

APPENDIX H

Design of a 360-Degree Azimuth Antenna
For the Microwave Landing System

## 1. Introduction

The purpose of this appendix is to outline the theoretical and design considerations involved in the achievement of an electronically scanned 360-degree-coverage azimuth antenna.

The appendix is presented in three sections. The first section after this one considers the basic array geometry and concludes that a circular array of radiating elements is preferable to a number of linear arrays. The next section addresses several alternative scanning techniques for circular arrays. The final section describes the particular scanning circular array that is being developed at NRL. Appendices I and J present the theory of a compact 3D lens configuration which will be used in the electronic scanning feed system.

It is assumed that the antenna will satisfy the following system requirements:

| | |
|---|---|
| Azimuth beamwidth | 4 degrees |
| Azimuth sidelobe level | 25 dB |
| Elevation pattern | Shaped |
| Theoretical gain | 31 dB |
| Antenna Losses | 4 dB |
| Net maximum gain | 27 dB |

## 2. Array Geometry

Two basic array geometries are available for achieving 360-degree azimuth coverage with an electronically scanned antenna--a circle or a polygon. The circular array is a single array with a single scanning feed system. The polygon is a set of independent linear arrays.

From the standpoint of system performance, the two geometries have the following features:

- The beamwidth changes with azimuth angle for the linear arrays. [illegible]width of the circular array degrades slightly with elevation [illegible] this application, for example, the phase error at 15 degrees [illegible] ±29 degrees.

b. The circular array produces a "planar" beam--that is, beam pointing direction is independent of elevation angle. Conversely, the linear arrays produce "conical" beams--that is, beam pointing direction varies slightly with elevation angle.

The conical beams produced by the linear arrays will produce an error in the azimuth indicated by MLS receivers. Over an azimuth region which increases with increasing elevation angle, the airborne receiver will receive two mainbeam passages rather than one. Provided that the receiver ignores the second beam, an error is generated, the maximum value of which increases rapidly with elevation angle. The maximum error for two elevation angles, together with the azimuth angle for which the error is obtained, are listed below. It is assumed that four linear arrays are used and that they point in the azimuth directions, n90°.

| Elevation | Azimuth | Error |
|---|---|---|
| 20° | n90°-45°$\pm$3.8° | .42° |
| 30° | n90°-45°$\pm$9.7° | 2.24° |

The use of linear arrays implies that a number of independent electronically scanned arrays will be used. The total number of array elements, and consequently phase shifters, is listed below for a four-degree beamwidth.

| Number of Arrays | Elements per Array | Total Number of Elements |
|---|---|---|
| 3 | 60 | 180 |
| 4 | 39 | 156 |
| 5 | 32 | 160 |
| 6 | 28 | 168 |

It is seen that the case of four arrays minimizes the number of phase shifters. However, the corresponding calculation for a circular array results in an array of about 108 elements. It will be shown that the most complex beam scanning system which could be used with the circular array would require about 94 phase shifters. The selected circular array scanning configuration requires 37 phase shifters and 37 3-way switches.

Therefore, the use of linear arrays involves both errors and increased hardware complexity, and the remainder of this appendix is devoted to the design of a scanning circular array.

It is assumed that the circular array design will be based on the following criteria:

a. Aperture/beamwidth. $\theta_{3dB}(\text{deg}) = 64\lambda/A$, where A is effective aperture. This relationship is determined by the 25 dB sidelobe requirement.

b. Aperture/diameter. $A = D \cos \theta_e$, where D is diameter of the circular array and $\theta_e$ is half the effective coverage angle of the circular array elements.

c. Element spacing. $S = \frac{\lambda}{1+\sin\theta_e}$. This relation comes directly from array theory, where $\theta_e$ is defined above.

The above criteria, together with the assumed system requirements and with $\theta_e = 60°$, result in the following antenna parameters:

| | | |
|---|---|---|
| $\theta_{3dB}$ | $= 4°$ | Beamwidth |
| A | $= 16\lambda$ | Effective aperture |
| D | $= 18.5\lambda$ | Array diameter |
| S | $= .536\lambda$ | Element spacing |
| N | $= 108$ | Number of elements |
| Dimensions | 1.1 m. diameter, ~ 1 m. height | |

3. Alternative Circular-Array Scanning Techniques

Two basic electronic-scan techniques are considered here. One is directly analogous to the phase-scanned linear array and will be referred to as phase scan. We define this as a configuration in which the individual element patterns are identical in amplitude but are orthongonal because of their differing phase centers. The other, which we will refer to as amplitude scan, is directly analogous to Interscan. In this configuration, the patterns are orthogonal based on their amplitude characteristics alone.

The radiating elements of a circular array do not satisfy either of the above criteria. The patterns are orthogonal, but not based on either phase or amplitude alone. Thus, there exists an essentially continuous range of orthogonal patterns available from the circular array, with phase orthogonal at one extreme and amplitude orthogonal at the other. We will examine techniques for transforming from the element patterns to any other set of orthogonal patterns.

Returning to the two types of electronic scan techniques, it is noted that the formation of pattern functions by these two methods represents the two classical synthesis procedures. In phase scan, the pattern is synthesized from element patterns which can be described as complex Fourier harmonics, and this is a Fourier synthesis. In amplitude scan, the pattern is synthesized in a Woodward fashion from element patterns which are essentially sin x/x functions. In the case of the Fourier synthesis, the number of harmonics used depends on the size of the aperture. In the Woodward synthesis, the number of sin x/x patterns

used depends on the precision required of the synthesis. An advantage of amplitude scan is that it requires fewer degrees of freedom for the synthesis of a directive pattern with control over a few sidelobes.

As is well known to workers in the field, amplitude scan consists of a coarse scan mechanism and a fine scan modulator. The coarse scan is accomplished by a switching network which selects the patterns that will be used in the synthesis. The fine scan modulator selects the specific amplitude weights that will be applied to the patterns. Now, in order to use phase control rather than amplitude control and thereby afford straightforward comparison among the alternative techniques, we choose to Fourier transform the amplitude weighting function supplied by the fine-scan modulator. This weighting function is sampled according to the pattern locations, and the sampling points translate with the beam scanning motion. The Fourier transform changes translation of one function into phase modulation of another function.

One might ask why we have bothered to use an amplitude scan configuration if we are going to transform it into a phase scan arrangement. The reason for using amplitude scan is the reduction in complexity. Fewer phase control devices will be required for the amplitude scanned antenna.

Scanning configurations are now described for the circular array. Figure H-1 lists the four patterns which will be used as examples. The patterns range from omnidirectional to the minimum beamwidth patterns available from the array, and the scanning techniques range from pure phase scan to pure amplitude scan. The second technique uses the pattern of the circular array radiating element directly, which has a beamwidth of about 90 degrees and useful coverage of about 120 degrees. All of the other patterns are obtained by suitably transforming the array element patterns.

For the pure phase scan case, the use of omnidirectional patterns represents the transformation of the circular array to an equivalent linear array, and Figure H-2 indicates how these patterns would be generated. A mode forming network such as a Butler matrix or a Rotman lens is used.

For the amplitude scan case, a microwave optical collimator or an appropriate network must be used to form the multiple directive patterns. Possible techniques are the Myers geodesic lens, the Luneberg lens, or transformation from the equivalent linear array to multiple patterns. The last example involves two transformations, one to the equivalent linear array and another to the multiple beams. Each transformation involves a Fourier transforming network such as a Rotman lens or a Butler matrix. Figure H-3 outlines the resulting configuration, showing the multiple-beam-forming device, the coarse switching network, and the fine scan modulator, with the number of interconnections. Using still another,

but small Fourier transform network, the fine scan modulator is realized with four phase shifters. Therefore, it is seen that phase scan uses a maximum number of phase shifters and no switches while amplitude scan uses a minimum number of phase shifters and a maximum number of switches.

Examples of two intermediate techniques are given. One uses the element pattern directly without translation and requires moderate numbers of phase shifters and switches. This is referred to as a cyclic scan technique. The other uses slight transformation of the element patterns, also requires moderate number of phase shifters and switches, and is called a hybrid scan technique.

The hybrid scan technique uses ten phase shifters and transformed patterns with about 36 degrees beamwidth. These patterns can be obtained by means of a partial focus lens, analogous to the Luneberg lens, which does not achieve perfect focus. The detailed characteristics of this lens are not known. However, the same performance can be obtained with an equivalent linear array and a set of small Fourier transform networks. Although the mix of switches and phase shifters for this configuration might be desirable, the lack of an available, practical device to achieve the partial focus precludes its consideration at this time.

The pure phase scan configuration, although it requires no switches, involves the use of a large network or lens to provide the equivalent linear array outputs. In addition, it requires about 100 phase shifters. This degree of complexity allows complete pattern synthesis--in theory, every sidelobe of the 360-degree pattern can be specified. Because of the excessive lens size and number of control devices, this alternative is rejected.

Figure H-4 illustrates the details of the various scanning techniques, assuming particular realizations for the lenses and transforming networks. The remaining choice lies between amplitude or Interscan and cyclic scan. The choice is somewhat subjective. If we prefer reduced sensitivity to component failure, we choose cyclic scan with 36 separate switches and 36 separate phase shifters. This alternative is selected and is described in the following section.

4. Cyclic Scan Circular Array

Referring again to Figure H-4, it is noted that cyclic scan is functionally similar to the other techniques except for the lack of a transforming lens between the array and the coarse scan switches. Furthermore, the fine scan network is the major part of the configuration, consisting of a lens, a power divider, and 36 phase shifters.

As was pointed out above, a smaller number of control devices produces a lesser degree of control over the synthesized pattern. The use

of 36 phase shifters will provide control over about 36 sidelobes, or about 120 degrees of the 360 degree antenna pattern. This is completely adequate to provide the desired beamwidth and sidelobe level.

Figure H-4 indicates a Rotman lens with dimensions larger than the array for the cyclic scan system. The Rotman lens is a Fourier transforming device which is planar in construction, generally using a parallel-plate transmission medium. An alternative three-dimensional lens has been devised, which can provide the same transfer characteristics as the Rotman lens in a more compact manner. This lens concept is described in Appendices I and J. It is shown that the three-dimensional lens must have 37 ports, and its dimensions are about .6 m, which is significantly smaller than the circular array. Thus, the entire feed system can be packaged within the circular array aperture.

The resulting antenna design has the following parameters:

| | |
|---|---|
| Circular array diameter | 1.09 m. |
| Number of elements | 111 |
| Element spacing | 3.09 cm. |
| Switches | 37, 1P3T |
| Phase shifters | 37 |
| Lens | Cylindrical, ~.6 m. long by ~.6 m. diameter. 37 ports on each side |

1. MODE PATTERNS - PURE PHASE SCAN
   (ALL OMNIDIRECTIONAL)

2. ELEMENT PATTERN FOR CYCLIC SCAN
   (CYCLIC IN ~4° INTERVALS)

3. BEAM PATTERN FOR HYBRID SCAN
   (CYCLIC IN ~4° INTERVALS;
   ~ 40° BEAMWIDTH)

4. BEAM PATTERNS FOR INTERSCAN
   (CYCLIC IN ~4° INTERVALS;
   ~ 4° BEAMWIDTH)

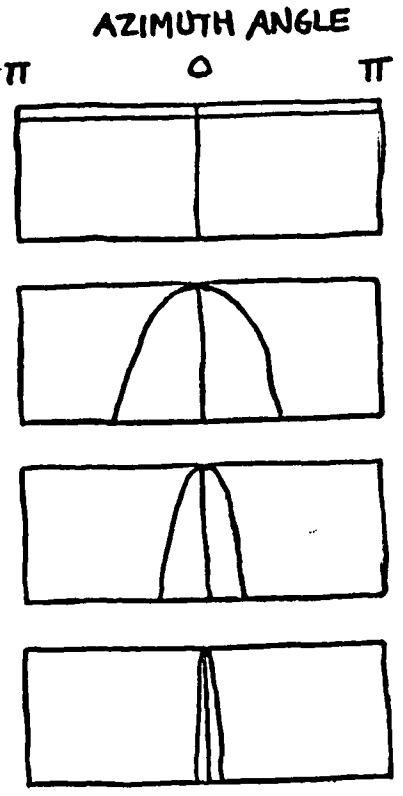


Fig. H-1 — Comparison of patterns used in scanning techniques.

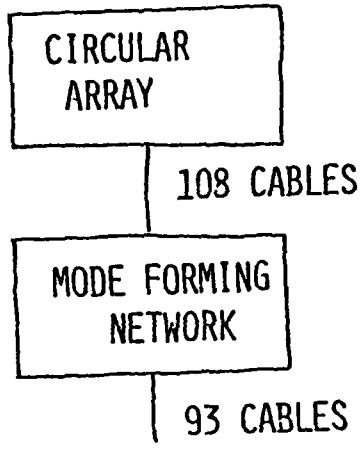


MODE FORMING NETWORK IS THE SAME AS A MULTIBEAM NETWORK FOR A LINEAR ARRAY. IT CAN BE A BUTLER MATRIX OR A ROTMAN LENS.

EACH OUTPUT PRODUCES AN OMNIDIRECTIONAL PATTERN WITH PHASE CHARACTERISTIC

$$\phi_n(\theta) = n\theta \quad (-46 \leq n \leq +46)$$

$\theta$ = AZIMUTH ANGLE

Fig. H-2 — Transformation of circular array to equivalent linear array.

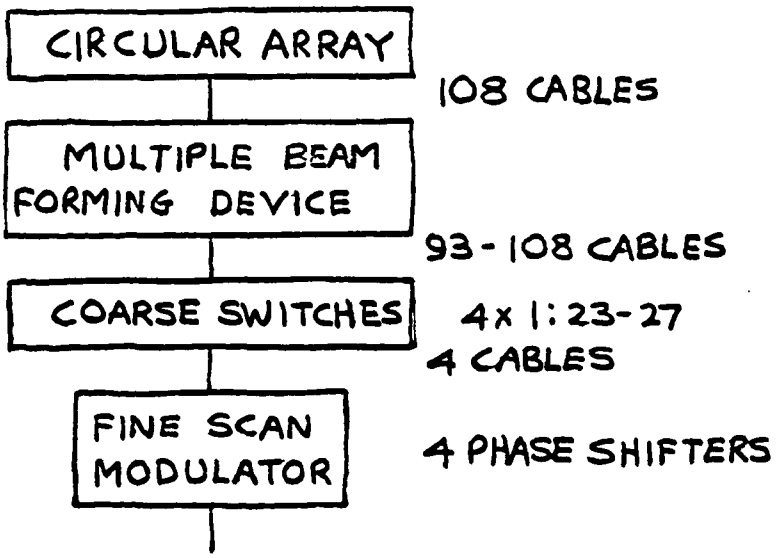


Fig. H-3 — Interscan technique.

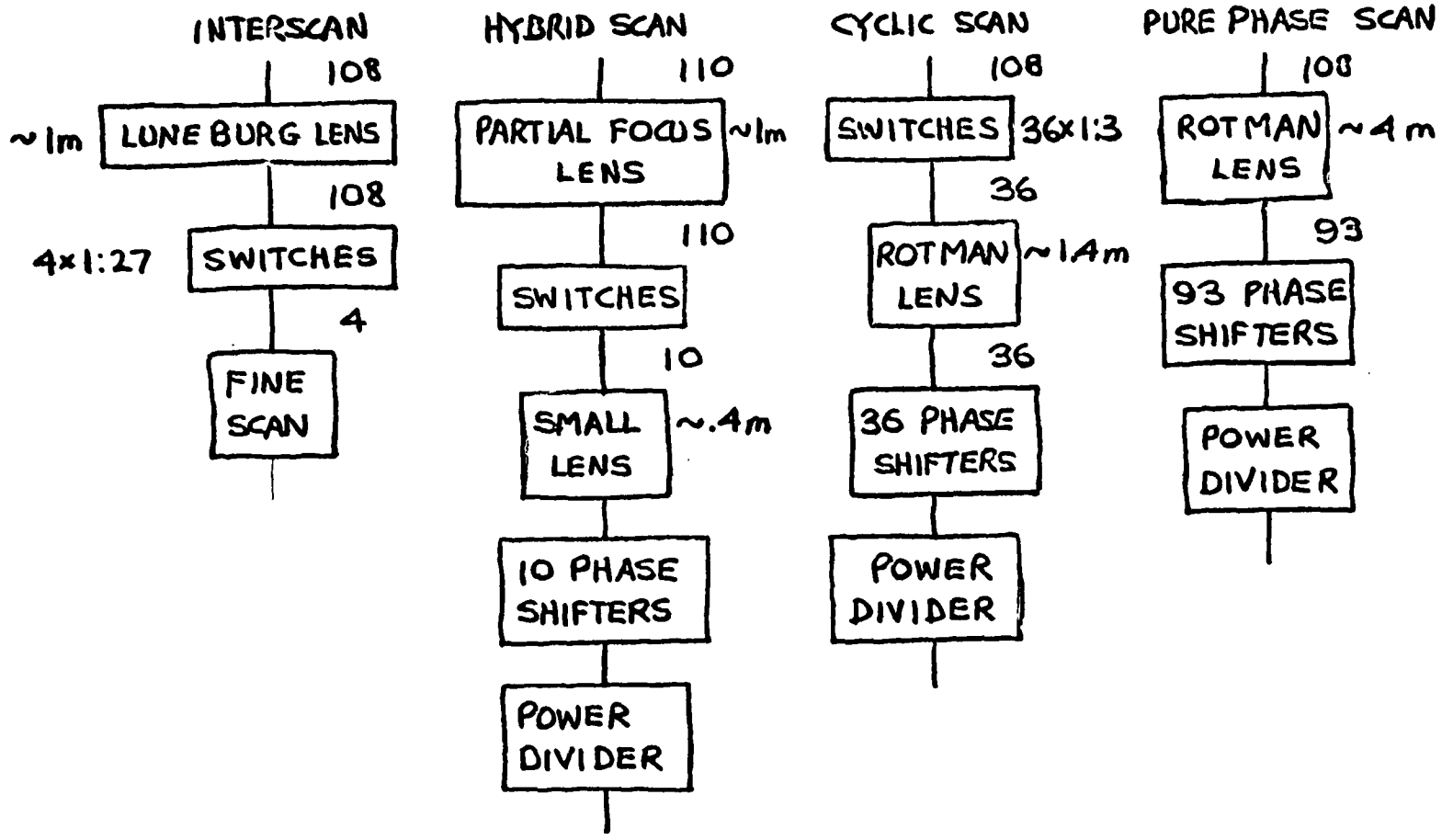


Fig. H-4 — Comparison of scanning techniques.

## APPENDIX I
## THREE-DIMENSIONAL BOOTLACE LENSES

Introduction. Previously published work on bootlace lenses has predominantly treated two-dimensional configurations and linear antenna arrays. A three-dimensional bootlace lens offers the principal advantage of achieving multiple beams from a planar array with frequency-independent collimation and beam positions. When used with circularly polarized lens and feed radiators, small phase adjustments are easily made by rotating the radiators. Because of the inherent polarization diversity of the transmission medium, the use of dual-polarized lens and feed radiators enables the realization of two lenses in one structure, capable of independently feeding two arrays.

Two different design approaches to the three-dimensional bootlace lens are presented and analyzed here. Equations and plots of performance and design parameters are presented. A technique is described in Appendix J for appropriately configuring a 3D bootlace lens so that its outputs can be connected to a linear array to produce multiple beams. The result of this procedure is to reduce greatly the overall size of lens required to obtain multiple beams from a linear array.

Air-Filled 3D Lens. It is well known that an air-filled 3D bootlace lens exhibits astigmatism as its dominant aberration for off-axis feed positions. Although it is possible to achieve a quadrufocal design with one focus on-axis and the other three symmetrically spaced off-axis, it is found that minimum aberration is obtained with all foci collocated on the lens axis.

A "universal" 3D air-filled bootlace lens design has been derived by requiring that, for any radial distance off-axis, with both feed point and lens surface points located at this radius, the astigmatism should be minimum. The lens and feed surfaces are also required to be symmetric. The cross-section of the resulting lens is shown in Figure I-1. Points on the lens surface are defined by $(x,z)$, and points on the feed surface are defined by $(x,-z)$. The axial points of these surfaces are $\pm z_o$. The lens surface is generated by the equation

$$(x^2+z^2)^{\frac{1}{2}} + z + (2x^2+4z^2)^{\frac{1}{2}} = 4\left[x^2+(z_o+z)^2\right]^{\frac{1}{2}} - 4z_o \qquad \text{(I-1)}$$

The length of the transmission line between a point on the lens surface and the aperture is given by

$$L(x) = 2z_o - \left[x^2+(z_o+z)^2\right]^{\frac{1}{2}} \qquad \text{(I-2)}$$

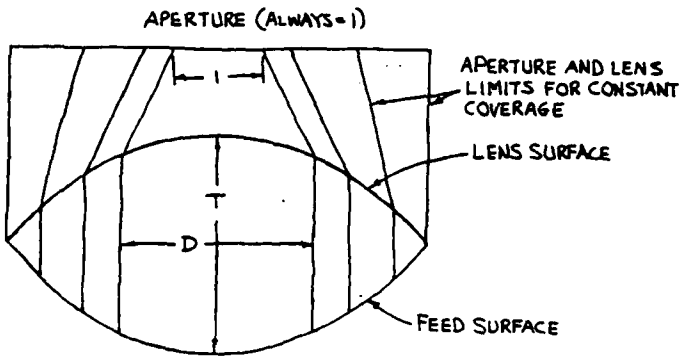


Fig. I-1 — 3D air-filled bootlace lens.

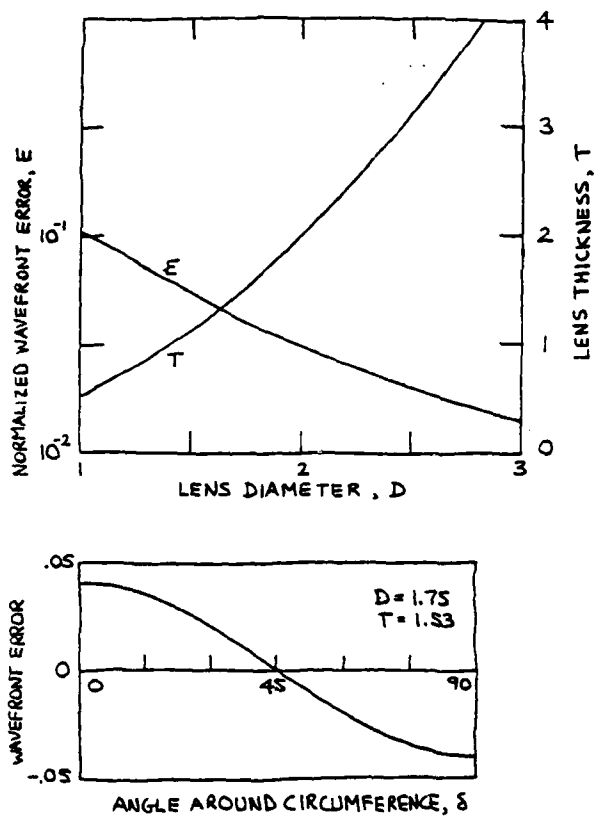


Fig. I-2 — Characteristics of 3D air-filled bootlace lenses.

If the lens diameter is taken to be a particular value of x, then the aperture size for hemispheric coverage is

$$A(x_1) = 2[(x_1^2+z_1^2)^{\frac{1}{2}} - z_1] \qquad \text{(I-3)}$$

In the plots of Figure I-2, all parameters are scaled for unity aperture diameter and hemispheric coverage. The astigmatic wavefront error is cosinusoidal in $\delta$ and exhibits a maximum deviation of $\pm E$ relative to the aperture size. In the limit of large D, E varies inversely as $D^2$. For the lens configurations of most likely practical interest, E ranges from .1 to .01.

3D Fisheye Lens. The lens configuration of Figure I-3 has inhomogeneous dielectric loading in the region between the feed and lens surfaces. This region is obtained by cutting out a portion of a Maxwell fisheye lens, which has a refractive index given by $n = 2/(1+r^2)$.[1] The lens and feed surfaces are spherical with radii of $\sqrt{2}$, defined by

$$r^2 \pm 2r\cos\phi - 1 = 0$$

All transmission lines are of equal length, and the lens has one feed point of perfect focus on the axis. It can be shown that the lens is anastigmatic, and the dominant off-axis aberration is coma. The lens and feed surfaces are geodesics--that is, the surfaces contain ray paths. Thus, the surfaces appear to be planar to the radiators located on them. Furthermore, all rays through the center of one surface intersect the opposite surface normally. In this regard, the lens is optically equivalent to the 2D spherical geodesic bootlace lens proposed by Wild [2].

Analysis of the optical performance of this lens requires the calculation of the optical path length between any two points in the Maxwell fisheye medium. In general, it is very difficult to calculate optical path lengths in inhomogeneous media. However, because the fisheye is an ideal optical system and because all ray paths are circles, it is always possible to find an arc on the unit circle that is optically equal to a given ray path. In this way the lens can be analyzed by straightforward geometric techniques. The optical path length between any two points is given by

$$\gamma = \pi - \tan^{-1}[\cot\alpha\sqrt{1+a^2}] - \tan^{-1}[\cot(\theta-\alpha)\sqrt{1+a^2}] \qquad \text{(I-4)}$$

$$\tan\alpha = (R_2 - R_1\cos\theta)/R_1\sin\theta$$

$$a^2 = 4(R_1^2+R_2^2 - 2R_1R_2\cos\theta)/\sin^2\theta$$

$$R_1 = (1-r_1^2)/r_1$$

$$R_2 = (1-r_2^2)/r_2$$

where $r_1$ and $r_2$ are the radial distances of the two points and $\theta$ is the angle between them.

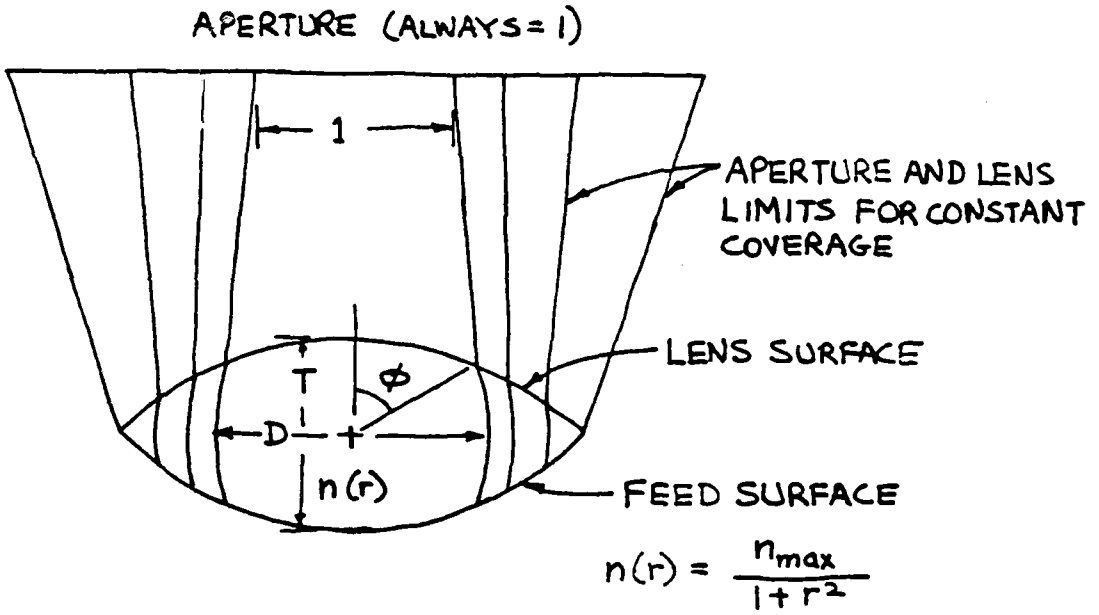


Fig. I-3 — Fisheye bootlace lens.

AD-A089 168 NAVAL RESEARCH LAB WASHINGTON DC F/G 17/7
SUMMARY REPORT ON NRL PARTICIPATION IN THE MICROWAVE LANDING SY--ETC(U)
AUG 80 J P SHELTON, J K HSIAO
UNCLASSIFIED NRL-MR-4305 DOT-FA75WAI-556

2 OF 2
AD-A089 168

END
DATE FILMED
10-80
DTIC

If the lens and feed points are defined by $\phi$ and $\delta$, where $\phi$ is shown in Figure I-3 and $\delta$ is the angle between the radii as seen vertically along the axis (separation is minimum for $\delta$=0 and maximum for $\delta$=180°), the optical path length is given by

$$\tan(\gamma/2) = \left[\frac{1-\sin^2\phi\cos^2\delta/2}{1-\sin^2\phi\sin^2\delta/2}\right]^{\frac{1}{2}} \qquad \text{(I-5)}$$

The desired optical path length is given by

$$\gamma_o = \pi/2-(L/2)\cos\delta \qquad \text{(I-6)}$$

$$L = \pi-4\tan^{-1}(\cos\phi)$$

Equations (I-5) and (I-6) are used to determine wavefront error, $\varepsilon=\gamma-\gamma_o$.

As in the case of the 3D air-filled bootlace lens, the fisheye bootlace lens is also universal in that a smaller portion of the lens can be used to obtain improved optical performance. If the edge of the feed and lens surface is defined by $\phi$ and all parameters are scaled so that the aperture diameter is unity and coverage is hemispheric, the plots of Figure I-4 are obtained. Note that for $\phi < 90°$, the maximum value of r is less than one, so that the minimum value of the refractive index n is greater than one. The index and lens dimensions have also been scaled in Figure I-4 so that the minimum index is one and the maximum index at lens center is as shown. The comatic wavefront error is essentially cubic in cos$\delta$. In the limit of small $\phi$ or large D, E varies inversely as $\phi^4$. For the lens configurations of most likely practical interest, E ranges from .07 to .0007.

The performance of the fisheye lens, although inferior to that of the conventional 2D bootlace lens, is far superior to that of the 3D air-filled lens.[3]

References


1. S. Cornbleet, Microwave Optics, Academic Press, 1976, p. 121.
2. J. P. Wild, "Geodesic Lens," U.S. Pat. No. 4114162, Sep. 12, 1978.
3. J. P. Shelton, "Focusing Characteristics of Symmetrically Configured Bootlace Lenses," IEEE Trans. Antennas Propagat., Vol. AP-26, No. 4, Jul. 1978, pp. 513-518.

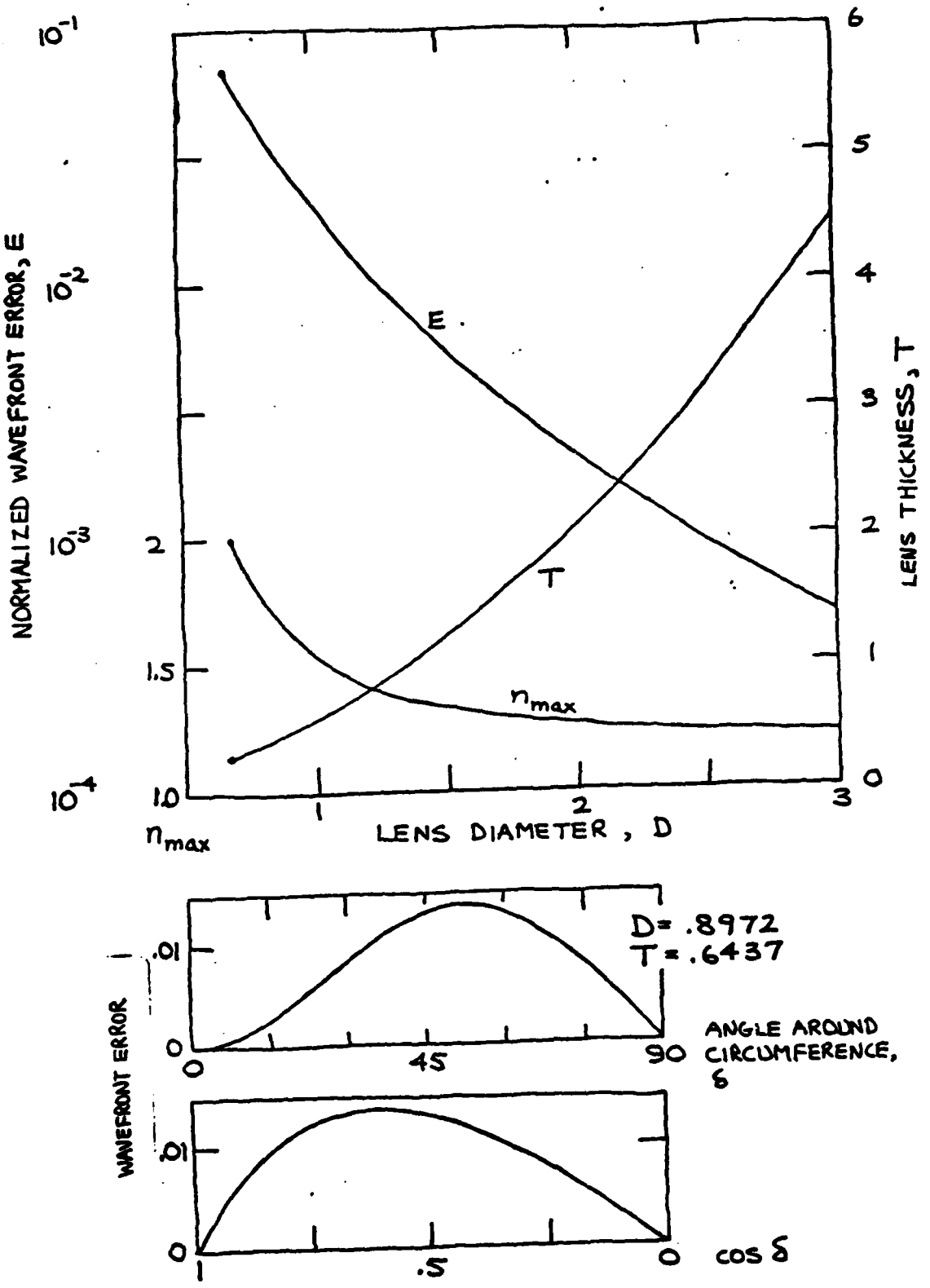


Fig. I-4 — Characteristics of 3D fisheye bootlace lenses.

## APPENDIX J
## Using 3D Lenses to Obtain Multiple Beams from Linear Arrays

In Ref. [1] Shelton discussed the conditions under which multiple beams can be obtained from planar arrays with lossless hybrid networks. It was shown that such multibeam systems are realizable only if the array satisfies a tiling condition--that is, the infinite regular lattice of radiating element locations can be completely filled by translations of the planar array. It was also shown that certain planar arrays can be fed by linear-array multibeam networks. In particular, all square arrays and all symmetric hexagonal arrays fall in this special category. Figure J-1 shows a 19-element hexagonal array with adjacent arrays in a tiling configuration. The elements are numbered so that arithmetic modulo-19 progressions are obtained along any linear cut through the array. The modulo-19 sequence is constrained to the integers between -9 and +9, inclusive. Figure J-2 shows the beam positions of the multiple beams from the array of Figure J-1 and some of the grating lobe locations for these beams.

It was shown in [1] that the integer steps from element to element can be determined by requiring that the tiled arrays all have the same integer patterns on them. If a is the integer step along the $\vec{a}_1$ lattice vector and b along the $\vec{a}_2$ lattice vector, the equations can be shown to be

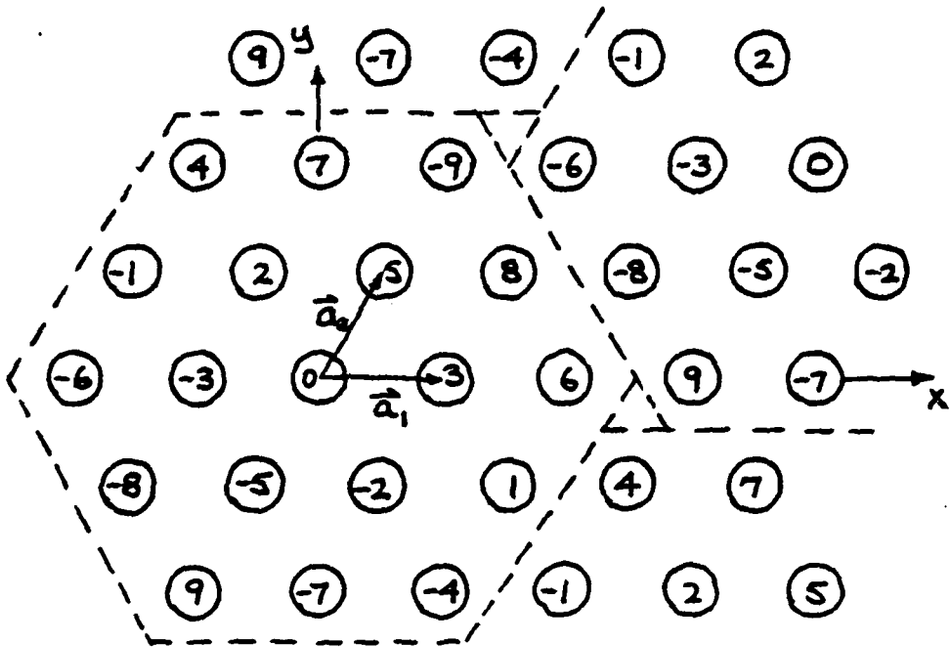


Fig. J-1 — 19-element hexagonal array showing adjacent arrays in tiling arrangement.

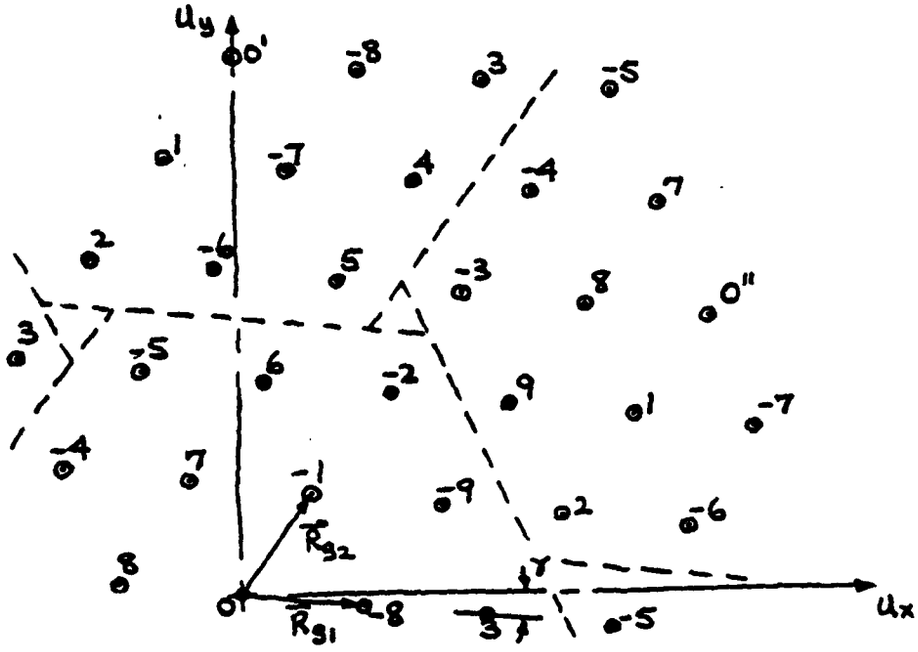


Fig. J-2 — Beam positions for array of Figure J-1.

$$\begin{cases} 5a - 3b = 19m \\ 3a + 2b = 19n \end{cases} \qquad \text{(J-1)}$$

for $m = 0$, $n = 1$, equations (J-1) yield $a = 3$, $b = 5$.

These conditions can also be applied to planar and linear arrays fed by bootlace lenses because bootlace lenses can be theoretically equivalent to a hybrid multibeam network [2]. The logical extension of the above conclusions is that, for the special square and hexagonal arrays, if a three-dimensional lens can generate multiple beams, then the same lens can be used to feed a linear array with the same number of elements.

We use the 19-element array of Figure J-1 as an example, and we assume that a 3D bootlace lens is used. The feed and lens surfaces will consist of 19-element hexagonal arrays. The parameters which must be determined at this point are the orientation of the lens and feed arrays, the correct scaling of the lens dimensions, and the assignment of lens and feed elements. The required orientation is first derived.

The grating lobe locations 0, $0'$, and $0''$ in Figure J-2 are determined by the geometry of the planar array lattice. The lattice vectors for this array are given by

$$\begin{aligned} \vec{a}_1 &= s\vec{x} \\ \vec{a}_2 &= s(\vec{x}/2 + \vec{y}\sqrt{3}/2), \end{aligned} \qquad \text{(J-2)}$$

where s is spacing between nearest radiators and $\vec{x}$ and $\vec{y}$ are unit vectors in the x and y directions. All element locations in the lattice are given by linear combinations of $\vec{a}_1$ and $\vec{a}_2$ :

$$\begin{aligned} \vec{r}_e &= n\vec{a}_1 + m\vec{a}_2 \\ &= s[(n + 1/2)\vec{x} + m\vec{y}\sqrt{3}/2], \end{aligned}$$

where $\vec{r}_e$ is the vector from the origin to the element location and m, n assume all positive and negative integer values. The grating lobe locations are defined in the $u_x$, $u_y$ plane by

$$\vec{R}_g = \vec{R}_o + 2\pi k(\vec{u}_x + \vec{u}_Y/\sqrt{3}) + \ell\vec{u}_y(4\pi/\sqrt{3}) \qquad \text{(J-3)}$$

where $u_x = (2\pi s/\lambda)\sin\theta_x$ and $u_y = (2\pi s/\lambda)\sin\theta_y$, $\vec{u}_x$ and $\vec{u}_y$ are unit vectors, k, $\ell$ also assume all integer values, and $\vec{R}_o$ is the location of any one of the grating lobe maxima. Note that the minimum nonzero magnitude of $\vec{R}_g - \vec{R}_o$ is $4\pi/\sqrt{3}$.

It is clear that the on-axis beam is obtained with the on-axis feed element and that the off-axis beams are obtained by elements of the feed array that are correspondingly displaced off-axis. Thus, if the beam is located at $\vec{R}_g$ in the $u_x$, $u_y$ plane, the feed element will be located at a point in the projected feed array plane, x, y, given by $-c\,\vec{R}_g$, where c is a constant of proportionality.

Given the on-axis location of one of the beams and the lattice geometry defined by equations (J-2), the grating lobe maxima must be located as given by equation (J-3) for $\vec{R}_o = 0$ and as shown in Figure J-2. The locations of the remaining 18 beams generated by the lens can only be as shown in Figure J-2 (or as a mirror image in the $u_y$ axis obtained by multiplying all values of $u_x$ by -1).

The basis vectors for the multiple beam locations are given by

$$\vec{R}_{g_1} = (2\pi(2n+1)/N)\vec{u}_x - (2\pi/\sqrt{3}N)\vec{u}_y \qquad \text{(J-4)}$$

$$\vec{R}_{g_2} = (2\pi(n+1)/N)\vec{u}_x + (2\pi(3n+1)/\sqrt{3}N)\vec{u}_y,$$

for the symmetrical hexagonal array with n rings of elements and number

of elements $N = 3n^2+3n+1$. Note that $|\vec{R}_{g_1}| = |\vec{R}_{g_2}| = 4\pi/\sqrt{3N} = |\vec{R}_g - \vec{R}_o|/\sqrt{N}$. As pointed out previously, the feed element locations will be opposite the multiple beam locations. Whereas the radiating array and lens array locations given by equations (J-2) lie on a triangular lattice with basis vectors oriented at integral multiples of 60 deg relative to the x-axis, the feed array basis vectors given by equations (J-4) are rotated with respect to the x-axis by an angle $\gamma$ given by

$$\cot\gamma = -\sqrt{3}(2n+1),$$

for the symmetrical hexagonal array. For the 19-element array, $\gamma = 6.5868$ deg.

It is interesting to consider that for any orientation of feed and lens arrays other than the one derived here, the antenna system will not be optimum in the sense of producing lossless, orthogonal, maximum gain multiple beams from a planar array.

A similar analysis can be carried out for arrays with $n^2$ elements, for which the lens and feed arrays are square and located on square element lattices. Here again it is found that the feed array must be rotated with respect to the lens array. In this case the rotation angle $\gamma$ is given by

$$\tan\gamma = m/n,$$

where m is an integer constrained by $0 < m < n/2$, and m cannot be a factor of n other than one.

We now have two steps remaining to complete the analysis of the use of 3D lenses to form multiple beams from linear arrays. The first is the proper scaling of the lens to achieve the necessary phase relationships. The second is to relate the lens elements to the elements of the

linear array and to relate the feed elements to the beam positions formed by the 3D lens/linear array combination.

Design formulas for 3D lenses are based on the assumptions that the aperture size is unity, the maximum path delay across the aperture for an edge feed position is also unity, and the feed and lens surfaces are geometrically similar. Referring to the modulo-19 number of the elements of the array of Figure J-1, we note that these numbers should be multiplied by $\lambda/19$ to give path delay, and that the modulo-19 numbering should first be discarded at the edge of the array, as shown in Figure J-3. The feed position indicated by dashed circle c produces a path delay of $20\lambda/19$ between lens elements a and b, and the feed position indicated by dashed circle d produces a path delay of $40\lambda/19$. The geometry of the elements at a, b, and d before scaling is shown in Figure J-4. The gap between the edges of the feed and lens surfaces is G, the diameter of these surfaces is D, and the rotation angle between lens and feed arrays is $\gamma$. The path delay between paths ad and bd is given by

$$\Delta\ell = \sqrt{G^2+D^2\cos^2\gamma/2} - \sqrt{G^2+D^2\sin^2\gamma/2}$$

We also have $\sqrt{G^2+D^2} - G = 1$ or $D^2 = 2G+1$.

It is seen that $\Delta\ell = 1$ for $\gamma = 0$ and decreases with increasing $\gamma$. Therefore, we scale the lens dimensions by the factor $40\lambda/19\Delta\ell$. For lens designs of maximum compactness $\Delta\ell$ becomes significant: For $G = 0$ and $\gamma = 6.5868$ deg, $\Delta\ell = .9409$. However, for a lens with $G = 1$, $D = \sqrt{3}$, $\Delta\ell = .9926$.

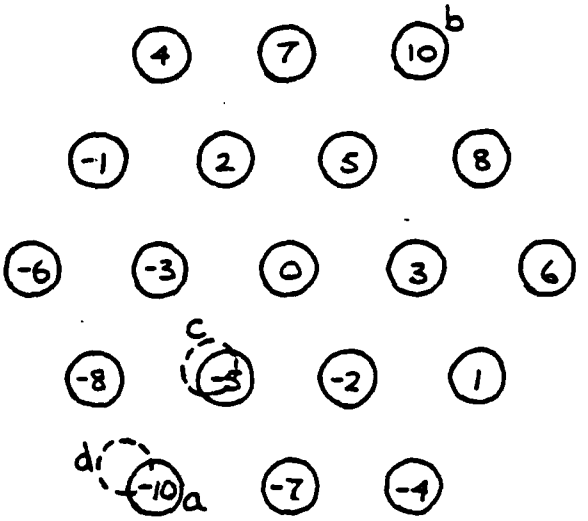


Fig. J-3 — Lens array showing relative locations of elements a,b and feed points c,d.

Fig. J-4 — Geometry of lens points a,b and feed point d.

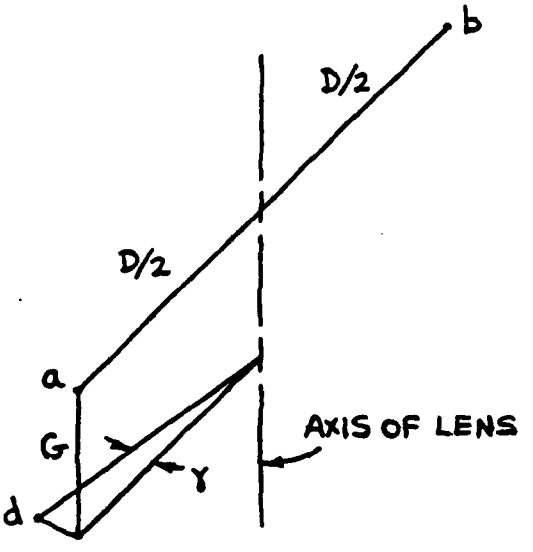

For the 19-element array shown in Figure J-1, the numbers show the connections to the elements of the linear array. Figure J-2 shows the positions of the multiple beams produced by the linear array. If one off-axis beam position can be determined, as in the case of beam number one in Figure J-3, then all beam positions are defined by extending the linear progression. This results first in numbering the row of beams consisting of 0 through -5 in Figure J-4, then the rows -4 to -8 and -5 to -7, based on the tiling characteristics of the grating lobes of the multiple beams. Continuing, we can number the rows -8 to 7, 8 to 3, and finally 3 to 0' and 3 to 0", to complete the numbers of all beam positions. Note that for both arrays the elements around the center element can be defined by three integers, 2, 3, 5 for the lens array and 1, 7, 8 for the feed array. These sets of integers are sufficient to define all elements for the arrays. Other sets of integers can be obtained by forming integer multiples, modulo 19, of the initial sets. The result is that lens and feed arrays can be formed with any combination of three sets of integers, 2, 3, 5, and 1, 7, 8, and 4, 6, 9.

This appendix has outlined a procedure for feeding a linear array with the outputs of a 3D bootlace lens. The procedure involves the following steps:

1. Select either a square or regular hexagonal array.
2. Determine the rotation angle between feed and lens arrays.
3. Compute the appropriate scale factor for the lens.
4. Determine the connections from the lens arrays to the linear arrays and the beam positions assigned to elements of the feed array.

REFERENCES

1. J. P. Shelton, "Multibeam Planar Arrays," Proc. IEEE, Vol. 56. No. 11, Nov. 68, pp 1818-1821.

2. J. P. Shelton, "Focusing Characteristics of Symmetrically Configured Bootlace Lenses," IEEE Transactions Antennas Propagation, Vol. AP-26, No. 4, Jul 78, pp 513-518.

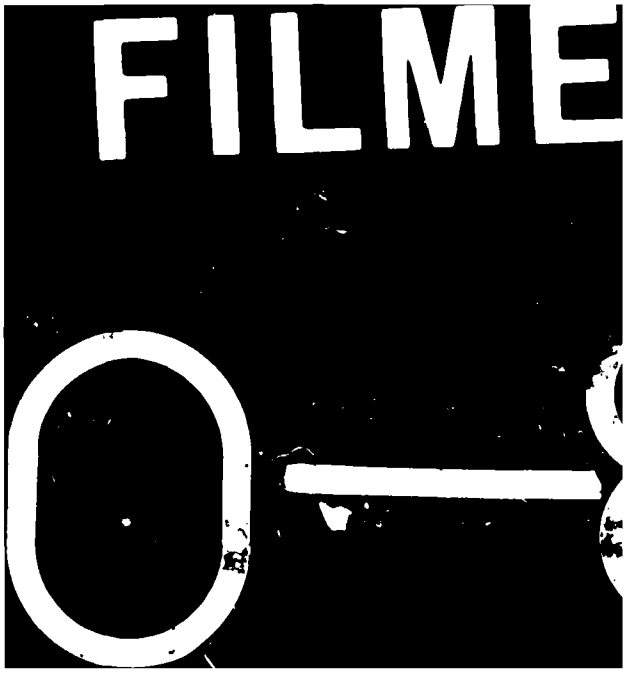
FILME